



**TECHNISCHE
UNIVERSITÄT
DRESDEN**

Faculty of Forest, Geo and Hydro Sciences

Detection of land cover changes in El Rawashda forest,
Sudan:

A systematic comparison

Dissertation for awarding the academic degree
Doctor of Natural Science (Dr. rer. nat.)

Submitted by

MSc. Wafa Mohamed Tahir Nori

Supervisor:

Mr. Prof. Dr. Elmar Csaplovics
Technical University of Dresden / Institute of Photogrammetry and Remote
Sensing

Mr./Mrs. Prof. Dr. xxx xxxxxxxxxxxxx
University / Institution...

Dresden, March 2012

Explanation of the doctoral candidate

This is to certify that this copy is fully congruent with the original copy of the dissertation with the topic:

„ Detection of land cover changes in El Rawashda forest,
Sudan:
A systematic comparison “

Dresden, 24.05.2012

.....
Place, Date

Nori, Wafa

.....
Signature (surname, first name)

Declaration

I hereby declare that this thesis entitled “Detection of land cover changes in El Rawashda forest, Sudan: A systematic comparison” submitted to the Faculty of Forest, Geo and Hydro Sciences, Technical University of Dresden, is my own work and, it contains no materials previously published or written by another person and has not been previously submitted or accepted elsewhere to any other university or institute for the award of any other degree.

Wafa Mohamed Tahir Nori

Dedicated to my Father
A very special man

Contents

1	Introduction.....	1
1.1	Background	1
1.1.1	Forest in Sudan.....	1
1.1.2	Remote Sensing for Ecosystem Management.....	3
1.2	Problem definition	4
1.3	Motivation	5
1.4	Current status of research	7
1.5	Objectives.....	9
1.6	Structure of the thesis.....	10
2	Review of forest change detection techniques	12
2.1	Introduction.....	12
2.1.1	Image acquisition	12
2.1.2	Pre-processing	13
2.2	Visual interpretation	13
2.3	Pixel-based methods	14
2.3.1	Single-date indices	14
2.3.1.1	Spectral reflectance.....	14
2.3.1.2	Vegetation indices	15
2.3.1.3	Principal Components	15
2.3.1.4	Tasseled cap components.....	16
2.3.1.5	Spectral Mixture Analysis	16
2.3.1.6	Classification	17
2.3.2	Multi-date transformation.....	17
2.3.2.1	Image differencing	17
2.3.2.2	Change vector analysis	18
2.3.2.3	Multitemporal principal component analysis.....	19
2.3.2.4	Multitemporal Kauth-Thomas transformation	20
2.3.2.5	The Multivariate Alteration Detection	20
2.3.2.6	Chi square transformation	21

2.3.3	Change detection algorithms	21
2.3.3.1	Post-classification comparison (PCC).....	22
2.3.3.2	Thresholding.....	22
2.3.3.3	Classification	23
2.4	Object-based methods.....	23
2.4.1	GIS-data.....	24
2.4.2	Image segmentation.....	25
2.5	Change mapping	26
2.6	Method comparison	27
3	Study area and research data acquisition	28
3.1	Study area	28
3.1.1	Location of the study area	28
3.1.1.1	Topography	28
3.1.1.2	Geology	28
3.1.1.3	Soil	28
3.1.2	Physical Characteristics of El Rawashda Reserved Forest..	30
3.1.2.1	Climate	30
3.1.2.2	Vegetation	31
3.1.3	Social and land-use characteristics	32
3.1.3.1	Population in Gedarif State with special reference to El Rawashda	32
3.1.3.2	Land-use, land use changes and their influence on the forests	33
3.1.3.3	Socio-economic background of the nomad	34
3.1.4	Management Units	34
3.1.4.1	El Rawashda model I.....	35
3.1.4.2	El Rawashda Model II.....	35
3.2	Research data acquisition.....	35
3.2.1	Field sampling	35
3.2.2	Data collection for study area	36
3.2.2.1	Landsat Imagery.....	36

3.2.2.2	Aster Imagery	37
3.2.3	Image pre-processing.....	37
3.2.3.1	Atmospheric correction.....	37
3.2.3.2	Image to image registration	38
4	Methods of Change Detection.....	39
4.1	Descriptions of land cover classes.....	39
4.2	Classification of images using Maximum likelihood Classifier	39
4.3	Accuracy assessment of classified images	41
4.4	Calculation of Vegetation Indices as independent variables.....	41
4.4.1	NDVI	42
4.4.2	NDVI-RGB.....	42
4.4.3	SAVI	42
4.4.4	TDVI	43
4.5	Index Differencing.....	43
4.6	Tasseled Cap Transformation.....	43
4.6.1	RGB-TCG.....	43
4.7	Change Vector Analysis.....	44
4.8	Mapping with Conventional and Selective Principal Component Analysis	44
4.8.1	Multitemporal PCA: the conventional approach	44
4.8.2	Selective PCA	44
4.9	Change Detection by Multivariate Alteration Detection.....	45
4.10	Accuracy assessments for change detection techniques	45
4.11	Object-Oriented Classification of references data by eCognition....	46
5	Results	48
5.1	Classification and Change Detection Accuracy	48
5.2	Post Classification Change Detection	50
5.3	Change detection based on Vegetation Indices	55
5.3.1	Vegetation Indices differences.....	55
5.3.2	5.3.2 RGB-NDVI.....	56
5.4	Application of Tasseled Cap for change detection	59

5.4.1	Derivation of Tasseled Cap Transformation.....	59
5.4.2	Derivation of Greenness component for change detection...	60
5.5	Change Vector Analysis: An Approach for Detecting Forest Changes	62
5.5.1	Analysis of the change image 2000/2003	62
5.5.2	Analysis of the change image 2003/2006	63
5.6	Mapping with Conventional and Selective Principal Component Analysis	63
5.6.1	Generation of PCA Components	63
5.6.2	Change detection with Multitemporal PCA: the conventional approach	65
5.6.3	Change detection with Selective PCA	69
5.7	Change Detection based on Multivariate Alteration Detection (MAD).	70
5.7.1	MAD Interpretation	71
5.7.2	Maximum autocorrelation factor (MAF) analysis	74
5.8	Accuracy assessments for change detection techniques	76
6	Discussion	82
7	Conclusions and outlook.....	90
7.1	Conclusions	90
7.2	Outlook	92
8	References	94

List of Figures

Figure 1.1: Sudan location.....	2
Figure 1.2: Sudan Humanitarian.....	2
Figure 1.3: Herd of animals grazing in El Rawashda Forest.....	6
Figure 1.4: Gathering wood in El Rawashda forest	6
Figure 1.5: Charcoal production in earth-pit kilns in Gedarif.....	6
Figure 2.1: The process for detecting the direction of change (a) and the magnitude of change (b) within change vector analysis.....	19
Figure 2.2: Geometric interpretation of principal component analysis ..	19
Figure 2.3: MAD procedure	21
Figure 2.4: Object-oriented, knowledge-based analysis with eCognition..	24
Figure 3.1: Location of the study area	29
Figure 3.2: El Rawashda Reserved Forest, Sudan, showing excavation running along the forest	30
Figure 3.3: Average Annual Rainfall, El Rawashda Region, 2002-2009...	31
Figure 3.4: Map of Gedarif showing the situation of El Rawashda forest	32
Figure 3.5: Livestock raising in the traditional seasonal transhumance in El Rawashda forest.....	33
Figure 3.6: Movement of nomad groups in El Rawashda forest	34
Figure 3.7: Field observation points.....	36
Figure 4.1: Land cover classes in El Rawashda forest.....	40
Figure 4.2: Samples representing the land cover classes according to the spectral radiance of Aster (pc1, pc2, pc3) in the study area ...	41
Figure 4.3: Change and no change error matrix.	46
Figure 4.4: Classification of the reference imagery by eCognition.....	47
Figure 4.5: Segmentation based on pixel-based	47
Figure 4.6: Segmentation based on object-based	47
Figure 5.1: Supervised classification of ETM 2000.....	51
Figure 5.2: Supervised classification of ETM 2003.....	51
Figure 5.3: Change map.....	51
Figure 5.4: Supervised classification of ETM 2003.....	52
Figure 5.5: Supervised classification of Aster 2006.....	52
Figure 5.6: Change map.....	52

Figure 5.7: Resultant images of NDVI, SAVI and TDVI transformation and image differencing.	57
Figure 5.8: Simplified interpretation of three-date RGB-NDVI color composite imagery	58
Figure 5.9: RGB composite of Tasseled Cap Transformation of ETM 2000 (left), ETM 2003 (middle) and Aster 2006 (right).	60
Figure 5.10: A comparison of the Greenness component of TCT (right) with the Normalized Difference Vegetation Index NDVI (left) for ETM 2000	60
Figure 5.11: Simplified interpretation of three-date RGB-TCG color composite imagery	61
Figure 5.12: Change vector based on Tasseled Cap images from the year 2000 to 2003, magnitude (left) and direction (right)	62
Figure 5.13: Change vector based on Tasseled Cap images from the year 2003 to 2006, magnitude (left) and direction (right)	63
Figure 5.14: Images of the first three Principal components generated from ETM 2000 (left), ETM 2003 ETM 2003 (middle) and Aster 2006 (right)	64
Figure 5.15: PCA generated from 10 bands combination of ETM_2000 and ETM-2003	67
Figure 5.16: PCA generated from 10 bands combination of ETM 2003 and Aster 2006	68
Figure 5.17: PC2 generated from NIR of ETM_2000 and NIR of ETM_2003 (left), and PC2 generated from NIR of ETM_2003 and NIR of Aster-2006	70
Figure 5.18: Scatter plot MAD1 vs. MAD2	71
Figure 5.19: MAD components of ETM2000 and ETM2003 and the first three components as RGB	73
Figure 5.20: MAD components of ETM2003 and Ater2006 and the first three components as RGB	73
Figure 5.21: MAD/MAF components of ETM2000 and ETM2003 and the first three components as RGB	74
Figure 5.22: MAD/MAF components of ETM_2003 and Aster_2006 and the first three components as RGB.....	75
Figure 5.23: Changes given by the MAD/MAF of the first three components from ETM_2000 and ETM_2003 (left) and from ETM_2003 and Aster_2006 (right) with automatic threshold.....	75

Figure 5.24: Change / no change map given by different change detection techniques (2000-2003).....	77
Figure 5.25: Change / no change map given by different change detection techniques (2003-2006).....	77
Figure 5.26: Classification of the references images	79
Figure 5.27: Accuracy map given by different change detection techniques (2000-2003)	80
Figure 5.28: Accuracy map given by different change detection techniques (2003-2006)	81
Figure 6.1: Change of forest classes	86
Figure 6.2: Accuracy assessments of change detection techniques	87

LIST OF TABLES

Table 3.1: Satellite imagery and its specifications used for bi-temporal change detection	37
Table 3.2: Landsat specification.....	37
Table 3.3: Aster specification	37
Table 5.1: Error matrix of ETM 2000.....	49
Table 5.2: Producer's and user's accuracy of ETM 2000 classification	49
Table 5.3: Error matrix of ETM 2003.....	49
Table 5.4: Producer's and user's accuracy of ETM 2003 classification	49
Table 5.5: Error matrix of Aster 2006	50
Table 5.6 Producer's and user's accuracy of Aster 2006 classification	50
Table 5.7: Comparison of classifications, absolute number of pixels (GL = grassland, CF = close forest, OF = open forest, BL = bare land)	53
Table 5.8: Comparison of classifications, relative number of pixels in percent (basis: all image pixels)	53
Table 5.9: Comparison of classifications, relative number of pixels in percent (basis: image pixels of each class in 2000)	54
Table 5.10: Comparison of classifications, absolute number of pixels (GL = grassland, CF = close forest, OF = open forest, BL = bare land)	54
Table 5.11: Comparison of classifications, relative number of pixels in percent (basis: all image pixels)	54
Table 5.12: Comparison of classifications, relative number of pixels in percent (basis: image pixels of each class in 2003)	55
Table 5.13: The percentage of increase, decrease and no change in vegetation cover	57
Table 5.14: PCA Statistics of ETM_2000.....	64
Table 5.15: PCA Statistics of ETM_2003.....	66
Table 5.16: PCA Statistics of Aster_2006	66
Table 5.17: PCA Statistics of 10 bands combination of ETM_2000 and ETM_2003 data	67
Table 5.18: PCA Statistics of 10 bands combination of ETM_2003 and Aster_2006 data	68
Table 5.19: PCA Statistics from 10 bands of ETM_2000 and ETM_2003 data by band wise	69
Table 5.20: PCA Statistics from 10 bands of ETM_2003 and Aster_2006 data by band wise	69

Table 5.21: Correlation matrix of the MAD components with the original ETM_2000 and ETM_2003 bands	72
Table 5.22: Correlation matrix of the MAD components with the original ETM 2003 and Aster 2006 bands	72
Table 5.23: Percentages of Reforestation, Deforestation and No change (2000-2003)	78
Table 5.24: Percentages of Reforestation, Deforestation and No change (2003-2006)	78
Table 5.25: Comparison between different change detection techniques and its overall accuracy [%] (2000-2003)	80
Table 5.26: Comparison between different change detection techniques and its overall accuracy [%] (2003-2006)	81

LIST OF ACRONYMS

ATCOR	ATmospheric CORrection
CCA	Canonical Components Analysis
CIA	Central Intelligence Agency
CVA	Change Vector Analysis
DN	Digital Number
EROS	Earth Resource Observation System
ETM	Enhanced Thematic Mapper
FAO	World Food and Agriculture Organization
FNC	Forestry National Corporation
GCP	Ground Control Points
GIS	Geographical Information System
GLCF	Global Land Cover Facility
GEF	Global Environment Facility
GPS	Global Positioning System
HRVIR	Haute Résolution Visible et InfraRouge
LULC	Land Use/Land Cover
MAD	Multivariate Alteration Detectio
MEPD	Ministry of Environment & Physical Development
MKT	Multitemporal Kauth-Thomas
MMU	Minimum Mapping Unit
MPCA	Multitemporal Principal Component Analysis
MSS	Multispectral Scanner

NDMI	Normalized Difference Moisture Index
NDVI	Normalized Difference Vegetation Index
NDWI	Normalized Difference Water Index
NIR	Near-Infrared
PC	Principal Component
PCA	Principal Component Analysis
PCC	Post-Classification Comparison
RGB	Red-Green-Blue (color composite)
RMSE	Root Mean Square Error
SAVI	Soil Adjusted Vegetation Index
SMA	Spectral Mixture Analysis
SPOT	Syst`eme Probatoire pour l'Observation de la Terre
SWIR	Short-Wave InfraRed
TCA	Tasseled Cap Analysis
TDVI	Transformed Difference Vegetation Index
TM	Thematic Mapper
UNEP	United Nations Environment Program
UNDP	The United Nations Development Program
UTM	Universal Transverse Mercator

ACKNOWLEDGEMENTS

I would like to express my deepest gratitude to my supervisor Professor Dr. Elmar Csaplovics who heavily supported my research through many useful thoughts and clarifications for finalizing the study. I am also indebted to him for giving me the opportunity to finish my study at The Technische Universität Dresden.

My deepest gratitude goes also to my former supervisor Junior Professor Dr. Irmgard Niemeyer. After the initial assistance and various views on how the work should be conducted she let me develop the thesis work and provided me with full support. I am thankful to Dr.Elnour Abdalla Elsiddig and Dr. Amna Ahmed Hamid for their strong support.

I am very grateful to Technische Universität Bergakademie Freiberg and PHD program for their financial support to carry out the field work. Very special thanks extended to Dr Corina for her strong helps.

I am thankful to my colleagues in the Forest National Cooperation (FNC) offices in Gedarif, for their unlimited support during the field work. Special thanks go also to Taghreed Siddig and Dr. Hussein Suleiman for their help. Sincere thanks to my colleagues at the Technische Universität Bergakademie Freiberg and at The Technische Universität Dresden.

I am thankful to the Ministry of Higher Education and Scientific Research (Sudan) and University of Kordofan for their financial support for the study.

Finally I am deeply indebted to my family for their support and encroachment throughout the period of this study, special thanks to my sisters Afaf and Khalda. My heartfelt thanks to my husband Abdelmoneim, who was there to support me every step of the way. Special gratitude to my daughter Riham and my sons Awab and Nori for their great patience during my long absence.

1 Introduction

1.1 Background

1.1.1 Forest in Sudan

Sudan's total land area amounts to some 1,861,484 sq km (CIA World Factbook, 2011). Its vast area includes stretches of tropical forests, marshlands, mountains in southern and central parts to savannah, stone sand deserts and mountains in the north, east, and west (Mustafa, 2006). As it is shown in figure 1.1, Sudan is bordered by Egypt to the north, the Red Sea to the northeast, Eritrea and Ethiopia to the east, South Sudan to the south, the Central African Republic to the southwest, Chad to the west and Libya to the northwest. Sudan's population is 45,047,502 includes the population of South Sudan (8,260,490), estimated urban population at 40% and the rural population at about 60 % (including nomadic groups). The population growth rate is 2.4%, the population density per square kilometers is estimated to be 24.2 persons (CIA World Factbook, 2011). This figure, however, can be a misleading indicator if the population distribution is not considered. In Sudan, a great deal of land is desert, desert-like, or simply non-arable. Therefore, when land area is limited to that which has some potential arability, population density would increase to 31.4 persons/square km, and go as high as 370 persons/ square kilometer when considering land presently cultivated (MEPD, 2003). Figure 1.2 shows Sudan 2011 Humanitarian, The secession of southern Sudan has led to the displacement of the population on a large scale. In Darfur, while there have been several outbreaks of localized fighting since, a growing number of refugees and displaced persons to more stable areas has been seen. At the same time, a large-scale movement of South Sudanese from Sudan to South Sudan continues.

Forests in Sudan occupy an area of about 69,949,000 hectares, about 29.4% of the country's area (Including forest area in South Sudan). Of this area 20% is classified as primary forest, 71% is classified as naturally regenerated forest and only 9% is planted forest (FAO, 2010). The forests reserve has a large potential economic value. It can provide the basis for a sustainable timber industry, wildlife tourism and other forest products. Currently, forest resources are used mainly for gum Arabic production and subsistence needs. Although forestry sector contributes as much as 13 percent to the gross domestic product of Sudan, this valuable resource is threatened, however, by deforestation driven mainly by human activities (UNEP 2007).

Forests are considered among the most important natural features in the Sudan, they form, with other varying intensities of plant cover, the base for the terrestrial ecosystems of the country. Forests perform a series of vital environmental functions at local, regional and global level. At local level environmental services provided by forests include the maintenance of soil, water and climate quality that support productive agriculture, also their canopy protects soil from rainfall thereby regulating run-off and slowing down erosion. On the global scale, forests have two fundamental functions, namely the role of carbon sinks in the global carbon cycle and as pools of biodiversity. In terms of social and economic importance and livelihood support, trees and forests occupy a central position in providing the greater part of fodder for both domestic livestock and wildlife in addition to being the main source of energy and build-



Figure 1.1: Sudan location

Source: Sudan location map.svg, 2011

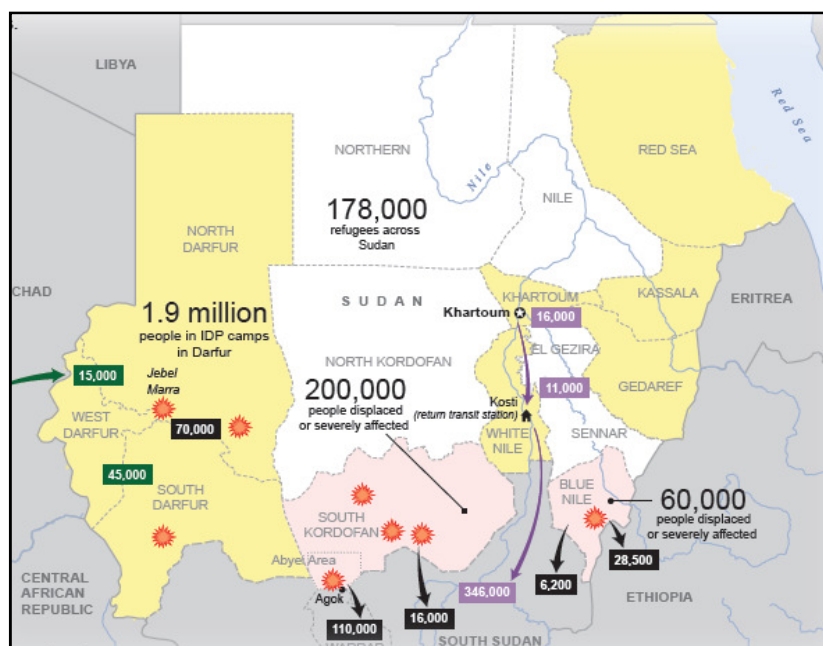


Figure 1.2: Sudan Humanitarian

Source: Relief Web (2011)

ing material for households (FAO, 2006). FAO stated that information on Sudan forest cover extends and composition is neither accurate nor reliable. While a recent report of FAO revealed that Sudan is one of the ten countries with the largest net loss per year. In the period 1990–2000 Sudan had net loss of forest area of 589 million hectares (0.8%) and reduced to 54 million hectares (0.08%) (FAO, 2010).

The Forests National Corporation (FNC) with the cooperation of FAO was able to undertake a National Forest Inventory in 1997, which covered the central part of the country between latitudes 16°N and 10°N. The area covered was 62.3 million ha (622.700 km²) or 24.9% of the total area of the Sudan. The area covered is mainly in the low rainfall savanna region, where almost all-present activities of irrigated and rain-fed agriculture, forestry, grazing, human settlements and oil fields are concentrated. A large part of forest products come from this inventoried area. This survey resulted in a forest cover in the inventoried area of 12% based on the FAO Definition of Forest (10% canopy cover) (HCENR, 2009).

1.1.2 Remote Sensing for Ecosystem Management

Population, community and physiological ecology provide many of the underlying biological mechanisms influencing ecosystems and the processes they maintain. Yet, for too long in all countries, development priorities have focused on human needs from ecosystems, and without paying much attention on the impact of our actions (White et al. 2000).

Vegetation cover is one of the most important components of the earth's surface. It strongly influences evapotranspiration, infiltration, runoff and soil erosion. Vegetation cover is also the principal factor limiting stocking rates in managed grazing lands. It has been widely recognized as one of the best indicators for determining land condition (Booth and Tueller, 2003; Bastin and Ludwig, 2006; Wallace et al., 2006). Therefore, land condition can be assessed and monitored according to vegetation cover and its variations in time and space. This component is often used as the key indicator in the remote sensing of the land condition.

Information and data needs have been growing in scope and complexity (de Sherbinin 2005). For the past couple of decades the application of remote sensing (RS) not only revolutionized the way data has been collected but also significantly improved the quality and accessibility of important spatial information for natural resources management and conservation. The rapid acceptance of the use of remote sensing for conservation and nature protection coincides with the frequent reporting of wide spread modification of natural systems and destruction of wildlife habitats during the past three to four decades. Concerns about the increase in adverse environmental conditions prompted the remote sensing experts and users to quickly catch up with the evolving technology. The parallel advance in the reliability of Geographic Information System (GIS) has allowed the processing of the large quantity of data generated through remote sensing (Lunetta et al. 1999).

Environmental Assessment to evaluate growth and its impact is important for informed planning for future growth. This can be done through improved methodologies in line with the latest scientific developments to analyze land cover changes over time using remote sensing, in an approach called change detection. Change detection is a process that measures how the attributes of a particular area have changed between two or more time periods. Change detection often involves comparing aerial photographs or satellite imagery of the area taken at different times (Wang, 1993). The

basic promise in using remote sensing data for change detection is that changes in land cover result in changes in radiance values, and changes in radiance due to land cover change are large with respect to radiance changes caused by other factors such as differences in atmospheric conditions, differences in soil moisture and differences in sun angles (Mas, 1999). Some of the most commonly used change detection techniques are image differencing, post-classification comparison, principal component analysis, and change vector analysis (Singh 1989, Fung 1990, Lambin and Strahler, 1994, Kwarteng and Chavez, 1998). These techniques have been used successfully to identify areas of change in different urban regions but, most of these techniques focused on areas located in semi-arid regions with low vegetation and thus radiance values change associated with city growth can be easily captured. Since urban growth is not limited to semi-arid regions, it is essential to evaluate the effectiveness of these techniques in identifying change in different sites through the world (Pilon, et al., 1988, Sohl, 1999).

This research evaluates the effectiveness of pixel Post-Classification Comparison (PCC), image differencing of different vegetation indices (Normalized Difference Vegetation Index NDVI, Soil-Adjusted Vegetation Index SAVI and Transformed Difference Vegetation Index TDVI), Principal Component Analysis (PCA), Multivariate Alteration Detection (MAD), Change Vector Analysis (CVA) and Tasseled Cap Analysis (TCA). detection techniques for monitoring urban growth in a semi-arid and temperate climatic setting, with additional attention being placed on each technique's strengths and weaknesses

1.2 Problem definition

Between 1990 and 2010, Sudan lost an average of 321,600 ha or 0.42% per year. In total, between 1990 and 2010, Sudan lost 8.4% of its forest cover or around 6,432,000 ha (FAO 2010). It is driven principally by energy needs and agricultural clearance. Between 1990 and 2005, the country lost 11.6 percent of its forest cover or approximately 8,835,000 ha. United Nations Environment Programmers (2007) stated that: two-thirds of the forests in north, central and eastern Sudan disappeared between 1972 and 2001.

Degradation of deforestation rates indicate that forest cover could reduce by over 10 percent per decade. In areas under extreme pressure, UNEP estimates that total loss could occur within the next 10 years. These negative trends demonstrate that this valuable resource upon which the rural population and a large part of the urban population depend completely for energy is seriously threatened.

Within the last six decades, the Gedarif State in eastern Sudan lost its status as one of the major sources of food production in the country, due to large-scale degradation of its rich soil as well as other natural resources, mainly through unsuccessful land use policies and practices (Elsiddig 2003).

According to available records, planned forest management in the Sudan has since 1932 been based on a government policy that restricts the access of local communities to the forests except with special permits (Elsiddig 2003). Natural forest reserves and land proposed for reservation in Sudan sum up to about 14.5 million hectares, but a negligible part of that is put under proper management (Elsiddig 1996). Although the forest policy called for protection of natural forest reserves against illicit cutting, grazing and fire, so far, all the management activities executed within the natural forest reserves are concerned mainly with protection and patrolling exercised by forest

guards (Elmoula 1985; Elsiddig 2003), a practice that renders the policy more oriented towards control and punishment than towards development of the forests and fulfilment of people's needs.

In the absence of clear management practices and the absence of local people's involvement in the management process, natural forest reserves and forests outside the reserves are continuously subjected to heavy pressures from the forest-dependent local people. Benefiting from ineffective control and the easy access to the forest that is often provided by the official forest harvesting, they engage in random felling (inside and outside reserves, where it is also forbidden), removal of vegetation by overgrazing (Figure. 1.3), gathering wood (Figure. 1.4) and charcoal burning (Figure. 1.5).

In Sudan, the major causes of soil degradation have been ranked as intensive grazing for extended periods of time, or without sufficient recovery periods, depletion of soil nutrients through poor farming practices, forest harvesting by itself tends to have minor impacts on soil quality and long-term site productivity, and over-exploitation of the vegetation for domestic uses. Studies proved that, the impact of overgrazing leading to degradation of approximately 30 million ha, mostly in the arid zone, causing widespread wind erosion. Further, erosion in the semi-arid zone, attributed to human factors such as deforestation, overgrazing and overexploitation. A high population imbalance in some areas further increased soil degradation (Laxen, 2007). Studies revealed that goat grazing is the main cause for deterioration of *Acacia senegal* tree in many of its natural habitats. Tree seeds and seedlings are also suppressed by different causes namely insects, lack of water and high soil temperatures (Hussein 1991). The permanent settlement of semi-nomadic or nomadic ethnic groups and their livestock has a negative effect on vegetation. Large herds of livestock have destroyed the possibility of the vegetation to regenerate (Laxen, 2007).

There is a definite need for baseline information on prevailing land-use systems in Sudan so as to facilitate the design, implementation and evaluation of forestry interventions and to assist the local people in the conservation, management and protection of dry land forests.

1.3 Motivation

Forest in Sudan was estimated in 2000 as 61.6 million hectares, or 25.9 percent of the total area. Between 1990 and 2000, forest area was decreasing at a rate of 1.4 percent per year. The decline in forest resources not only due to the expansion of mechanized agriculture in central Sudan, but also to an increase in overgrazing and overexploitation to meet the demands of growing population and aggressive urbanization.

Devolving control over natural forest resources is a positive step for the government and local people in the Sudan (Abdelnour, 1999). In eastern Sudan, however, things are not all going according to the plan. Despite ten years of negotiations the real question of who has the power over decision-making is still unanswered. Forests are under great stress in Sudan. In the mid-fifties, forests constituted about 36% of the total area of the Sudan (90,000,000 km²). Today, most of this forest land has been depleted to meet the demands for fuel wood and timber.

The motivation for doing this research in forest landscape through remote sensing using innovative change detection techniques is that the interest in the field of forest

vegetation change detection and its monitoring is growing rapidly because the existence of human and natural world depends on forest. Accelerating deforestation in



Figure 1.3: Herd of animals grazing in El Rawashda Forest.

Photograph by the author, 2006



Figure 1.4: Gathering wood in El Rawashda forest

Photograph by the author, 2006



Figure 1.5: Charcoal production in earth-pit kilns in Gedarif

Photograph by Glover, 2005

Sudan threatens has a major global implications for biological diversity, altering the composition of the atmosphere and contributing to climate change. Studies revealed that deforestation releases about 17% of all annual anthropogenic greenhouse gas (GHG) emissions. Tropical deforestation releases large amounts of CO₂, because of the carbon stored in the vegetation and released when tropical forests are cut down (Gorte and Sheikh 2010). There are many causes of deforestation, in Sudan deforestation driven principally by energy needs and agricultural clearance (UNEP, 2007).

Remotely sensed data, because of the advantages of repetitive data acquisition and its digital format suitable for computer processing have become the major data source for forest change detection. Moreover, information derived from monitoring forests via satellite imagery is useful in identifying appropriate forest management strategies. Many methods have been devised to detect changes in forest biomass, with varying degrees of effectiveness. Efficient and effective methods of using remote sensing imagery to monitor forests are needed because they continue to be a paucity of good, practical examples of satellite remote sensing imagery used in detection of silvicultural, partial harvest, and natural forest changes (Franklin et al., 2002).

An analysis of the literature reviewed indicates that there are very few studies concerned with comparative evaluation of change detection techniques and the majority of these comparative studies have not supported their conclusion by quantitative analysis of the results (Mas, 2007), so the study also seeks to compare the relative effectiveness of different techniques in detecting land cover changes in an arid zone using images captured at different times.

1.4 Current status of research

Many researchers have used remotely sensed imagery to monitor land cover changes through time, for example (Mas 1999; Franklin et al., 2000, 2002a, 2002b; Fuller, 2001; Hansen et al. 2001; Sader, 2001). The use of satellite imagery allows researchers to inventory and study the state of vegetation in a large region, while reducing the need to be in the field. The results produced by remotely sensed imagery can provide valuable information to resource managers by aiding in the management decision making process (Franklin et al, 2002a). Forest managers are frequently interested in information regarding canopy changes caused by short-term natural phenomena, including insects, flood, drought, human activities, and reforestation (Coppin and Bauer, 1994).

Woodcock et al. (2001) produced a map of forest change in the Cascade Range of Oregon by applying a new approach to monitor large areas by extending the application of a trained image classifier to data beyond its original temporal, spatial, and sensor domains. The method showed accuracies comparable to a map produced with current state-of-the-art methods and their results highlighted the value of the existing Landsat archive and the importance for continuity in the Landsat program.

Desclée et al. (2006) developed a new method of change detection for identifying forest land cover change in temperate forests using three SPOT-HRV images covering a 10-year period. Combining the advantages of image segmentation, image differencing and stochastic analysis of the multispectral signal, this method is called object-based and statistically driven. They assessed the performances of this method using two sources of reference data, including one independent forest inventory and a pixel-based

method using the RGB-NDVI technique. High detection accuracy (>90%) and overall Kappa (>0.80) were achieved.

Kennedy et al. (2007) described and tested a new conceptual approach to change detection of forests using a dense temporal stack of Landsat Thematic Mapper (TM) imagery. They used Trajectory-based change detection for automated characterization of forest disturbance dynamics. The authors proposed that many phenomena associated with changes in land cover have distinctive temporal progressions both before and after the change event, and these lead to characteristic temporal signatures in spectral space, so instead of searching for single change events between two dates of imagery, they searched for these idealized signatures in the entire temporal trajectory of spectral values. The authors pointed that, this trajectory-based change detection is automated and has the advantages of requires no screening of non-forest area, and requires no metric-specific threshold development. More advantage is that, the method simultaneously provides estimates of discontinuous phenomena (disturbance date and intensity) as well as continuous phenomena (post-disturbance regeneration).

Masek et al. (2008), for the first time mapped the disturbance and early recovery of a forest across North America for the period 1990–2000 using the Landsat satellite archive. The detection was performed using the temporal change in a Tasseled-Cap (Disturbance Index) calculated from the two images. The authors used a sample of biennial Landsat time series from 23 locations across the United States for validation. Their results indicate disturbance rates of up to 2–3% per year across the US and Canada due to harvest and forest fire.

Mitchard et al. (2009) conducted a long-term (1986–2006) quantification of vegetation change in a forest–savanna boundary area in central Cameroon. They performed across-calibrated normalized difference vegetation index (NDVI) change detection method to compare three high-resolution images from 1986, 2000, and 2006. The result indicated that the largest changes were in the lower canopy cover classes whereas the higher canopy classes showed significant positive change. The authors attributed this due to a reduction in human pressure caused by urbanization, as rainfall did not alter significantly over the study period. They stated another possibility that increasing atmospheric CO₂ concentrations are altering the competitive balance between grasses and trees. The study proved that forest encroachment into savanna is an important process, occurring in forest–savanna boundary regions across tropical Africa.

Sakthive et al. (2010) precisely analyzed the trend of forest cover changes over the time span of 70 years, in the Kalrayan hills in India using satellite data acquired in 1931, 1971 and 2001. The forest cover, in the study area, during 1931 and 1971 were derived from the Survey of India top sheets of 1931 and 1971. The authors focused on the role of remote sensing and geographic information system (GIS) in assessment of changes in forest cover. Their results clearly proved that forest cover has increased between 1931 and 1971 and decreased between 1971 and 2001.

More recently, Bharti et al. (2011) reported an upward shift of timberline vegetation by 300 m in Nanda Devi Biosphere Reserve (NDBR). The detection performed by Panigrahy et al. in 2010, they detected timberline changes in the subalpine vegetation, using post classification comparison method. The authors managed to compare fir patches to see the changes in timberline vegetation. Bharti et al recommend use of Temporal Trajectory Analysis (TTA) for detecting changes due to different phenol-

phases and suggest large scale mapping of major vegetation categories using remote sensing and ground truth verification so that to detect minor vegetation change more accurately.

Experiences from El Rawashda are quite obvious and consistent with the findings of Yacouba (1999), Wily (2003), and FAO (2002 b). These previous studies pointed out that weak and insecure property rights over land shortens the time-frame used by farmers, making it less likely that to take measures against land degradation and this will achieve a return in the planning horizon of the land user. The earlier investigations emphasized that where the occupier of land is unsure of the future, extraction will occur to ensure that these resources are not lost to the individual. A farmer with clear title to the land is more likely to consider investment of money, labour and land in conservation, because benefits in production which may only accrue after many years will still be retained by the individual who implemented the measures.

In Sudan, there are long-term processes evident in the loss of forestry in the last three decades. The (UNEP)'s Post Conflict Environmental assessment of Sudan (2007), stated that northern, eastern and central Sudan have already lost the great majority of their forest and estimated that deforestation in Darfur has lost more than 30 percent of its forests, the study also confirmed that south Sudan has lost some of its forests especially around major towns such as Malakal, Wau and Juba. The effects of these processes on the availability of fuel wood are stark, with significant scarcity across large parts of Darfur. In addition to the local demands, UNEP estimates that within five to ten years the northern states may totally depend on west of Sudan for charcoal aggravate local conflict to control natural resources. Monitoring of forestry in the country therefore should be made at national level rather than regional level.

1.5 Objectives

The general objective of the research is to develop a monitoring scheme for operational use to allow assessment, mapping and evaluation of forest cover and its changes for sustainable management.

In addition to the general objective, the research has formulated primary and specific objectives.

The primary objective was to evaluate the potential for monitoring forest change in El Rawashda forest, Sudan, using Landsat ETM and Aster data. This was accomplished by performing eight change detection algorithms: pixel post-classification comparison (PCC), image differencing of Normalized Difference Vegetation Index (NDVI), Soil-Adjusted Vegetation Index (SAVI), Transformed Difference Vegetation Index (TDVI), Principal component analysis (PCA), Multivariate alteration detection (MAD), Change Vector Analysis (CVA) and Tasseled Cap Analysis (TCA). Another principal objective of this project was to compare the results, qualitatively and quantitatively, of these different land use and land cover change detection approaches.

The specific objectives were to:

1. Develop an appropriate classification system to represent the forest cover according to the existing management plan.
2. Determine the appropriate methods to detect vegetation change.
3. Perform these types of change-detection methods to map the changes in vegetation in El Rawashda forest.

4. Perform an accuracy assessment on the change-detection methods and
5. Compare the change-detection methods in order to select the best one that detects changes between two consecutive years. The selected algorithm will be used to produce the land cover change maps that will permit the efficient thematic updating.

1.6 Structure of the thesis

The research has assessed and evaluated the forest cover and its changes in the study areas of El Rawashda forest, Sudan using multitemporal Landsat and Aster imagery of the years 2000, 2003 and 2006 respectively.

The present research is elaborated in six chapters.

The Introduction (Chapter 1) opens the main research topic of this study through a short definition of change detection and outlines some of the most commonly used changed detection techniques. Chapter 1 further highlights the problem statements by introducing the opportunities and constraints of using remote sensing nature conservation in ecosystem monitoring in general. The main objectives and sub-objectives which facilitate the task of achieving the higher goal are also narrated in this chapter. The chapter further describes the structure of the study.

Chapter 2 reviews existing change detection methods developed or applied over forest ecosystems. Focused on techniques using high resolution satellite images, these techniques were grouped into three different categories of change detection approaches including visual interpretation, pixel-based and object-based methods. These approaches are divided into steps for assessing their assets and weaknesses and screening out appropriate elements for the development of forest change detection.

Chapter 3 introduces the study area (El Rawashda forest, Sudan), its physical characteristics (location, area, climate, vegetation, topography and soil), its social and land use characteristics. The chapter further illustrates the various data sets used in the study. Landsat 7 Enhanced Thematic Mapper (ETM) data acquired on March 22, 2003, (ETM) data acquired on May 29, 2000 and Aster data acquired on February 26, 2006 were used for analyzing an area covering approximately 1.101.789 km² as area of interest.

Chapter 4 describes in details the methods employed in achieving the objectives and addressing the research motivations. These methods are: supervised change detection using pixel post-classification comparison (PCC), image differencing of different vegetation indices (Normalized Difference Vegetation Index NDVI, Soil-Adjusted Vegetation Index SAVI and Transformed Difference Vegetation Index TDVI), principal component analysis (PCA), multivariate alteration detection (MAD), change vector analysis (CVA) and tasseled cap analysis (TCA).

Chapter 5 presents the various outputs and their analysis. This chapter illustrates all tested techniques used to map land cover changes over time. Simple differencing techniques and change vector analysis and multivariate alteration detection help to pinpoint the relevant changes and provide a significant basis for the analysis. Supervised change detection post-classification comparison enables to interpret and quantify the changes. This chapter further performs an accuracy assessment on the change-detection methods to compare these methods in order to select the best one

that detects changes. The selected algorithm was used to produce the land cover change maps that will permit the efficient thematic updating.

Chapter 6 and Chapter 7 the final chapters of the thesis, summarize the work, draws conclusion and provides discussion of the results and their relation with other studies.

2 Review of forest change detection techniques

This chapter reviews the literature on the techniques for forest change detection using satellite imagery. Given that the methods are becoming more numerous and complex, we displayed a categorization to summarize the different approaches from visual interpretation to pixel-based and object-based methods. The different techniques are described and compared in order to assessing their assets and weaknesses and screening out appropriate elements for the development of forest change detection.

2.1 Introduction

From the beginning of earth observation systems, different satellite remote sensing systems and techniques have been developed for different forest ecosystem and resource requirements using high resolution optical remote sensing. These techniques are focused on the identification of forest cover change, described by Geist (2006), including forest clearing, the spatial extent of forest cover, forest type and disease. Different reviews have been proposed in the literature for summarizing and comparing these different approaches (Singh, 1989; Coppin and Bauer, 1996; Lu et al., 2004b; Coppin et al., 2004). However, new change detection methods are still designed and with the recent improvement in image segmentation applications, change detection approaches are grouped into three categories: (1) visual interpretation, (2) pixel-based and (3) object based methods.

2.1.1 Image acquisition

The essential aspect for change detection is selection of the appropriate satellite images. Recently with the development of earth observation systems, much variety of satellite data is now available. High resolution optical data provide a detailed view of forest depletion. This category includes satellite imagery acquired from sensors such as SPOT-HRVIR, Landsat TM or ETM, IRS-LISS and ASTER which have a spatial resolution from 5 to 30 m. New sensors, i.e. DMC, can acquire high resolution data (32 m) over a wide swath (600 km per orbit) which makes it well adapted for large-scale change detection (Collins and Woodcock, 1999).

There have been few global modeling studies dealing with the impact of temporal frequency on forest change detection. Wilson and Sader (2002) recently proposed an image overlay technique based on band ratios like NDVI and normalized difference moisture index (NDMI) rather than spectral bands and applied this technique to temperate forests in Maine. They concentrated their discussion on the accuracy using both indices and they found that NDMI worked better than NDVI. High accuracies in classification were reached especially on the shorter time intervals (two or three years) and even in application of the same method to tropical rainforests., Jin and Sader (2005a) discriminated clear-cut which can be detected with image acquisition interval up to 5 years from small harvest requiring one or two years interval. Comparing change detection results using 3, 7 and 10-year intervals for detecting clear-cut, Lunetta et al. (2004) found that 3-year interval between image acquisition provides more accurate results applied on tasseled cap brightness and greenness.

2.1.2 Pre-processing

All change detection process depends on the quality of satellite images to detect land-cover change. This quality is ensured by several pre-processing steps which include (1) geometric correction, (2) radiometric and atmospheric correction, and (3) masking.

Satellite sensor imagery; usually suffers from geometric distortions due to many factors which include: radial symmetric distortion, earth curvature, atmospheric refraction and relief displacement in the sensor's field of view. Accurate geometric correction is essential for a proper spatial correspondence of multi-date images. Misregistration error must be <50 % of the pixel size to produce accurate detection. Random distortions can be reduced by measuring the shift of ground control points (GCP), distinctive geographical features of known location on the image, and re-sampling or re-forming the original image to a new one accordingly. Digital Elevation Model (DEM) becomes more popular and is required since parallax effect is of the same order of magnitude as the pixel size. The higher spatial resolution and the advanced capabilities of recent sensors have increased this effect thus rendering more complex its correction. New automated image registration procedure is still under investigation but until now, such system has not reached the high precision required for performing change detection (Descl'ee, 2007).

Radiometric corrections are of two types, absolute correction and relative correction; these two types are mainly used to normalize multi-temporal remotely-sensed images for time-series comparison. (Schott et al., 1988). Absolute radiometric correction involves extracting and converting the digital number (DN) recorded by the sensor to spectral radiance detected by the sensor using sensor-specific calibration parameters. This method requires the input of simultaneous atmospheric properties and sensor calibration, which are difficult to acquire in many cases, especially in historic data. Relative radiometric correction is aimed towards reducing atmospheric and other unexpected variation among multiple images by adjusting the radiometric properties of target images to match a base image, thus it is also called relative radiometric normalization. Relative radiometric normalization is an image-based correction method that uses a base image to adjust the radiometric properties of other images with the expectation of reducing atmospheric influences and other external variation among multiple images. In this method, reflectance of invariant targets with in multiple scenes can be used to render the scenes to appear as if they were acquired with the same sensor, with the same libration, and under identical atmospheric conditions, without the need to be absolutely corrected to surface reflectance. Most relative methods assume that radiometric relationships between the target image and the base image are linear (Song et al., 2001). The linear normalization function is defined by visual interpretation of the density ridge. Canty et al. (2004) developed an automatic normalization method instead of selecting Pseudo Invariant Features visually, based on Multivariate Alteration Detection (MAD) (Nielsen et al., 1998). For characterizing early succession forest patterns, the automatic normalization method of Canty et al. (2004) was found efficient for reducing the differences between multitemporal images (Schroeder et al., 2006).

2.2 Visual interpretation

Visual interpretation using single or multi-date images needs human expertise for detecting and labeling areas that are considered as changed. With visual interpretation one can make full use of an analyst's experience and knowledge. The criterion for

identification of an object with interpretation elements is called an interpretation key. The image interpretation depends on these elements. The interpretation key are, texture, shape, size and patterns of the images. (Lu et al., 2004b). Although this technique is time-consuming and requires skilled analysts, visual interpretation is still widely used (Anttila, 2002; Asner et al., 2002; Franklin et al., 2000; Sunar, 1998). So far, it is not possible to detect land cover changes made by the combination of several factors such as the stage or change in the area size with automatic change detection algorithm (Büttner et al., 2002).

2.3 Pixel-based methods

Digital pixel-based methods aim to analysis the remote sensing image according to the spectral information in the image and offer repeatable procedures for detecting land cover change. These approaches are referred as pixel-based methods given that every pixel is compared from one date to another independently from their neighbours. Each pixel-based method is characterized by a specific combination of three key steps, namely single-date indices, multi-date transformation and change detection algorithms (Lillesand, 2001).

2.3.1 Single-date indices

Single-date indices are derived from each satellite image of the multi-date data set. The single-date indices highlight the absence of temporal information at this stage. Single-date indices include either the reflectance of the different spectral bands or a combination of both, or also the result of single date land-cover classification. In change detection, a combination of different spectral bands into indices mostly is preferred instead of directly analyzing reflectance values for different reasons. First, it reduces data redundancy between spectral bands and processing time for the analysis due to data volume reduction. Second, it facilitates the direct interpretation of the change types. However, it is important to first assess the expected improvement using these indices instead of individual spectral bands. Required for the post-classification comparison, land-cover classification can also be considered as a single-date index (Sader et al., 2001). Finally, single-date indices can be summarized in six groups: (1) Spectral reflectance, (2) Vegetation index, (3) Principal component, (4) Tasseled cap component, (5) Spectral Mixture Analysis and (6) Land-cover classification.

2.3.1.1 Spectral reflectance

Spectral reflectance is the primary source of data for change detection. Many techniques directly use reflectance value from the different spectral bands, but only few studies have compared the contribution of each spectral band in change detection performances. Lu et al. (2005) found that the Short-Wave Infrared (SWIR, Landsat TM5) band provided the best change detection results, followed by the Red band (Landsat TM3) for land-cover changes in tropical regions. In the other side it has been noted that the utility of pixel classification of spectral reflectance for identifying areas of land modification, or land conversion is limited, as a result of various sources of error or uncertainty that are present in areas of significant landscape heterogeneity (e.g. forest silvicultural thinning). For urban areas, the complex mosaic of reflectance creates significant confusion between land-use classes that possess reflectance characteristics similar to those of land-cover types (Prenzel and Treitz, 2003).

2.3.1.2 Vegetation indices

Vegetation index reflects the approximation relation between the spectral response and vegetation cover. The essential characteristic of desertification is the lower the productivity of land. Changes in vegetation index can reflect the changing process of land productivity. Therefore vegetation index can be used as desertification monitoring indicators to monitor land desertification and dynamic changes (Kumar et al., 2010).

Vegetation indices are dimensionless calculations of radiometric measures of vegetation that function as indicators of relative abundance and activity of green cover, depending on the physical ability of vegetation (Jensen 2000). Vegetation indices based on reflectance factors of red and near-infrared bands. Vegetation indices heavily rely on the contrasting intense of chlorophyll pigment absorption and the high reflectance of leaf mesophyll in the red band and the near-infrared respectively (Maselli, 2004). The purpose of vegetation indices is to maximize sensitivity to plant biophysical parameters, normalize external effects for consistent temporal comparisons (e.g., sun angle and viewing angle), normalize internal effects (e.g., canopy background, topography, and soil), and be associated with some measurable biophysical (Jensen 2000).

Vegetation indices have been widely applied in change detection. The Normalized Difference Vegetation Index (NDVI) has been the most popular and the most commonly used index in change detection due to its close relationship with leaf biomass and its simplicity of computation and interpretation (Hayes and Sader, 2001; Michener and Houhoulis, 1997; Sader and Winne, 1992; Volcani et al., 2005). Heute (1988) proposed a vegetation index called soil adjusted vegetation index (SAVI) to overcome the limitation of NDVI and so it is intended to minimize the effects of soil background. Incorporating a constant soil adjustment factor L into the denominator of the NDVI equation minimizes the effect of soil background on the vegetation signal. L varies with the reflectance characteristics of the soil, e.g. color and brightness. Apparently the problem is more common in semi arid and arid environments where the green canopy cover is less than 30% (Schmidt and Karnieli, 2001). Another vegetation index, the Normalized Difference Moisture or Water Index (NDMI or NDWI), is more sensitive to changes in water content (Hardisky et al., 1983). This last index was found less affected to atmospheric effects than NDVI (Gao, 1996). Wilson and Sader (2002) found better accuracy using NDMI than NDVI for detecting forest harvest. Other studies have combined several vegetation indices in order to improve the detection capability (Coppin et al., 2004). Various indices have been developed but no single vegetation index can be considered as better than the others in all change detection cases (Lyon et al., 1998; McDonald et al., 1998). However, by reducing data redundancy, vegetation indices can also be less sensitive for detecting vegetation changes than the original reflectance values (Chavez and MacKinnon, 1994; Lu et al., 2005)

2.3.1.3 Principal Components

Principal Components (PCs) are obtained by linear transformation of spectral bands into a new coordinate system. Principal Component Analysis (PCA) reduces the number of channels and increases the information content on a single RGB image. To monitor the degraded areas caused by gold miners, Almeida-Filho and Shimabukuro (2002) applied a PCA separately on each of the 6 Landsat TM images. The third PC of each image was selected for performing the change analysis due to the enhancement of degraded areas relative to surrounding savanna vegetated terrain. According to

Cakir et al. (2006), the first Principal Component (PC1) corresponds to sharp contrast between vegetation and non-vegetation features.

Many studies have used principal component analysis to detect change and attained satisfied results (Byrne et al., 1980, Duggin et al., 1986, Sunar, 1998, Li and Yeh, 1998). Sunar (1998) characterized principal component analysis as very useful for highlighting differences distinctly attributable to changes. Li and Yeh (1998) compared principal component analysis to post classification techniques and concluded that principal component analysis was much more accurate than post classification techniques and therefore suggested it as an accurate alternative for detecting land use change. Fung and LeDrew (1987) found that the eigenvectors used for rotation could vary significantly depending upon whether the standardized or non-standardized form was chosen, as well as whether the whole data set or a subset was used for generating the eigenvectors. They suggested that the eigen structure derived from the entire data set is more valid for land cover change detection. On the other hand many studies using principal component analysis have produced rather poor results. Toll et al. (1980) reported that the use of principal component analysis for urban change detection produced poor change detection results compared to simple image differencing of Landsat MSS bands 2 and 4. Fung (1990) compared principal component analysis to differencing of both the raw images and Tasseled Cap transformations and found that both techniques were not able to detect all types of land cover change in the tested study area.

2.3.1.4 Tasseled cap components

Tasseled cap transformation was developed by Kauth and Thomas in 1976 for Landsat MSS data (Kauth & Thomas, 1976) and was improved and extended to Landsat TM data in the mid-1980s by Crist and Cicone 1984. Tasseled cap transformation is a kind of orthogonal transformation; it rotates the original data plane so that the vast majority of data variability is concentrated in the features (Kauth & Thomas, 1976; Lillesand & Kiefer, 1994). The first and second features of TM are brightness and greenness, respectively. The third feature is termed “wetness” because it is sensitive to soil and plant moisture (Crist & Cicone, 1984). The TCT have been used in several change detection studies (Jin and Sader, 2005a; Franklin et al., 2002; Lunetta et al., 2004; Healey et al., 2005) and more recently the method had been applied by Zhang and Ban, 2010 who conducted detection of impervious surface sprawl using tasseled cap transformation within the conceptual framework of Vegetation-Impervious surface-Soil (V-I-S) model.

2.3.1.5 Spectral Mixture Analysis

In spectral mixture theory, the signal recorded for a pixel is assumed to be a mixture of the radiances of the component endmembers contained within that pixel. Knowing or deriving spectrally pure endmembers of all the components within a pixel allows one to quantify the endmember fractions occurring within the pixel using linear or nonlinear mixture approaches (Sabol et al., 2002).

In recent years, spectral mixture approaches with remote sensing data has rapidly progressed. Many Studies derive land cover component fractions via sub pixel interpretation (García-Haro et al., 1996). IKONOS imagery had derived endmember information of urban areas using spectral mixture analyses (Small, 2002) and also it has been used to derive component fractions within ETM+ pixels instead of using ground truth data (Yang & Huang, 2002). Asner et al., 2003; Greenberg et al., 2005; Lu

et al., 2004 detected changes by comparing the endmember proportions between multitemporal images and they concluded that, this approach can detect finer changes but the critical steps of SMA are the time consuming selection of reference end members which can be derived either from the image or from the field.

2.3.1.6 Classification

Classification is the most appropriate and logical approach for predicting target class for each case in the data (e.g. forest cover classes) of an observation (pixel), based on its intrinsic traits (measurement vector of spectral band responses) (Franklin et al., 2003). Supervised classification requires prior knowledge about the spectral properties and/or the statistical nature of the categorical classes to be determined (Mather, 1987) or access to ancillary data, which can be used to build spectral statistics.

Knowledge about the spectral information is sometime derived from fieldwork, aerial photo interpretation or from the study of appropriate large scale maps. Supervised classification procedure allows the analyst to predict the classification process. A priori selection of categorical classes, analyses of training site statistics, specification of sampling approaches and of training site geometry are possible with the supervised classification (Franklin et al., 2003).

Classification can be carried independently on each image to convert it into thematic map for advance comparison. The process can be performed by different ways (unsupervised or supervised) from simple algorithm (e.g. maximum likelihood) (Currit, 2005; Petit et al., 2001) to more advanced classifiers such as Artificial Neural Networks (ANN) (Gopal and Woodcock, 1996) or fuzzy classification (Deer, 1998). This process provides detailed land-cover information, however its application on each image is region-specific.

2.3.2 Multi-date transformation

The multi-date transformation is an intermediate step in the change detection process for combining the spectral and temporal information from all satellite images. Different techniques can compare images acquired at different dates for producing multi-date change index analyzed by the change detection algorithm. These transformations include (1) Image differencing, (2) Change vector analysis, (3) Multitemporal principal component analysis, (4) Multitemporal Kauth-Thomas transformation, (5) Multivariate alteration detection, (6) Chi square transformation.

2.3.2.1 Image differencing

Due to its simplicity image differencing is a popular method for change detection. When appropriate radiometric and atmospheric corrections have been applied, the distribution mean tends to zero. Image differencing is a point-to-point operation where the indices (instead of raw pixel values) are subtracted from one another. Index differencing negates the effect of multiplicative factors acting equally in all bands such as topographic effects and temperature differences (Lillesand and Kieffer, 1987) and has the advantage of emphasizing differences in spectral response curves. The main disadvantage with index differencing is that it can enhance random or coherent noise not correlated in different bands (Singh, 1989).

The differencing is generally performed on vegetation indices (Coppin et al., 2004; Jin and Sader, 2005a; Lyon et al., 1998) or tasseled cap components (Coppin et al., 2001; Jin and Sader, 2005a). Other studies have subtracted the PC1 from the two images

(Cakir et al., 2006; Lu et al., 2005). Image differencing can be also applied on endmember fraction images derived from SMA (Lu et al., 2004a; Rogan et al., 2002). Image differencing usually it is not applied on all spectral bands due to the difficulty of combining the change detection results from each difference band. Lu et al. (2005) compared the performance of each spectral band using image differencing as well as the combination of them by a majority rule. They concluded that change detection using the combination of all spectral bands provided the best accuracy, even better than based on NDVI.

2.3.2.2 Change vector analysis

Change vector analysis (CVA) is one of the most useful radiometric techniques for change detection. However, the method is a promising tool for determining changed category when deciding how to reasonably determine thresholds of change magnitude and direction (Zhu et al., 2010).

The CVA method was first developed by Malila (1980) using Brightness and Greenness layers for detecting changes in northern Idaho forests. The technique is flexible enough to be effective when using different types of sensor data and radiometric change approaches (Johnson and Kasischke, 1998). The process measures the displacement of a pixel from date-1 to date-2 in the multidimensional space defined by the different spectral bands. Two outputs are derived from each change vector: the magnitude and the direction of the vector. The magnitude, calculated by the Euclidean distance between the two positions, measures the intensity of the change in surface reflectance. The direction, depending on the relative values of the axis coordinates, gives information about the type of change (Michalek and Wagner, 1993).

Change direction is measured as the angle of the change vector from a pixel measurement at time 1 to the corresponding pixel measurement at time 2 (Figure 2.1a). The decrease in brightness is indicated by angles measured between 90° and 180°. Lorena et al. (2002) stated that, this change direction represent regeneration of vegetation. The increase in brightness is indicated by angles measured between 270° and 360°. They designated this change direction to represent loss of vegetation. Angles measured between 0° and 90° and 180° and 270° indicate either increases or decreases in both bands of greenness and brightness. They designated this as indication of no change, which is representative of neither an increase nor decrease in vegetation (Figure 2.1 b).

The extension of CVA to three input bands required an appropriate definition of change direction angles. Extended CVA techniques measured absolute angular changes and total magnitude of tasseled cap components (Brightness, Greenness, and Wetness) (Allen and Kupfer, 2000 and Nackaerts et al., 2005). Finally, CVA technique was also applied over all spectral bands only for deriving the change magnitude (Häme et al., 1998).

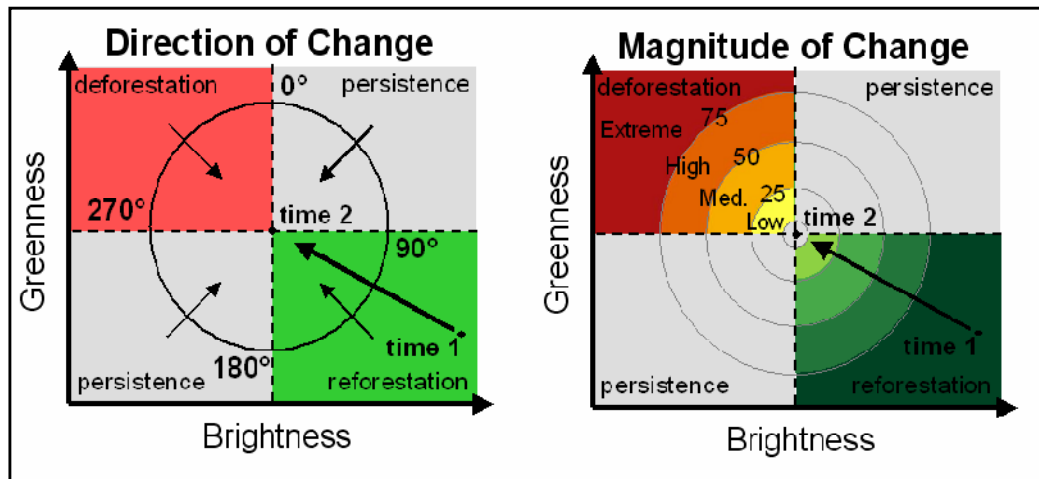


Figure 2.1: The process for detecting the direction of change (a) and the magnitude of change (b) within change vector analysis

Source: Kuzera et al., 2005

2.3.2.3 Multitemporal principal component analysis

Principal component analysis (PCA) is a linear transformation technique related to Factor Analysis. It produces a new set of images from a given set of original image bands, the new set of images, known as components that are uncorrelated and are ordered in terms of the amount of variance explained in the original data. Most commonly, principle component transformations are designed to remove or reduce redundancy in multispectral data by compressing all the information contained in the original *n-channel* data into fewer than *n* –new channels or components (Fung and LaDrew, 1987). The new components are then used instead of the original data because the new component images are more interpretable than the original images. Geometric interpretation of PCA is shown in figure 2.2.

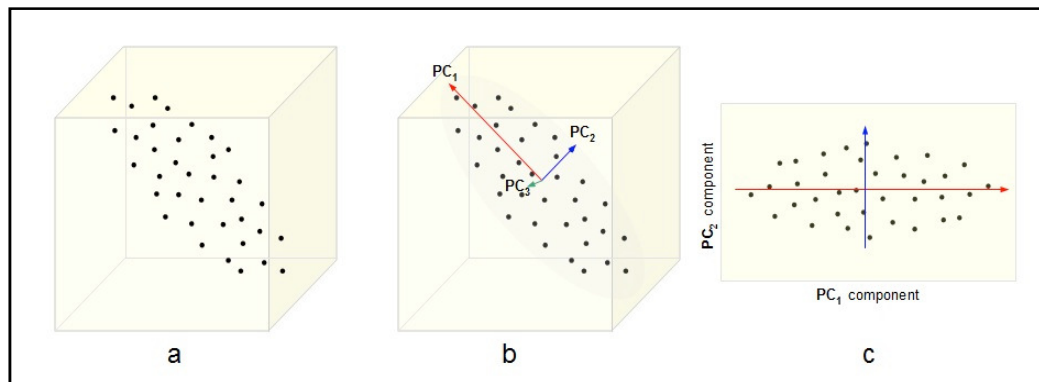


Figure 2.2: Geometric interpretation of principal component analysis

Source: www.dgp.toronto.edu/~aranjan/tuts/pca.pdf

The Multitemporal Principal Component Analysis (MPCA) is based on the same principle as the PCA described in Section 2.3.1.3 except that it is applied on the complete multi-date data set. It is expected that one or more multitemporal principal components to be directly related to land cover changes (Byrne et al., 1980). The main difficulty of this approach is the selection of the components of interest which is mainly done by visual interpretation (Michener and Houhoulis, 1997).

The Selective principal component analysis is based on the concept that using only two bands as inputs, so the information that is common to both bands will be mapped to the first component, and information that is unique to either band will show up in the second component. This also makes the imagery much easier to interpret, since the relevant output of the procedure is a single grey tone image (Kwarteng and Chavez, 1998)

2.3.2.4 Multitemporal Kauth-Thomas transformation

Multitemporal Kauth-Thomas (MKT) transformation is the generalization of the Kauth-Thomas transformation for multi-date data (Collins and Woodcock, 1996). The MKT approach produces six main components from a multi-date dataset including the mean (the stable components) and the difference (the change components) of the three tasseled cap components between the two images. Combined with image differencing, the MKT approach was found superior to MPCA due to the physically-based variables produced by MKT compared to the image-dependent components derived by PCA (Rogan et al., 2002).

2.3.2.5 The Multivariate Alteration Detection

Multivariate alteration detection (MAD) method is based on canonical components analysis (CCA). According to MAD method, two images acquired at different times and covering the same geographic area are taken as two sets of random variables, then by applying MAD transformation a new set of variates, called MAD variates which are uncorrelated with each other. In this way, actual changes in all channels can be detected by removing as much as possible correlations between channels (Zhang Lu, 2004).

The MAD was applied by Canty et al. (2004); Nielsen et al. (1998), using traditional canonical correlation analysis (CCA) which proposed by Hotelling, 1936 to find linear combinations between two groups of variables ordered by correlation, or similarity between pairs. One of the main advantages obtained by using MAD is the automatic identification of "no change pixels". Moreover, basic data come from the same image, uncorrelated with changes in the overall atmospheric conditions or statistic image noise. In MAD process, the no-change thresholds can be set easily, because the standardized MAD components are approximately chi square distributed (Schroeder et al., 2006). The MAD components have maximum variance in its pixel intensities, so that the pixels are statistically uncorrelated with each other. The last MAD component has maximum spread in its pixel intensities and, ideally, maximum change information. The second-to-last component has maximum spread subject to the condition that the pixel intensities are statistically uncorrelated with those in the first MAD component, and so on (Canty et al., 2003).

Figure.2.3 summarizes the procedure of the MAD transformation of medium resolution images for change detection. Two sets of registered data with N spectral channels are thresholds.

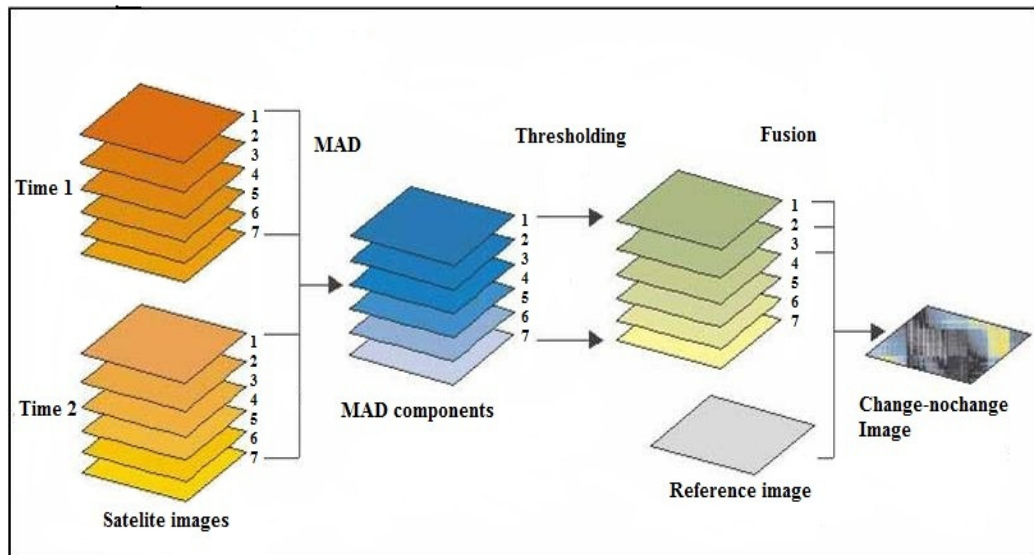


Figure 2.3: MAD procedure

Source: Niemeyer and Canty, 2002

This method has been successfully applied to multispectral images by Niemeyer et al., 1999, Canty and Niemeyer, 2002 and more recently by Crocetto and Tarantino (2009) who applied the method because of its high level of automation and reliability in the enhancement of change information among different images.

2.3.2.6 Chi square transformation

The strong point of the chi-squared is that it can be used to test if a data sample belongs to a process with a determined distribution (Tarongi and Camps, 2010). The Chi square transformation is a test for combining all spectral bands of image difference into one single change image. The change index is obtained by computing the distance between the difference value of each pixel and the difference mean for all pixels in the multidimensional space defined by the number of spectral bands. This method is based on the assumption that only a small proportion of the image is changed. A disadvantage of this technique is that change observed in a specific spectral band might not be readily identified in the change image but its flexibility allows its application over various environments (Ridd and Liu, 1998).

2.3.3 Change detection algorithms

A basic change detection algorithm takes the image sequence as input and generates a binary image called a change mask that identifies changed regions (Pacifi, 2007). The goal of a change detection algorithm is to detect significant changes while rejecting unimportant ones. Sophisticated methods for making this distinction require detailed modeling of all the expected types of changes (important and unimportant) for a given application, and integration of these models into an effective algorithm. These algorithms which include post-classification comparison, thresholding and classification make the final decision for distinguishing change and no-change features. Preliminary

steps were only required for optimizing the input data for the algorithm in order to better discriminate change classes. Whereas thresholding only gives a binary change/no-change response, post-classification comparison and classification provide information about the change types (Radke et al., 2004).

2.3.3.1 Post-classification comparison (PCC)

The most widely used change detection algorithm is the post classification comparison which detects changes between hand-labeled region classes (Currit, 2005; Deer, 1998; Gopal and Woodcock, 1996; Miller et al., 1998; Petit et al., 2001). This technique provides detailed change trajectories between the two images. Moreover, the independent classification processes reduce the impact of multitemporal effects due to atmosphere or sensor differences (Lu et al., 2004b).

Post classification comparison performs change detection by comparing the classification maps obtained by classifying independently two remote sensing images of the same area acquired at different times. In this way, it is possible to detect changes and to understand the kinds of changes that have taken place. Moreover, the classification of multitemporal images does not need to normalize for atmospheric conditions, sensor differences, between the acquisitions. However, the performances of the PCC technique essentially depend on the accuracies of the classification maps. In particular, the final change detection map shows an accuracy close to the product of the accuracies yielded at the two times (Yuan, 1998). This is due to the fact that PCC does not take into account the dependence existing between two images of the same area acquired at two different times (Pacifi, 2007).

2.3.3.2 Thresholding

For many approaches relying on direct multi-date analysis, a critical step is the selection of appropriate threshold boundaries between change and no-change pixels (Franklin et al., 2002; Greenberg et al., 2005; Häme et al., 1998; Jin and Sader, 2005a; Skakun et al., 2003). Given that threshold values are scene-dependent, they should be calculated dynamically based on the image content. However, the thresholds can be determined by three approaches: (1) interactive, (2) statistical and (3) supervised. In the first approach, thresholds are interactively determined visually or by trial and error tests. The second approach is based on statistical measures from the histogram of multi-date change indices. Using image differencing, the threshold selection is commonly based on a normal distribution characterized by its mean m and its standard deviation σ . Values outside the level of confidence determined by $[m - x\sigma, m + x\sigma]$ are considered as changes, where x is the number of standard deviations from the mean determined a priori. Third, the supervised approach derives thresholds based on a training set of change and no-change pixels. Techniques for selecting appropriate thresholds are based on the modelling of the signal and noise (Radke et al., 2005; Rogerson, 2002; Rosin, 2002). Whereas thresholds are usually set at equal distance from the change index mean, Cakir et al. (2006) proposed to find different and optimal values for low-end and high-end thresholds.

Bruzzone and Pireto (2000) proposed two automatic techniques based on the Bayes theory for the analysis of the difference image. The first technique allows an automatic selection of the decision threshold that minimizes the overall change detection error probability under the assumption that pixels in the difference image are spatially independent. In the hypothesis of Gaussian distribution for changed and unchanged classes, the estimation of the parameters of the Gaussian model is carried out using

the Expectation Maximization (EM) algorithm. The other technique analyzes the difference image using a Markov Random Field (MRF) approach that exploits the inter-pixel class dependency in the spatial domain by considering the spatial contextual information included in the neighborhood of each pixel to improve the accuracy of the final change detection map according to the use of a regularization term (Pacifi, 2007).

2.3.3.3 Classification

Classification is the direct analysis of the multi-date dataset for detecting and characterizing areas of change. The multi-date dataset can be either the different single-date indices stacked together (Jolly et al., 1996; Sader et al., 2001; Woodcock et al., 2001) or the change indices derived from the multi-date transformation (Cohen and Fiorella, 1998; Lunetta et al., 2004; Rogan et al., 2002). Change is expected to show statistics significantly different from no change, so that they can be grouped in specific classes. Like for single-date classification, different methods have been used for multi-date classification going from common algorithm (Cohen and Fiorella, 1998) to more advanced classifiers such as decision trees (Rogan et al., 2003) and ANN (Woodcock et al., 2001). Sader et al. (2001) have stacked the NDVI of 3 dates in a red, green and blue composite to perform an unsupervised classification. This specific multi-date classification denoted as RGB-NDVI avoids the need of setting a predefined histogram threshold, but it requires training sample data to label classes.

2.4 Object-based methods

Recently, object based approach have been performed to detect forest change Combining analysis of visual interpretation with the quantitative aspect of the approach based on the pixels. Instead of analyzing pixels independently of their location, the object approach combines the similar adjacent pixels into one object. At the outset, object border specified by forest stand striation vectors were derived from a Geographic Information System (GIS) (Rosin, 2002). The interest for object-based methods has increased with the improvements in image segmentation techniques. Objects are first extracted from each image to be analyzed and a site model is constructed containing image segmentation maps and extracted object features, then, Object-level Change Detection (OLCD) is accomplished by comparing objects extracted from a new image to objects recorded in the site model and the differences are highlighted. Image segmentation is the division of the satellite image into spatially continuous and homogeneous regions, hereafter named as objects. The most important advantage of object-based approaches is the integration of contextual information in the change analysis (Desclée, et al., 2006). Furthermore, the segmentation reduces the local spectral variation inducing better differentiation between the types of land cover. However, despite the fact that the demarcation of the object remains conclusive; a limitation is the definition of a Minimum Mapping Unit (MMU). Defined initially to control the visual interpretation process (Saura, 2002), this parameter determines the minimum size of the object as calculated by the number of pixels included. Thus, change areas smaller than this constraint cannot be detected by analyzing the change (Radke et al., 2004).

The technique performed by the software eCognition shows some fundamental differences compared with other techniques (pixel-based) that perform traditional image analysis. An essential part of the system rules is the invention of new technology to extract knowledge from image object primitives in various resolutions,

the so-called multi-resolution. The segmentation functions as a measure of improvement heuristic, which reduces the heterogeneity of the average image of the objects for a particular resolution on the whole scene. The goal is to build a hierarchical network of image objects in which fine objects are sub-objects of coarser structures. Because of the hierarchical structure, data is represented at one time in the form of various resolutions. Each object knows its context, its neighborhood and its sub-objects. Subsequently, it is possible to identify the relationships between objects. The defined local object-oriented context information can then be used together with other (spectral, form, texture) image features to classify objects (Niemeyer and Canty, 2001). Fig. 2.5 summarizes the different steps in the object-oriented, knowledge-based analysis: multi-resolution segmentation, knowledge-based feature extraction, semantic modeling and classification.

2.4.1 GIS-data

Geographic information systems and remote sensing, updating represent an important tool to measure and display presentation of the various spatial and temporal information, allowing better knowledge of past, present, and long-term as result of human activities in ecosystems (Desclée, et al., 2006).

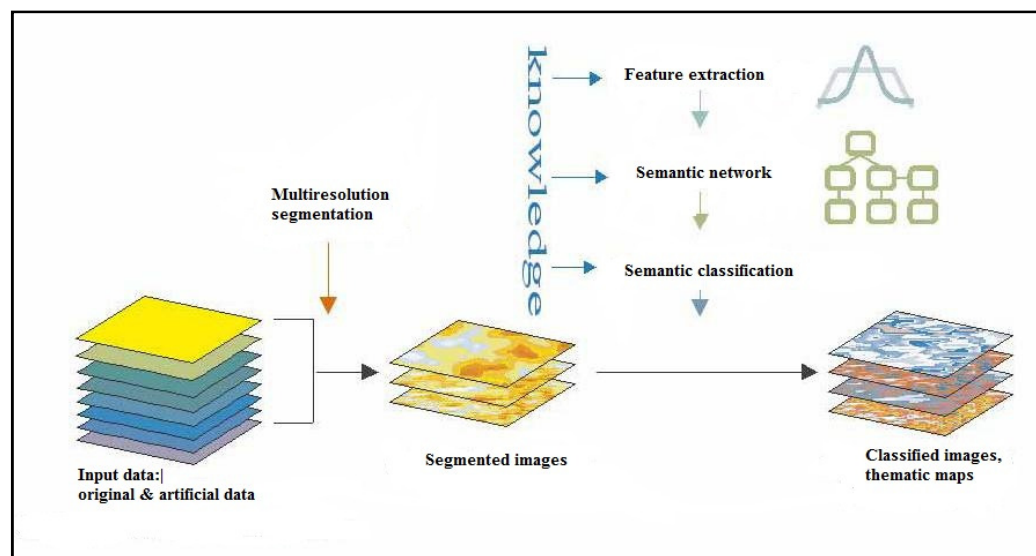


Figure 2.4: Object-oriented, knowledge-based analysis with eCognition

Source: Niemeyer and Canty, 2001

Map covered by forest geographical information system and database are important data in forest management planning field operations. The outcome of these geographic information and remote sensing data had been useful to minimize the spectral noise of pixel analysis and integrate shape and context aspects into parcel-based analysis. While forest stands delineation had been accompanied by satellite images, to map forest precisely. (Kayitakir'e et al., 2002), it has also been applied for detecting forest disturbances and updating forest information using multi-temporal image data set. Spectral information within each object defined by stand boundaries is summarized

and analyzed the change from different algorithms. The performance of this approach depends greatly on geometric accuracy of both data, in spite of its multisource information (Walter, 2004).

2.4.2 Image segmentation

Segments can be defined as areas that produced by one or more criteria of homogeneity in one or more dimensions and so they have additional and spatial information compared to single pixels (Hay and Castilla, 2008). It has been well known that the spatial dimension is crucial to object based image analysis methods, and that this is the main reason behind the rapid rise in the use of segmentation-based methods in recent years, compared to the use of image segmentation in remote sensing during the 1980s and 1990s (Gamanya et al., 2009).

In general terms, segmentation method could be interpreted as a collection of methods, which identifies groups of entities or statistical samples that share certain common characteristics. The sample characteristics are used to group the samples. Grouping can be arrived at, either hierarchically partitioning the sample or non-hierarchically partitioning the samples. Thus, segmentation methods include probability-based grouping of observations and cluster (grouping) based observations. It includes hierarchical (tree based method – divisive) and non-hierarchical (agglomerative) methods. Segmentation methods are thus very general category of methodology, which includes clustering methods also (Saksa et al., 2003).

The objects can also be directly delineated from satellite image thanks to image segmentation algorithms. Image segmentation is the division of satellite image into spatially continuous and spectrally homogeneous regions or objects. While many image segmentation algorithms have been developed in pattern recognition science for several decades (Pal and Pal, 1993), they were only rarely applied in remote sensing applications due to their complexity and difficulty to process large satellite images. Recently, such algorithms have been considerably improved and integrated in remote sensing (Soille and Pesaresi, 2002). Indeed, the analysis of very high resolution satellite images has required finding alternatives from traditional pixel based classification. These new tools now becomes adequate for many different operational applications in remote sensing but still rarely applied in change detection. Different segmentation algorithms exist and can be regrouped into two main categories, namely edge-based and region-based. Edge-based segmentation methods detect edges between different regions which sharply contrast and thus define objects delineated by these edges. These approaches are very numerous (Davis, 1975) and this provides the first step of detection. They generally rely on the computation of an intensity gradient and use edge detecting operators. Active contour models are a specific edge-based technique which adjusts arbitrary boundaries until it matches an object of interest (Kass et al., 1988). The segmentation process is repetitive by determining new groups at each iteration until all pixels are included into objects (Blaschke et al., 2004). Watershed algorithms are also region-based methods and effect the growth by simulating a flooding process, which progressively covers the region (Vincent and Soille, 1991). Some studies have combined region-based and edge-based techniques in order to improve their efficiency (Munoz et al., 2003).

Meinel and Neubert (2004) have qualitatively compared different existing segmentation tools provided in accessible software for remote sensing applications. They stated that much of the work referred to as object based image analysis originated around the software known as eCognition. eCognition was presented at various conferences in

1999 and 2000 and became available in 2000 as the first commercially available, object based, image analysis software (Benz et al., 2004). The eCognition software built on to the approach originally known as Fractal Net Evolution (Baatz and Schäpe, 2000) and developed into completely programmable workflows (Baatz et al., 2008). It is today known as Definiens produced high quality segmentation results which were also reproducible even if image size is modified (Lang and Tiede, 2007).

Change detection has still achieved very little applications using object-based approach while these segmentation tools have known a growing development in many other remote sensing applications. It becomes clear that the first years of the object based, image analysis developments were characterized by very little literature, but that the number of peer-reviewed journal articles has increased rapidly over the last four to five years. The pixel based analysis is beginning to show cracks and the object based image analysis methods are making considerable progress towards a spatially explicit information extraction workflow, such as is required for spatial planning as well as for many monitoring programmers (Blaschke, 2010).

2.5 Change mapping

Results from change detection include the change map and the derived area estimates. The change map is composed of categorical values which correspond to change classes. The number of classes can be limited to 2 classes (change and no-change) or extended to several change trajectories (the different “from to” classes). A transition matrix is produced by pixel-to-pixel matching of two land cover classifications and provides detailed change trajectories and their corresponding affected areas. The change representation is difficult given that change is generally rare and includes many change trajectories. Many change classes may thus cover a small portion of the study area. Moreover, many studies have pointed out the problem of noise in remote sensing data which induces strong “salt and pepper” effects in the change map. Indeed, each pixel is analyzed independently of its neighbours. Whereas recent studies propose to integrate spatial inter-pixel dependency in a post-processing step (Bruzzone and Prieto, 2000a; Nielsen et al., 1998), many change detection methods are still using filter to smooth out isolated change pixel.

The accuracy assessment of change map is crucial for evaluating the quality of change detection results. More complex than for classical thematic map, this procedure has to rely on specific statistical sampling designs and analysis technique (Biging et al., 1998). Except for the kappa coefficient, most accuracy indices are affected by the disproportion of reference data points for the change and the no-change category (Nelson, 1983). Fung and LeDrew (1988) also recommended kappa coefficient for determining optimal thresholds for change detection image. However, reliable change detection accuracy assessments are rather rare due to the difficulty of finding historical reference data and independent from the process of analysis. Finally, very few techniques have been designed for evaluating object-based change detection approach.

2.6 Method comparison

The comparison of change detection methods is rather complex for several reasons. First, each method focuses on specific changes of interest which are different from one study to another. Second, these approaches are based on different sets of satellite images having their own properties such as time interval and study region. Third, given that change indices are generally different from one study to another, change detection methods cannot be directly compared. Only few studies have quantitatively compared change detection methods. For detecting tropical forest clearing and re-growth on a 3-image dataset, highest performances were achieved using the multi-date NDVI classification, also called RGB-NDVI, compared to NDVI differencing and PCA (Hayes and Sader, 2001). With the recent complex techniques, change detection methods become more difficult to be indicator and results appear to be site and data-specific. The comparison is thus done by modifying only one step: the single-date index, the multi-date transformation, or the change detection algorithm. Comparing several change detection approaches for detecting forest changes, both Lu et al. (2005) and Nackaerts et al. (2005) clearly recommended to combine image differencing from all spectral bands for achieving the best results. Guild et al. (2004) have compared hybrid methods by changing only the multi-date transformation. Using tasseled cap components, the simple multi-date unsupervised classification was found better than the two other methods using multi-date unsupervised classification based either on multi-date PCA or on image differencing.

3 Study area and research data acquisition

3.1 Study area

3.1.1 Location of the study area

El Rawashda forest reserve, Gedarif State is situated at approximately latitude $14^{\circ} 15'$ N and longitude $35^{\circ} 45'$ E (figure 3.1). The official gazetted area is 27290 hectares. The State boarded by Kassala state to the north, Kahrtoom state to the northwest, Sinnar state to the south, Gezira state to the west and Eriteria to the east. Its average altitude is 600 meters above the sea level. The region under consideration is about 490 km from the capital Khartoum and 770 km from Port Sudan city, the main sea port of Sudan. Thus the region's geographical position is favorable to domestic and foreign trade (Omer, 1989). El Rawashda forest reserve lies in the semi-arid zone in the part of south central clay plains near to the transition between *Acacia mellifera* and *Acacia seyal-balanites* savannah woodland.

3.1.1.1 Topography

El Rawashda reserve forest is located in the part of the south central clay plains that slopes gently down from the basaltic Gedarif – Gallabat ridge at 650 m a.s.l. to the Atbara River. The elevation of El Rawashda forest is about 500 m a.s.l. The relief is very gently undulating, with slopes of 0.1- 0.5 percent (Eltayeb 1985; Vink 1987).

3.1.1.2 Geology

Underlying El Rawashda are non-out cropping tertiary basic volcanics, mainly basalts. Stoniness. Bedrock close to the surface is evident in just a few spots (Tohill, 1948). According to Laing (1953), the Characteristics for the reserve are the dark cracking clay vertisols formed on colluvio-alluvium derived mainly from basic rock.

3.1.1.3 Soil

The area is characterized by a semi-arid climate which is related to soils having dark colors, a high clay content and strong vitriolic properties. The area includes a large, rather uniform, clay plain intersected by small valleys. The clay content is very high and generally 75% to 80%. The color of the soils is very dark grayish brown. The organic matter and nitrogen content of the soil are low but as there is no deficiency of other plant nutrients, the soils are moderately fertile. The water holding capacity of the soil material is very high. This, in combination with the deep penetration of water in the soil through the vertisolic cracks, causes the available water holding capacity of the soil to be very high. This high water holding capacity allows crops to grow on stored water during dry spells and long after the rainy season. The soils also have undesirable physical characteristics, such as a low permeability when wet, causing soils in water receiving sites to be waterlogged for certain periods during the rainy season. Also, the soils are difficult to cultivate as they are very hard when dry and very sticky and plastic when wet, causing the moisture range at which the soils can be cultivated to be very narrow. Thus, mechanization of the land preparation operation is critical to work in this narrow time frame. In fact, without mechanization, it would be impossible to develop these vast areas of vertisols (Vink, 1987).

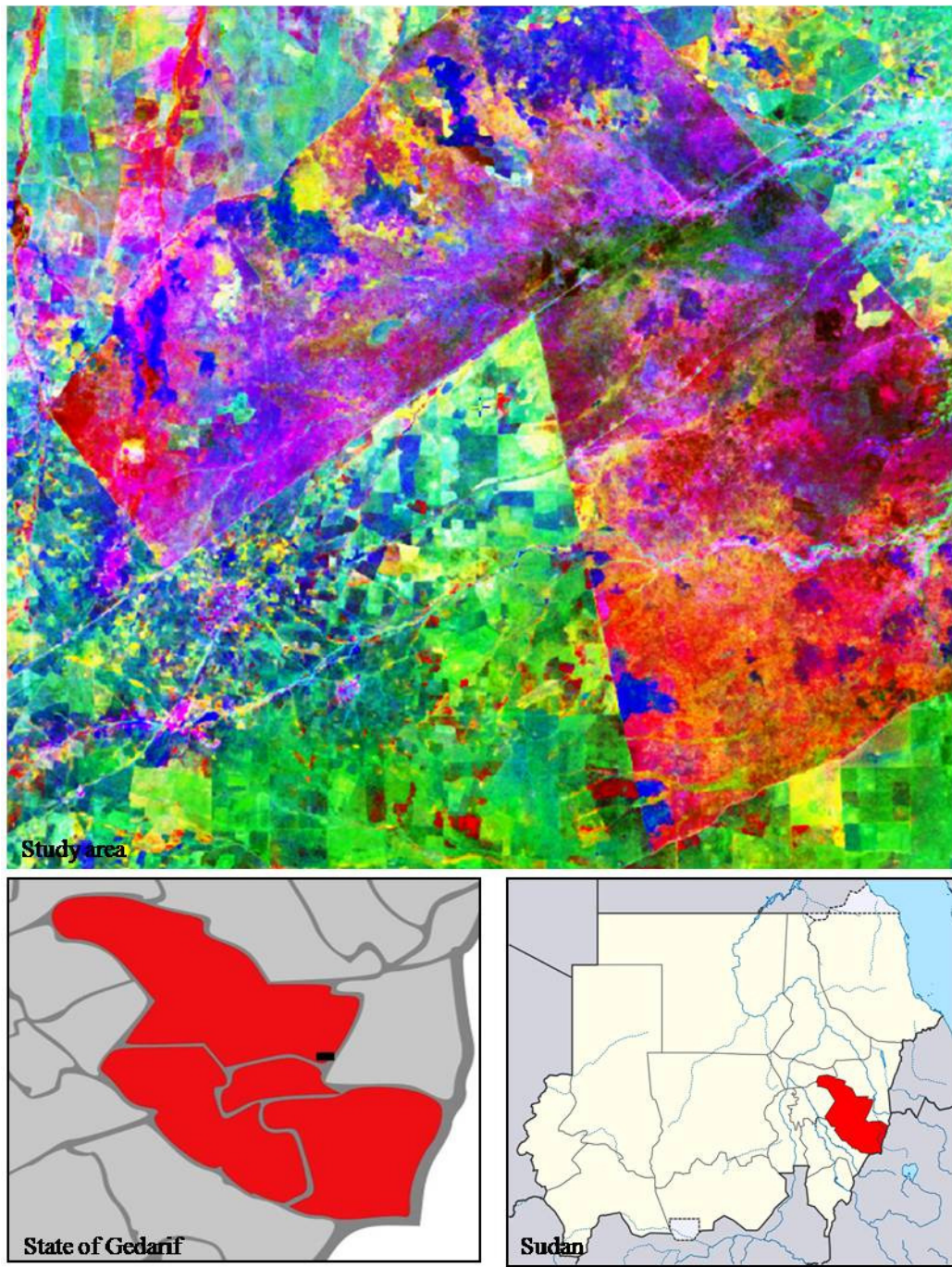


Figure 3.1: Location of the study area

3.1.2 Physical Characteristics of El Rawashda Reserved Forest



Figure 3.2: El Rawashda Reserved Forest, Sudan, showing excavation running along the forest
Photograph by the author. July 2005

3.1.2.1 Climate

Climatologically El Rawashda lies in the semi-arid zone, with summer rains and warm winters, characterized by a unimodal rainfall pattern. The length of rainy season fluctuates around seven months i.e. from April to October and the peak of rainfall is in August. The amount and distribution of rainfall in the study region varied during the period 2002-2009 (figure 3.3). Rainfall varied from 200 mm to over 500 mm with an annual average of 424 mm during this period. According to the figure, 2008 received the highest amount of precipitation (555.7 mm) followed by the year 2003 (524.8 mm); and the lowest amount of rainfall was recorded in 2004 and 2009 (293.8 and 344.7 respectively). Indeed, these variations affect the level of crop yields and hence comprise a major source of risk in the study area. Moreover, hazards of delays in rainfall commencement and subsequent poor rainfall distribution often necessitate re-planting and hence create additional cost of production. Rainfall is also considered as an important factor in determining the type and the variety of crops to be grown and the agricultural techniques to be used for optimum production.

The south- west monsoon maritime wind, responsible for bringing the rains of Sudan, blows across Gedarif area from May to October. From November to April, the area

experiences the prevailing northerly wind or what is the same as the dry North East Trade winds (Sudan Meteorological Department, 1970).

Temperatures are very high in summer and mild in winter. The average daily maximum temperature ranges from 25° to 40° C, while the average daily minimum temperature ranges between 13° and 20° C. Relative humidity rises from its normal level of around 20-30% through most of the year to 60- 70% in the wet season.

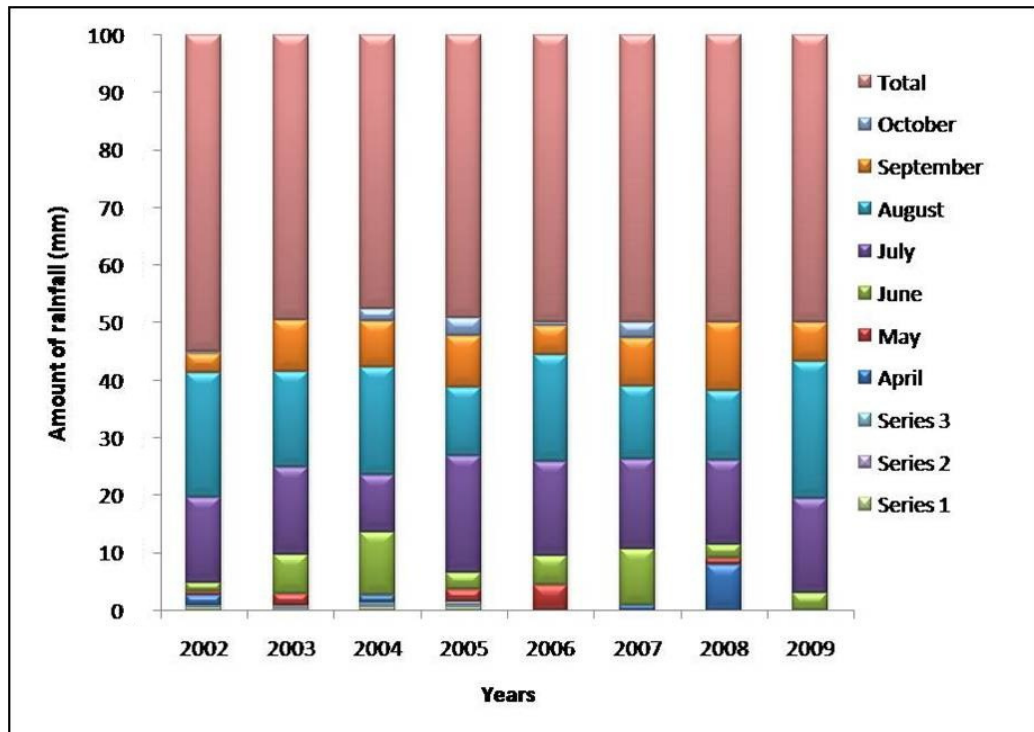


Figure 3.3: Average Annual Rainfall, El Rawashda Region, 2002-2009

Source: Meteorological Station, Gedarif, 2010

3.1.2.2 Vegetation

Gedarif State lies in the zone of low rainfall woodland savanna (Harrison and Jackson 1958). El Rawashda forest is located near the transition between two main vegetation types of low-rainfall woodland savanna on clay: *Acacia mellifera* at horn land and *Acacia seyal*-*Balanites aegyptiaca* woodland (Harrison and Jackson, 1958).

Acacia mellifera thorn land alternates with semi-desert grassland and occurs northward from the 400-500 mm isohyets (Vink, 1987); *Acacia mellifera* thickets dominate the vegetation. *Acacia seyal* – *Balanites aegyptiaca* wood land emerges with a sharp clear ecotone south of *Acacia mellifera* thorn land and with an increase in the annual rainfall to more than 500 mm (Harrison and Jackson 1958, Vink, 1987). The most dominant grass of the forest is *Cymbopo gonnervatus*.

3.1.3 Social and land-use characteristics

3.1.3.1 Population in Gedarif State with special reference to El Rawashda

El Rawashda area with its forest reserves is situated between two sizeable consumption centres of forest products, i.e. Showak and Gedarif (Figure 3.4). In 1982, the Gedarif State was estimated to have a population of 195,000 of which 27% were urban and 73% represented rural farmers (Elmoula, 1985). The total population in 1995 was estimated at about 1,230,000 persons (Elmubarak, 2002). The major ethnic groups are groups of Arabs comprising semi-nomadic, settled, rural and urban people. It includes mainly the Lahaween and the Shukriya and others. West Sudanese and West Africans, representing a large population of the labour force in the state, and a significant number of Ethiopian and Eritrean refugees have settled in the state. The estimated number of refugees according to the 1993 census was 360,000, representing 30% of the population (Elmoula, 1985; Eltayeb, 1985). According to the 1983 census and on a 1987 estimate, the population in El Rawashda area having close relation with El Rawashda forest reserves was registered as comprising 15,000 villagers and 4,500 refugees (Vink, 1987).

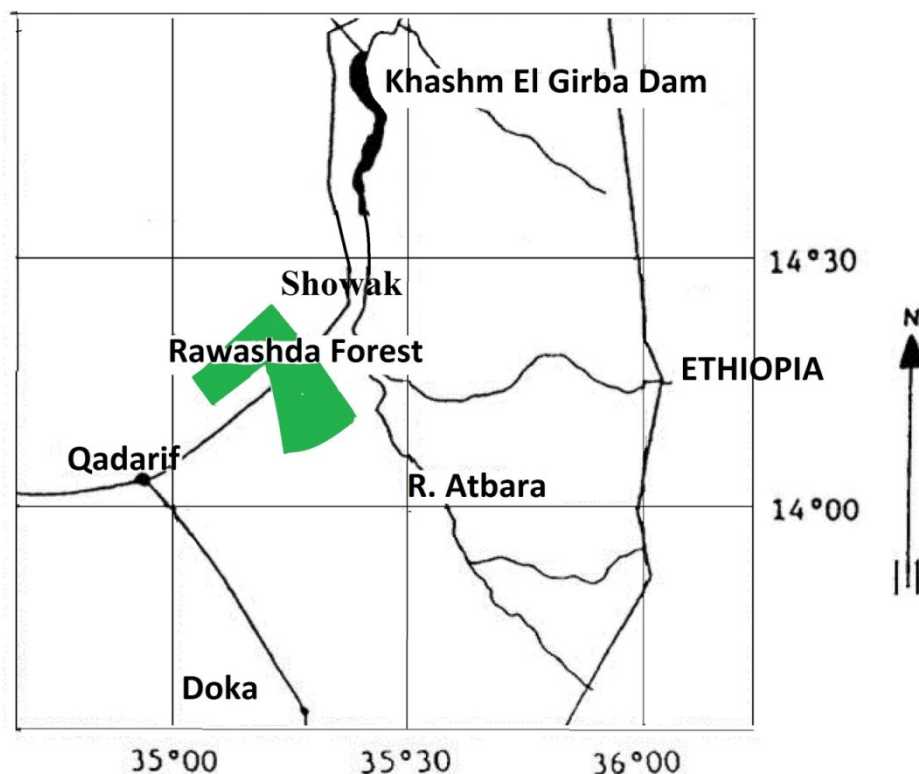


Figure 3.4: Map of Gedarif showing the situation of El Rawashda forest

Source: http://en.wikipedia.org/wiki/Districts_of_Sudan#Al_Qadarif

3.1.3.2 Land-use, land use changes and their influence on the forests

Agriculture is the main economic activity, followed by livestock raising in the traditional seasonal transhumance pattern (Figure 3.5), village livestock raising and, as a recent element, livestock raising by large-scale mechanized merchant-farmers investing surplus wealth in cattle. Gum tapping, collecting and trading forest products and charcoal burning are other traditional forms of economic activity. Thus, the people derive their income from various combinations of the three main forms of land-use: agriculture, grazing, and forest exploitation. Mechanized rain-fed crop production, has considerably reduced the land available for small-holder farming and for grazing (Glover, 2005). Elmoula (1985) stated that the traditional pattern of land-use has been profoundly changed by population growth, the influx of refugees from Ethiopia, a succession of drought years and more than anything else, the unbridled expansion of large-scale mechanized farming since the 1940s.



Figure 3.5: Livestock raising in the traditional seasonal transhumance in El Rawashda forest
Photograph by the author. 2006

By blocking the extension of traditional shifting cultivation as the population grows, the expansion of large-scale mechanized farming has gradually reduced the soil-restoring fallow period to zero, while creating landless peasants in the process. Continued mono-cropping on traditional and large scale mechanized agriculture has caused a decline in crop yields and an increase in infestation of cropland by the hemi-parasitic plant *Striga hermonthica*. Mechanized farming has taken over nomads' traditional grazing lands and blocked traditional migration routes (Glover, 2005).

3.1.3.3 Socio-economic background of the nomad

The nomads mainly belonged to the various branches of the Rashaida, who originally had emigrated from Saudi Arabia some 150 years ago. These people were of Middle Eastern or even Indian origin with colorful clothing (See figure 3.6).

The Rashaida stayed each year from late November until late June inside the New Halfa Scheme, after which they returned to Gedarif and Kassala plains when the rainy season started, for preparing their rainfed sorghum fields. The Rashaida moved around and lived in groups of five to ten families which could change in composition each year. The Rashaida could still have large herds of sheep and goats and a few camels. In 2002-2003 some households also had cattle that provided milk income. (Helsinki, 2007).

3.1.4 Management Units

Two kinds of management systems have been dominated the land use activities inside the natural forest reserves in the El Rawashda area. They are known as the El Rawashda Model I and El Rawashda Model II, respectively. Both models have one thing in common, i.e. the partnership between FNC and the local people in planting, protecting and deriving benefits from forest reserves.



Figure 3.6: Movement of nomad groups in El Rawashda forest

Photograph by the author, 2006

3.1.4.1 El Rawashda model I

The FAO Fuel wood Development for Energy Project in Sudan (1983-1989) designed a management plan for the El Rawashda forest (Vink, 1987; FNC, 2000; Ibrahim, 2000). The general theme of the plan was the participation of local inhabitants in the development of the reserved forest by their responsibilities to the forestry rehabilitation program (replanting trees in taungya system). The forest committee, which was formulated by the local inhabitants, was also responsible for the protection of the reserved forest against illicit felling, illegal grazing, etc. In return, the community of local inhabitants was eligible to forest products as determined by the forestry service in those compartments prescribed by the plan.

The centralized forest management system involved management control under the forestry authorities where tree establishment was carried out by different methods including local people, but protection was executed by the forest guards and officers (Glover, 2005).

3.1.4.2 El Rawashda Model II

In El Rawashda model II, selected blocks of degraded parts of El Rawashda forest reserve were allocated for integrated land use involving a rehabilitation process and a participatory approach. The model includes partnership between FNC and the local people in planting, protecting and getting benefits from forest reserves.

The model, designed by the forestry component of the Agricultural Development Project for the Eastern Sudan (ADES) is very similar to the FAO model, with the exception that the local inhabitants have nothing to do with the final felling. They are not allowed to collect firewood or other forest products other than those prescribed as rights and privileges in the Forest Act of 1989. The collaboration has been developed since 1994 on the basis of a contract between the two partners granting the farmers security of land tenure for crop (e.g. sorghum, millet and sesame) cultivation inside the reserve. The system grants each farmer land for cultivation each year, in a way that 75% of the land is used for crops and 25% for forest stand establishment. This is continued annually for four years until the whole piece of land is reforested. Then another piece of arable land within the forest reserve is targeted. The forest authorities provide the tree seeds and supervise the guarding and patrolling exercised by the farmers and forest guards as a joint activity. Farmers also accept to pay 10 to 20% of the grain products to the forest authorities, who issue licenses to the people and local bakeries, at low royalties, for gathering dead wood and fallen trees under the control of the forest guards.

The contract outlines the responsibilities and obligations of each farmer for cultivation inside the forest reserve. It implies that the government secures the land and the seeds to farmers. The contract also provides for efficient protection exercised by the farmers and the forest guards (Glover, 2005).

3.2 Research data acquisition

3.2.1 Field sampling

The Aster image was taken on 26 of February, 2006, while the first field work was undertaken about seven months later during the month of September, 2006. This is not an ideal situation and may give some inconsistencies between these two data types.

Ideally, field work and the images should be from about the same period of time so that the data correspond as much as possible. For that reason another field work was undertaken in March of 2007.

Fieldwork was carried out to collect data for training and validating land cover interpretation from satellite image of 2006, and for qualitative description of the characteristics of each land cover class. Also, it is necessary to collect other ancillary data and historical data required for classification of 2000 and 2003 images. In order to create a testing sample set, first of all a set of testing points was selected randomly. However, reaching all those random points in practice was found infeasible because El Rawashda forest is a very difficult to access, especially areas which are very far from the road/path. This resulted in the field check of 285 points (figure 3.7). For classification of images of 2000 and 2003, simple random sampling was applied.

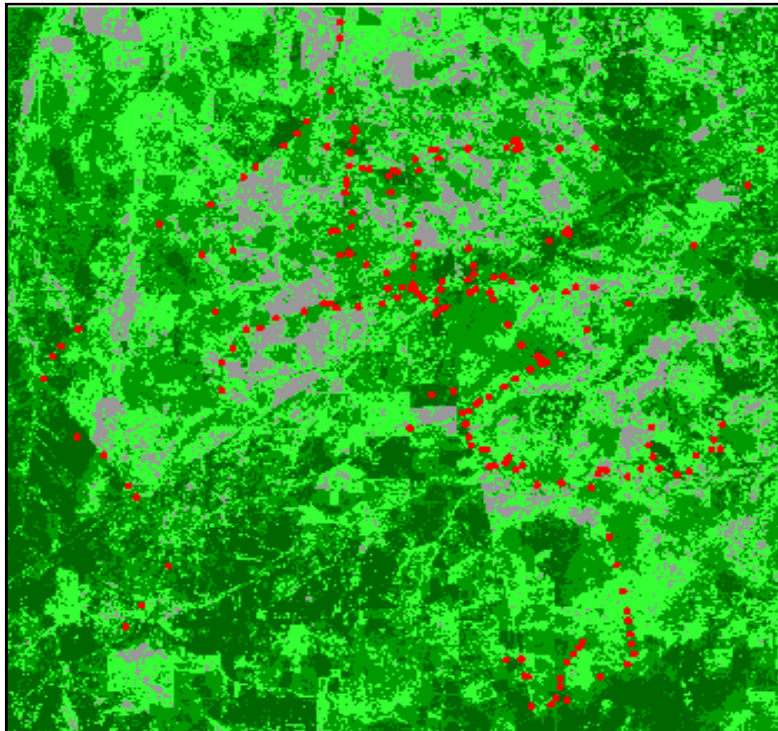


Figure 3.7: Field observation points

3.2.2 Data collection for study area

3.2.2.1 Landsat Imagery

Landsat ETM imagery of 29th March of the year 2000 and of 22th March of the year 2003 was acquired from the web based data archives of the Global Land Cover Facility (GLCF). This data is offered by the USGS for natural resources research. Data specifications are described in table 3.1 and 3.2.

Table 3.1: Satellite imagery and its specifications used for bi-temporal change detection

<i>Sensor</i>	<i>Platform</i>	<i>Date</i>	<i>Path/row</i>	<i>Band</i>	<i>Spatial resolution</i>
ETM+	Landsat 7	29-03-2000	171/50	1-5, 7	28.5m
ETM+	Landsat 7	22-03-2003	171/50	1-5, 7	28.5m
Aster	Terra	26-02-2006		3B(VNIR) SWIR	15m 30m

Table 3.2: Landsat specification

<i>Band</i>	<i>Spectral Resolution</i>
2 (Green)	0.53-0.61 μm
3 (Red)	0.63-0.69 μm
4 (Near IR)	0.78-0.90 μm
5 (Middle IR)	1.55-1.75 μm
7 (Middle IR)	2.09-2.35 μm

3.2.2.2 Aster Imagery

Aster of 26th February of the year 2006 was ordered from the web based data archives of the National Aeronautics and Space Administration (NASA). Data specifications are described in table 3.3.

Table 3.3: Aster specification

<i>Band</i>	<i>Label</i>	<i>Wavelength</i>	<i>Resolution</i>
B2	VNIR_Band2	0.63-0.69	15m
B3	VNIR_Band3N	0.76-0.86	15m
B4	VNIR_Band3B	0.76-0.86	15m
B5	SWIR_Band4	1.60-1.70	30m

3.2.3 Image pre-processing

3.2.3.1 Atmospheric correction

Several factors independent of ground cover can significantly affect spectral reflectance as measured by the sensor. Electro Magnetic Radiation (EMR) used for

remote sensing passes through atmosphere of the earth. The effects of the atmosphere on the signal are mainly caused by scattering and absorption. They vary with the path length, the atmospheric conditions and the wavelength. Atmospheric absorption results in the loss of energy to atmospheric constituents. (Lillesand and Kiefer, 2008). Scattering, the redirection of electromagnetic energy by particles suspended in the atmosphere, is the reason why the radiation arriving at the sensor consists of the following components:

- Radiance reflected from the earth's surface
- Radiation scattered directly to the sensor without reaching the earth's surface
- Radiation scattered to the ground (diffuse radiation, skylight) being reflected to the sensor
- Surface-reflected radiation partly scattered both directly to the sensor and to the ground.

Thus a sensor will receive not only the directly reflected or emitted radiation from a target, but also the scattered radiation from a target and the scattered radiation from the atmosphere, which is called path radiance (Lillesand and Kiefer, 2000).

Many correction methods have been proposed in several studies to remove the atmospheric effects. Song et al. (2001) made evaluation of several correction methods based on land cover classification and change detection accuracies applied on a multitemporal dataset of seven Landsat TM images.

In this research the algorithms available from PCI Geomatica Enterprises Inc. for ATCOR were used because the only ancillary data required are the solar zenith angle of each image and the location of stands.

The atmospheric models require the selection of atmospheric properties. These are predefined and are tropical, mid-latitude, or the US standard atmosphere and are also rural, urban, desert, or maritime. For this area the dry, arid and rural atmosphere best described the study area. The atmospheric model also uses sensor calibration defaults and solar zenith angles to calculate reflectance values. A variable, optical visibility has to be calculated for each image to perform the final algorithms in the atmospheric correction package. This requires the selection of a target with known reflectance values, which are compared with the reflectance values calculated within each image.

3.2.3.2 Image to image registration

Image registration is the process of making an image conform to another image and involves geo-referencing if the reference image is already rectified to a particular map projection. Thus image to image registration is usually used for time series data like multi-temporal images over the same region in order to place the same coordinate system to disparate images (Lee et al., 2007).

Therefore, the two Landsat images acquired in 2000 and 2003 were already rectified to Transverse Mercator projection and the third Aster image acquired 2006 was co-registered with image to image registration method. The total root mean square error (RMSE) of the registered images was 0.15 pixel, which was quite low to accept the RMSE limit required for the change detection. In general, RMSE limit for the change detection is preferred less than 0.5 pixel when registering the images.

4 Methods of Change Detection

4.1 Descriptions of land cover classes

This section describes the land classes used for land cover mapping from satellite images (Figure 4.1).

1. The closed forest class represents the evergreen forest; the crown coverage is over 60%.
2. The open forest class corresponds to forest which has been disturbed by human activities. It is composed predominantly of regeneration forest from the past disturbance such as slash and burn, or logging. The crown coverage is generally below 60 %.
3. Grassland represents small scrub species, Agricultural fields and early stage colonizing species. Some of the grassland is also included in this class since the area of grassland is negligible and often distributed near or mixed with shrub.
4. Bare land consists of crop fields, built-up areas, water bodies and bare soil. This is because it is very difficult to differentiate crop fields, especially the annual crops and bare soil. Also, the settlement area is often a mixture of scatter small gardens and built up objects, which makes it difficult to separate them in the image.

4.2 Classification of images using Maximum likelihood Classifier

The classification algorithm, which is based on the training sample information, is needed to classify the image. Algorithms like the parametric classifier require statistical information and are categorized as parallelepiped, minimum distance, and maximum likelihood approach. In this study the maximum likelihood algorithm has been applied. It is the most common approach and is frequently used in research and application (Heikkonen and Varjo, 2004).

The classification of the Landsat ETM 2000, 2003 and Aster 2006 imagery into land cover classes was carried out through a number of steps of supervised classification including: selection and use of training sets (sample points), classification using the maximum likelihood classifier, generation of output and accuracy assessment.

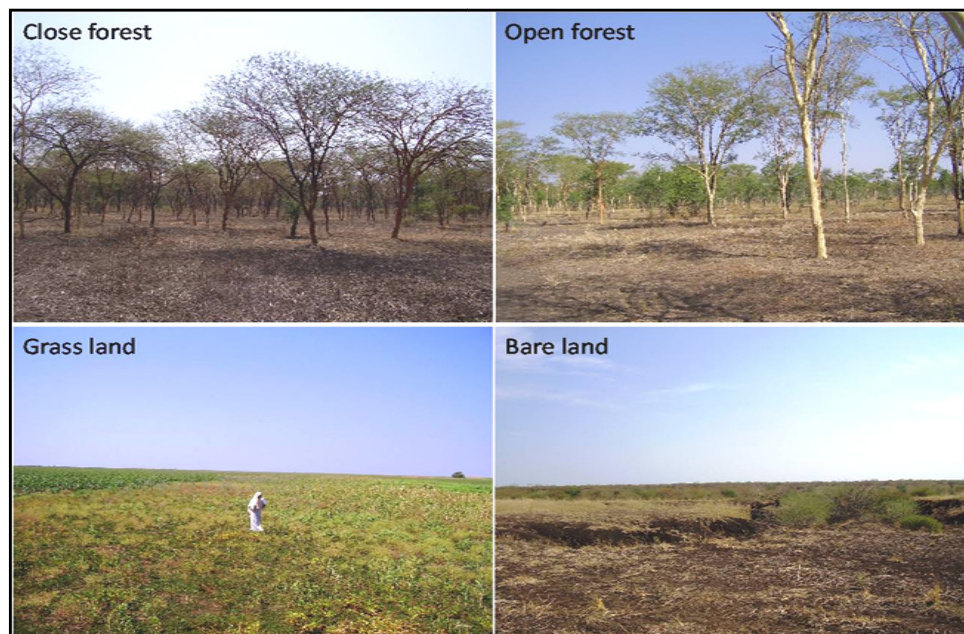


Figure 4.1: Land cover classes in El Rawashda forest

Photograph by the author, 2006

The classification was implemented using the maximum likelihood classifier methods of PCI Geomatica. At the outset, several classification trials and evaluation of the correspondent accuracy results in an iterative manner, aiming at refining the initial training set. The signature for each of the land cover types found in the study area was determined with the help of a training set of GPS coordinates corresponding to the cover types for Landsat image 2006. A number of pixels representing each cover type spectra were collected and assigned to the specific land cover classes for which the likelihood of being a number was maximum. The remaining set of points collected from the field representing each cover type was used as the validation set. The classes of forest cover degradation defined comprehended: close forest, open forest, grass land and bare land. Bare land and water bodies were grouped together during the data processing, since the occurrence of water represent non vegetated area. Agricultural schemes and grasses formed another combined group, considering the fact that the same indicators were useful for both. The direction of the influence of these indicators in forest cover was defined through the use of multivariate analysis (Principal Component Analysis); the scores generated in the PCA gave the clear expression of the vegetation cover. The classes were intended to provide a basis for the investigation of spatial distribution of vegetation cover variations in the forest area. The establishment of classes expressing the levels of vegetation cover can bring about some subjectivity, due to the need of use of qualitative endpoints.

4.3 Accuracy assessment of classified images

The overall classification accuracy is the percentage of correctly classified samples of an error matrix. It is computed by dividing the total number of correctly classified samples by the total number of reference samples.

To determine the accuracy of the image classification for the Landsat 2000 and Landsat 2003 images for which no ground validation data or aerial photography was available, the stratified random sampling method (Jensen, 1996) was used to generate 155 reference points for the whole study area. These points were collected according to the different strata and overlaid on the unclassified image to check if the class given falls into the same spectra as was used to collect the training samples. A comparison of the Landsat classified images was made with the classified Aster image for which ground validation points were available. The results of the overall classification accuracy, producer's and user's accuracies, and Kappa values for each land cover derived from the error matrix were used to determine how well the classification was done.

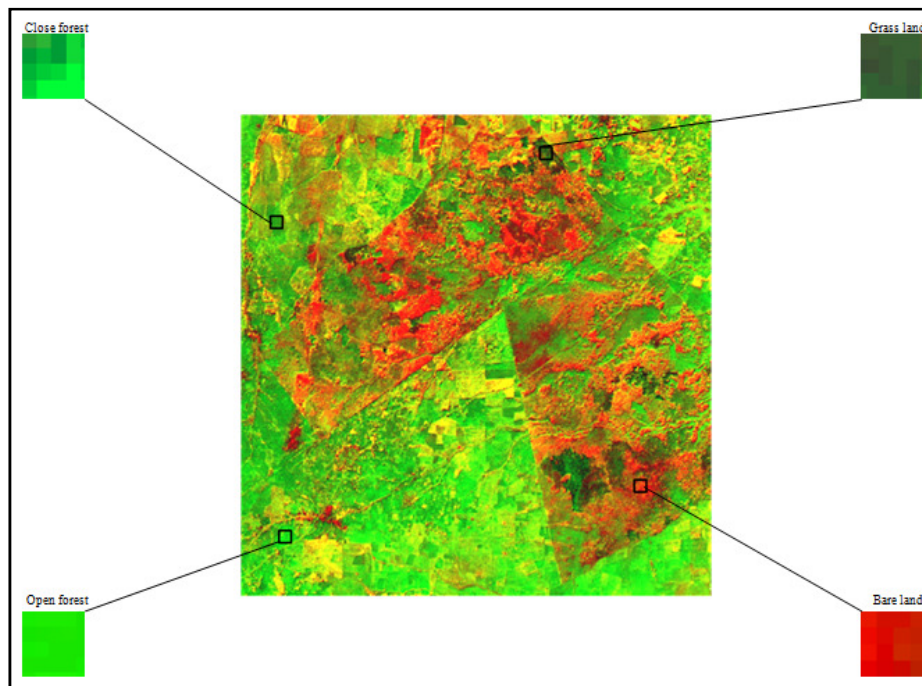


Figure 4.2: Samples representing the land cover classes according to the spectral radiance of Aster (pc1, pc2, pc3) in the study area

4.4 Calculation of Vegetation Indices as independent variables

Normalized Difference Vegetative Index (NDVI), Soil Adjusted Vegetative Index (SAVI), and Transformed Difference Vegetative Index (TDVI) were created for each

image collection date at each spatial scale, and were analyzed individually. The NDVI index was used because it is the most widely used in global vegetation studies today (Lunetta and Elvidge, 1999). The SAVI index was used because it was developed to minimize the influence of the soil background on the vegetative reflectance (Huete 1988). The TDVI index was used because it does not contain the saturation concerns that NDVI has and also minimizes the influence of the soil background, similar to the SAVI index (Bannari et al., 2002).

4.4.1 NDVI

The NDVI was derived from the difference between the maximum absorption of radiation in the red spectral wavelength and the maximum reflection of radiation in the near infrared spectral wavelength for each image where:

$$NDVI = \frac{NIR - Red}{NIR + Red}$$

4.4.2 NDVI-RGB

Three NDVI composites for the years 2000, 2003 and 2006 were projected on a RGB axis following the RGB-NDVI change detection strategy of Sader and Winne (1992). By simultaneously projecting each date of NDVI through the red, green, and blue (RGB) computer display write functions, major changes in NDVI (and hence vegetation cover) between dates appeared in combinations of the primary (RGB) or complimentary (yellow, magenta, cyan) colors. Knowing which date of NDVI is coupled with each display color, we visually interpreted the magnitude and direction of vegetation changes in the study area over the three dates to detect the major decreases or increases in green biomass associated with forest harvest or regeneration.

4.4.3 SAVI

Vegetation indices largely depend on the canopy of the forest, surface area of the green vegetation and their reflective value can be considerably affected by the reflection from the soil surface. Since the forest in the study area has a lot exposed bare ground and open forest and a sparse canopy in most areas, the SAVI index that includes a soil correction factor was used. This compensates for the relative soil effect while at the same time accounting for the amount of vegetation present. Being an open dry Acacia forest also, the effect of the soil background noise on the remotely sensed reflectance could cause giving biased strong relationship with biomass which would not be accurate. This index includes a soil adjustment factor that ranges from 0 for very high vegetation cover to 1 for very low vegetation cover. A value of $L = 0.5$ was used in this study and is recommended since it permits the best adjustment, by minimizing the secondary back scattering effect of the canopy transmitted soil background reflected radiation (Huete, 1988).

$$SAVI = \frac{(1 + L) \cdot (NIR - Red)}{(NIR + Red + L)}$$

4.4.4 TDVI

The Transformed Difference Vegetation Index (TDVI) developed by Bannari et al. (2002), was tested in this study. TDVI does not saturate like NDVI or SAVI, it shows an excellent linearity as a function of the rate of vegetation cover.

$$TDVI = 1.5 \cdot \left[(NIR - R) / \sqrt{NIR^2 + R + 0.5} \right]$$

4.5 Index Differencing

Image differencing was applied to vegetation images that were derived using three vegetation indices: NDVI, SAVI, and TDVI. In all cases, the 2000 transformed data were subtracted from 2003 transformed data and the 2003 transformed data were subtracted from 2006 transformed data, resulting in new images. A series of threshold values based on standard deviations from the mean were used on the new images to determine the changed from unchanged pixels. A visual assessment on the no-change/change pixels was performed to determine the threshold value with the highest accuracy. A process of labeling needs to occur to assign the appropriate "from" and "to" identifiers.

4.6 Tasseled Cap Transformation

The TCT was applied to each of the three images. The TCT coefficients in PCI Geomatica were used for this study. The results of the TCT produce an image file that consists of three bands which have been attributed to soil brightness, vegetation greenness, and soil or vegetation wetness.

The composite of the three TC components for all images was used to provide the change information over the entire temporal periods from 2000 to 2003 and from 2003 to 2006. The hypothesis was that the TC composite would detect more change than the vegetation indices because it takes into account all three of the spectral regions frequently used for vegetation studies (red band, near-infrared band and mid-infrared band), whereas the vegetation indices only consider two of the three.

For change detection purposes, the Tasseled Cap transformation results of Landsat and Aster data sets were utilized using the image differencing technique, only the greenness layer was used in pairs in order to delineate the variance in vegetation between the pairs of the two periods.

4.6.1 RGB-TCG

Three TCG (Tasseled Cap Green) layers composites for the years 2000, 2003 and 2006 were projected on a RGB axis following the RGB-NDVI change detection strategy of Sader and Winne (1992). This method was proposed because we found similar patterns of temporal change for the NDVI and TCG layer.

When determining change, RGB-TCG incorporated three dates at one time as opposed to two-date sequences used with other methods, moreover the method straightforward and time efficient. Finally, the analysis of cluster statistics and visual interpretation of RGB-TCG layers composites aided by additive color theory logic (Sader & Winne, 1992), facilitated identification of change representing forest clearing, no change and re-growth in a time.

4.7 Change Vector Analysis

For this study the change vector analysis technique was performed using a designed tool imported to IDL ENVI. Johnson and Kasischke (1998) suggest that CVA is most likely to be interpretable when multiple, phenomenological relevant spectral features are used as the input data rather than the raw data. This tends to be the case in the majority of CVA change detection studies and very seldom is the raw data used as an input. However, because some types of change are biophysical variables, this study relies on two different spectral data sets: original ETM and ASTER bands and the components of the Tasseled Cap transformation, brightness (B), greenness (G) and wetness (W). With this method, two images are computed: one image for the vector intensity and another for the vector direction. The first image contains the information of change, while the second contains information on the type of change.

4.8 Mapping with Conventional and Selective Principal Component Analysis

For the present study, PCA for change detection was applied by two ways: First, Multitemporal PCA. Second, Selective PCA for the three dates of Landsat and Aster images.

4.8.1 Multitemporal PCA: the conventional approach

Multitemporal PCA was performed using the 10 reflective bands of the two dates 2000 and 2003 and the two dates 2003 and 2006 images. More specifically a bi-temporal feature space was constructed by placing the two image vectors in the same space. By constructing a bi-temporal feature space, it is possible to use the general concept of principal components applied to change detection, which interprets that the pixels that have not suffered change will tend to lie around the first principal component and the changed pixels will tend to lie around the second principal component, which is orthogonal to the first. In this study all the bands are used to construct the bi-temporal feature space. By doing so, it is possible to project in two dimensions all the transformed data obtained from the images. This will lead to an easier interpretation of the results because all the change information will be expected to be in the second principal component. It also permits to take advantage of all the information in the images. This means that for every band there is going to be a second image component that will offer unique information of change.

4.8.2 Selective PCA

Selective PCA for change detection was applied by band wise for the two periods (2000-2003 and 2003-2006). PCA was performed for band1 time 1 and band1 time 2, band2 time 1 and band2 time 2...etc. This was applied to the original Landsat ETM and Aster dataset (bands 1-5). By using only two bands, the information that is common to both images is mapped to the first component and information that is unique to either one of the two bands (the changes) is mapped to the second component, so PCs2 were examined as a measure for change.

In both Multitemporal PCA and Selective PCA methods, the PCs were obtained with the correlation matrix, i.e., the PCs are standardized.

4.9 Change Detection by Multivariate Alteration Detection

In this study the applicability of the multivariate alteration detection (MAD) transformation with the maximum autocorrelation factor (MAF) post-processing to multivariate and bi-temporal change detection studies was demonstrated by cross-matrix between two images for the two periods (2000-2003 and 2003-2006). The statistical properties of the MAD variates are accurate which make them very useful for analyzing change information and for image. The MAF transformation serves to reduce dimensionality and to enhance spatial coherence of the difference components. In the present instance, we have used the MAF transformation to improve effectiveness of the MAD result and to find maximum change areas with high spatial autocorrelation. In this way, change information can be separated from noise to the greatest extent, so that we can solve the technical problem of effectively concentrating change information and we can produce difference image more clearly.

Interpretation of the resulting change images was based on correlations between the transformed variates and the original data.

Change-no change decision thresholds was applied to the MAF/MAD variates separately in order to generate color coded change images. The sum of squares of the standardized MAD components (the MAD components divided by their standard deviations) is approximately chi-square distributed, enabling no-change thresholds to be set easily.

4.10 Accuracy assessments for change detection techniques

From the outset of this research, it was known that accurate field or remote sensing based validation data for the images would be unavailable. As an alternative, validation was conducted by visually identifying areas of change or no-change in magnified displays of the RGB composites. This analysis was conducted for the original images to determine the best data transform. To accomplish this, a manual supervised classification was conducted to a subset of each image (64728 pixels) and then change detection was conducted by computing image difference. Hereafter the result map was used as a reference. The change detection was conducted with the transformed images to assess its completeness in spatially detecting vegetation change.

The accuracy assessment for change detection is particularly difficult due to problems in collecting reliable temporal field-based datasets. Therefore, much previous research on change detection cannot provide quantitative analysis of the research results. Although standard accuracy assessment techniques were mainly developed for single-date remotely sensed data, the error matrix-based accuracy assessment method is still valuable for evaluation of change detection results. Some other methods have also been developed to analyze the accuracy of change detection (Morissette and Khorram, 2000, Lowell, 2001).

In this study the accuracy assessment based on change/no-change pixels was performed. The result of the reference map for change/no change was subtracted from the result of change/no change map of each change detection technique, then the Pseudo Colour table of the software PCI Geomatica was adapted (figure 4.3).

	No change	Change
No change		
Change		

Figure 4.3: Change and no change error matrix.

4.11 Object-Oriented Classification of references data by eCognition

The classification of the reference imagery was done by the software eCognition (figure 4.4). Object-oriented classification is based on image segmentation and results in a more accurate mapping product with higher detail in class definition. The first step in object-oriented analysis with eCognition is a segmentation of the image. This process extracts meaningful image objects (e.g. roads, buildings, vegetation) based on their spectral (figure 4.5) and spatial characteristics (figure 4.6). In eCognition the segmentation is a semi-automated process where the user can determine specific criteria that affect size and shape of segments of the resulting image. The resulting objects are attributed not only with spectral statistics but also with shape and context information, relation to neighboring objects and texture parameters. The segmentation was performed by equally weighting of all bands, using the following parameters: Scale 10, Shape 0.1; Smoothness 0.5. The image classification in eCognition is based on user-defined fuzzy class descriptions based on spectral and spatial features. In general, the program uses a nearest neighbor algorithm, which performs class assignment based on minimum distance measures. The classification process includes a variety of different information, ranging from spectral mean values for each object, to measures of texture, context and shape. The aim of classification is to provide an accurate land cover classes that forms a reference of change map and further analysis to test the accuracy of other change detection methods. Accordingly, the definition of the land cover classes has to be based upon the major land cover classes: grass land, close forest, open forest and bare land.

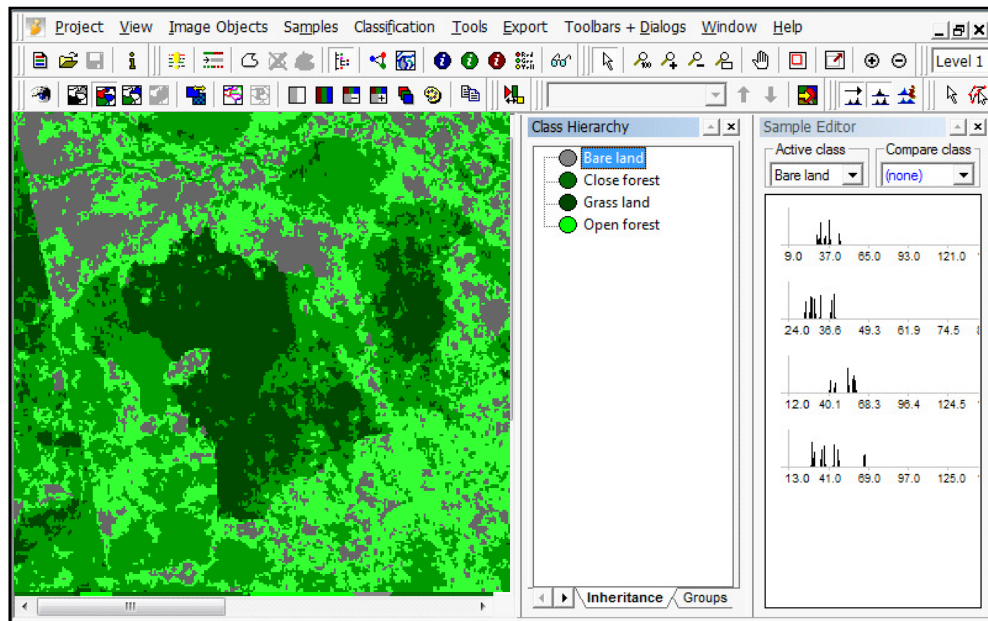


Figure 4.4: Classification of the reference imagery by eCognition

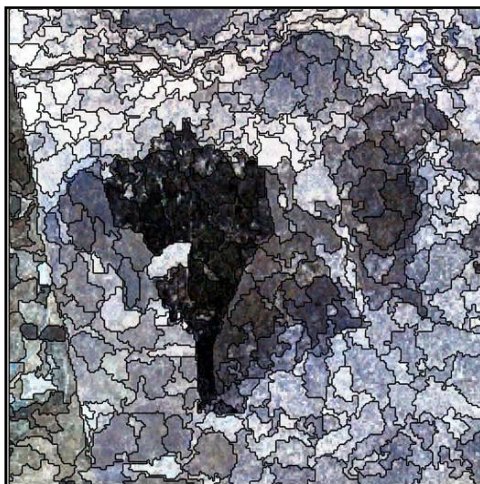


Figure 4.5: Segmentation based on pixel-based

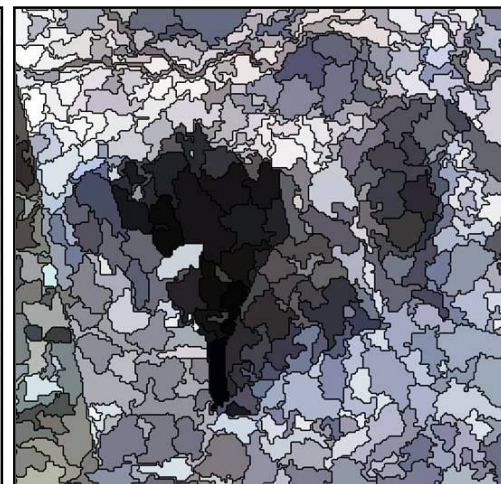


Figure 4.6: Segmentation based on object-based

5 Results

5.1 Classification and Change Detection Accuracy

The classification of change detection for El Rawashda forest was based on Maximum Likelihood supervised classification using 4 classes: Bare land, Grass land, Open forest and Close forest. At the outset of this research, it was known that accurate field or remote sensing based validation data for the years 2000 and 2003 would not be available. As an alternative, validation was conducted by visual interpretation, field data and with the help of unsupervised classification. The resulting 2000 and 2003 classifications and 2003 and 2006 classifications were used as inputs to produce change maps. This yielded change images in which 16 types of change between the two periods are potentially possible.

Overall classification accuracy and Kappa Coefficient were computed to provide measures of the accuracy of the classification. The user's and producer's accuracy as well as elements of the error matrix was calculated to assess error patterns of the respective classification. For this study a total number of 155 reference samples were used.

Landsat ETM 2000

Figure 5.1 shows the result of supervised classification and table 5.1 represents error matrix of Landsat ETM data of the year 2000. The Kappa coefficient was 0.79 and the overall accuracy was 88.4%. Areas highlighting grass class appeared with a user's accuracy of 84.6% and producer's accuracy of 100%, closed forest revealed user's accuracy of 92.2% and producer's accuracy of 80.5%. The lowest user's accuracy and producer's accuracy were obtained in open forest classes which were 80% and 70% consequently. Bare land showed a user's accuracy of 100% and producer's accuracy of 88.8% (table 5.2)

Landsat ETM 2003

Figure 5.2 shows the result of supervised classification and table 5.3 represents error matrix of Landsat ETM data of the year 2003. The Kappa coefficient came up to 0.89 and the overall accuracy was 91.9%. The sample pixels for most classes showed more or less high spectral variability which facilitated difficulties in separating each class from other. Areas highlighting grass class appeared with a user's accuracy of 92.6% and producer's accuracy of 97.4%, closed forest displayed high user's accuracy of 97.4% and producer's accuracy of 90.4%. The lowest user's accuracy and producer's accuracy were obtained in open forest classes which were both 76.9%; the spectral reflectance of the open forest training data was heterogeneous. Thus the problem in separating these classes was the major source of misclassification. Bare land showed a user's accuracy and producer's accuracy of 93.3% (table 5.4).

Table 5.1: Error matrix of ETM 2000

Reference Data					
Classified Data	Class1	Class 2	Class 3	Class 4	Totals
Class 1	33	0	3	0	36
Class 2	7	35	0	2	44
Class 3	2	0	37	0	39
Class 4	0	3	0	33	36
Totals	42	38	40	35	155

Table 5.2: Producer's and user's accuracy of ETM 2000 classification

Classes	Producer's accuracy	User's accuracy	Class No.	Land cover classes
Class 1	100%	84.6%	1	Grass land
Class 2	80.5%	92.2%	2	Close forest
Class 3	70.0%	80.0%	3	Open forest
Class 4	88.8%	100%	4	Bare land

Table 5.3: Error matrix of ETM 2003

Reference Data					
Classified Data	Class1	Class 2	Class 3	Class 4	Totals
Class 1	35	2	0	1	38
Class 2	0	35	3	2	40
Class 3	2	0	37	0	39
Class 4	4	0	1	33	38
Totals	41	37	41	36	155

Table 5.4: Producer's and user's accuracy of ETM 2003 classification

Classes	Producer's accuracy	User's accuracy	Class No.	Land cover classes
Class 1	97.4%	92.6%	1	Grass land
Class 2	90.4%	97.4%	2	Close forest
Class 3	76.9%	76.9%	3	Open forest
Class 4	93.3%	90.3%	4	Bare land

Aster 2006

Figure 5.5 shows the result of supervised classification and table 5.5 represents error matrix of Aster data of the year 2006. The Kappa Coefficient took a value of 0.89 and overall accuracy of 92.1%. In this classification, grassland, close forest and open forest showed a balanced producer's and user's accuracy and also the producer's accuracy was relatively low for open forest (88.8%) and confusion may be result from the presence of low height open forest stands in the forest as well as in the class boundaries. Bare land sample data appeared to be well defined with producer's accuracy of 96.8% and also with a user's accuracy of 93.9% (table 5.6).

Table 5.5: Error matrix of Aster 2006

Reference Data					
Classified Data	Class1	Class 2	Class 3	Class 4	Totals
Class 1	43	2	0	0	45
Class 2	1	40	3	1	45
Class 3	0	3	32	0	35
Class 4	1	0	0	29	30
Totals	45	45	35	30	155

Table 5.6 Producer's and user's accuracy of Aster 2006 classification

Classes	Producer's accuracy	User's Accuracy	Class No.	Land cover classes
Class 1	93.4%	95.5%	1	Grass land
Class 2	90.1%	90.1%	2	Close forest
Class 3	88.8%	91.4%	3	Open forest
Class 4	96.8%	93.9%	4	Bare land

5.2 Post Classification Change Detection

Maps of the major land cover types and the changes from 2000 to 2003 and from 2003 to 2006 are shown in Figure 5.3 and Figure 5. 6. There are several ways to quantify the land cover change results. One basic method is to tabulate the totals for each land use cover type and examine the trends between the years.

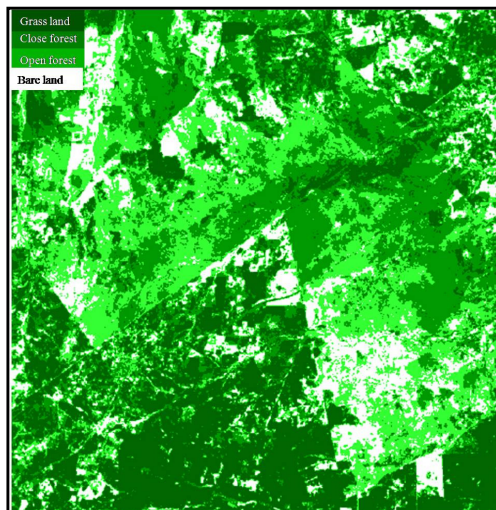


Figure 5.1: Supervised classification of ETM 2000

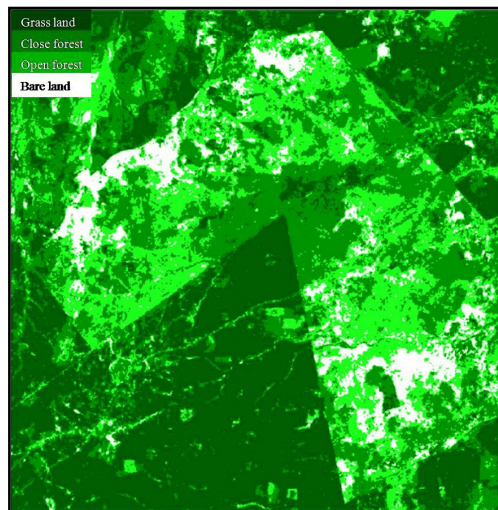


Figure 5.2: Supervised classification of ETM 2003

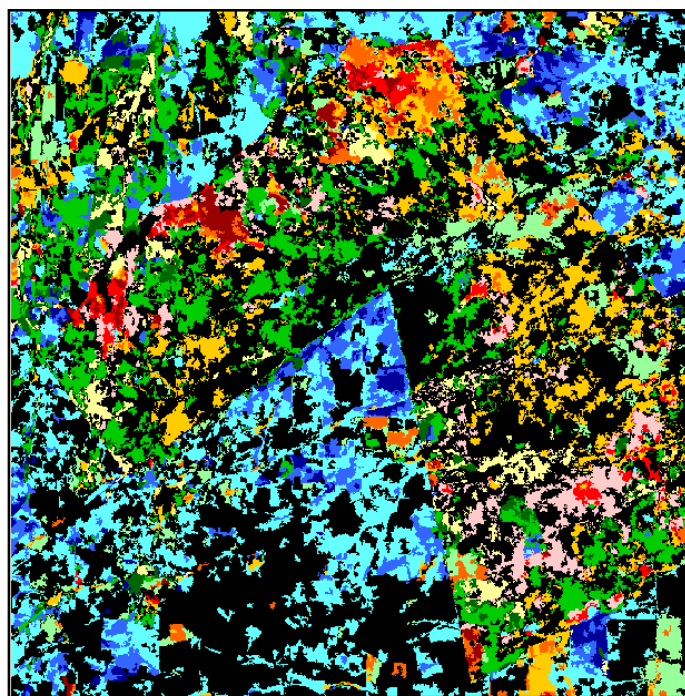


Figure 5.3: Change map

		Classification 2003			
		GL	CF	OF	BL
classification 2000	GL				
	CF				
	OF				
	BL				

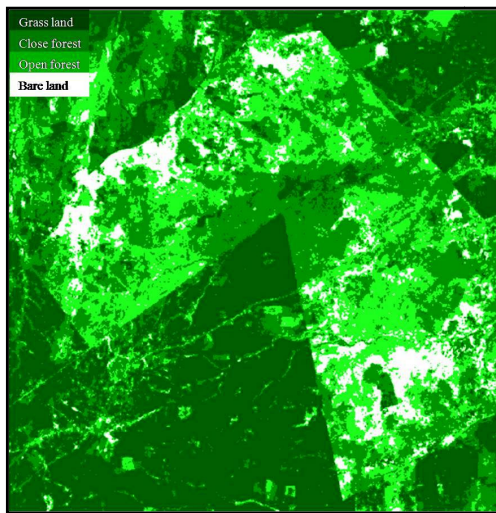


Figure 5.4: Supervised classification of ETM 2003

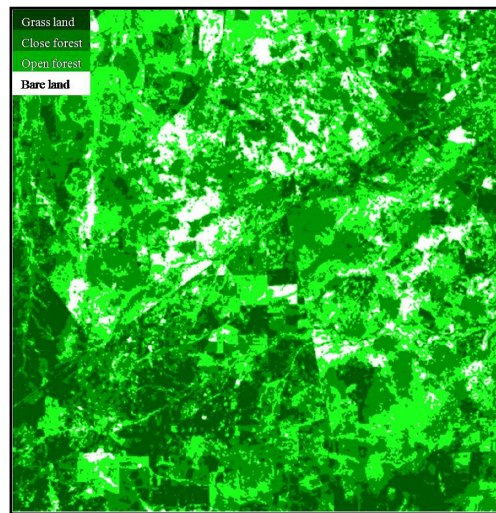


Figure 5.5: Supervised classification of Aster 2006

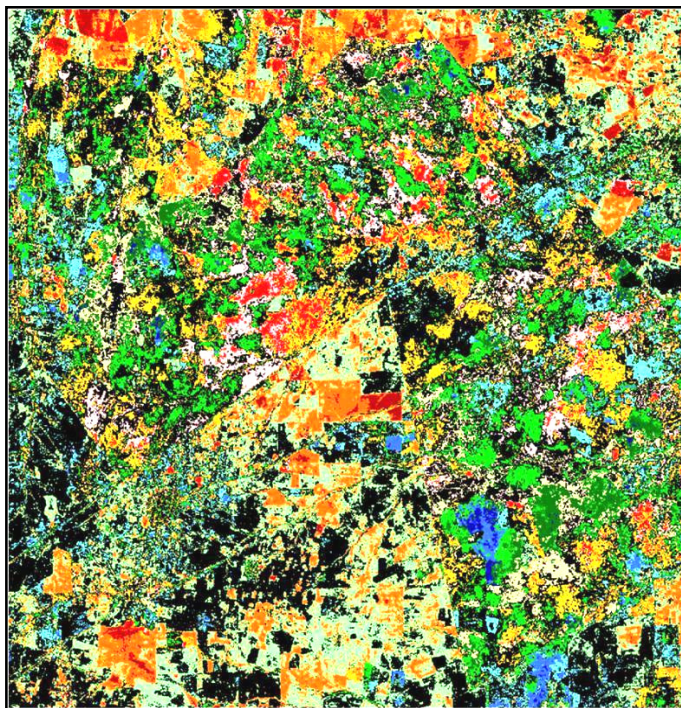


Figure 5.6: Change map

		Classification 2006			
		GL	CF	OF	BL
classification 2003	GL				
	CF				
	OF				
	BL				

The tables below demonstrate the kind of land cover changes, namely “from-to” information, that occurred during the period from 2000 to 2003. Note that the pixels without change are located along the major diagonal of this matrix.

Table 5.7: Comparison of classifications, absolute number of pixels (GL = grassland, CF = close forest, OF = open forest, BL = bare land)

		Classification 2003				Σ
		GL	CF	OF	BL	
Classification 2000	GL	223,023	47,160	23,087	12,598	305,868
	CF	176,265	179,793	84,826	16,951	457,835
	OF	64,648	108,040	142,052	38,700	353,440
	BL	25,872	23,824	33,775	23,596	107,067
	Σ	489,808	358,817	283,740	91,845	

Table 5.8: Comparison of classifications, relative number of pixels in percent (basis: all image pixels)

		Classification 2003				Σ
		GL	CF	OF	BL	
Classification 2000	GL	18.2	3.80	1.80	1.02	24.02
	CF	14.3	14.60	6.90	1.40	37.20
	OF	5.3	8.80	11.60	3.16	28.86
	BL	2.1	1.90	2.80	1.90	8.70
	Σ	40	29.1	23.1	7.5	100

Table 5.7 and 5.8 show the comparison of classification from Landsat (2000) classification and Landsat (2003) classification, i.e. absolute number of pixels and relative number of pixels (in percent of all image pixels). Grassland, close forest, open forest and bare land are the four major land cover classes. In 2000, 24.02% of all image pixels were classified as grassland, 37.2% as close forest, 28.86% as open forest and 8.7% as bare land. The total number of unchanged pixels in the two classification maps was 568.464 (46.4%). If the classes defined for 2000 are taken as basis (Table 5.9), the changes for each class turned up as follows: More than one third of closed forest (38.4%) was converted to grassland, one third of the open forest (30.5%) to close forest areas and also one third of bare land (31.5%) was turned to open forest. Only 22% of the pixels classified as bare land in 2000 do have the same class membership in 2003. The class grass land revealed fewer changes (27.1%). Less than half of the pixels in closed forest and open forest classes were assigned to the same class in 2003 (39.2% and 40.1% respectively).

Table 5.9: Comparison of classifications, relative number of pixels in percent (basis: image pixels of each class in 2000)

		Classification 2003				Σ
		GL	CF	OF	BL	
Classification 2000	GL	72.9	15.4	7.5	4.1	100
	CF	38.4	39.2	18.5	3.7	100
	OF	18.2	30.5	40.1	10.9	100
	BL	24.1	22.2	31.5	22.03	100

The tables below demonstrate the kind of land cover changes, namely “from-to” information, that occurred during the period from 2003 to 2006, note that the pixels without change are located along the major diagonal of this matrix.

Table 5.10: Comparison of classifications, absolute number of pixels (GL = grassland, CF = close forest, OF = open forest, BL = bare land)

		Classification 2006				Σ
		GL	CF	OF	BL	
Classification 2003	GL	168,68	170,22	111,15	16,59	466.66
	CF	44,17	173,48	120,87	28,56	367.09
	OF	14,83	100,84	129,62	43,71	289.01
	BL	4,52	32,50	39,84	24,56	101.43
	Σ	232,21	477,06	401,49	113,43	

Table 5.11: Comparison of classifications, relative number of pixels in percent (basis: all image pixels)

		Classification 2006				Σ
		GL	CF	OF	BL	
Classification 2003	GL	13.78	13.91	9.08	1.36	38.12
	CF	3.61	14.17	9.87	2.33	29.99
	OF	1.20	8.24	10.59	3.57	23.60
	BL	0.37	2.65	3.25	2.01	8.29
	Σ	18.97	38.97	32.80	9.27	100

Table 5.12: Comparison of classifications, relative number of pixels in percent (basis: image pixels of each class in 2003)

		Classification 2006				Σ
		GL	CF	OF	BL	
Classification 2003	GL	36.1	3.4	23.8	3.5	100
	CF	12.0	47.2	32.9	7.7	100
	OF	5.1	34.8	44.8	15.1	100
	BL	4.4	32.0	39.2	24.2	100

Table 5.10 and 5.11 show the comparison of classification from Landsat (2003) classification and Aster (2006) classification, i.e. absolute number of pixels and relative number of pixels (in percent of all image pixels). Grassland, close forest, open forest and bare land are the four major land cover classes. In 2003, 38.12% of all image pixels were classified as grassland, 29.99% as close forest, 23.6% as open forest and 8.29% as bare land. Three years later, the distribution of land cover classes changed in the following way: 18.97% grassland, 38.97% close forest, 32.8% open forest, 9.27% bare land. The percentage of unchanged pixels in the two classification maps was 496.361 (40.55%). If the classes defined for 2003 are taken as basis (Table 5.12), the changes for each class turned up as follows: Only 12% of closed forest was converted to grassland, more than one third of the open forest (34.8%) shifted to the class close forest areas. Only one third (36.1%) of the pixels classified as grassland in 2003 do have the same class membership in 2006. The class close forest implied fewer changes. About half of the class pixels (47.2%) remained close forest. For open forest, almost half of the class pixels (44.8%) were assigned to the same class in 2006. The class bare land includes the largest changes: One third (32%) of the class pixels were transformed to close forest, more than one third (39.2%) was turned to open forest. Only one fourth of the class pixels (24.2%) did not change.

5.3 Change detection based on Vegetation Indices

Vegetation index and difference images were constructed for all three vegetation indices (NDVI, SAVI and TDVI) and from all three scenes. Results showed that the vegetation index maps obtained by NDVI and SAVI transformations within each computational group were similar in terms of spatial distribution pattern and statistical characteristics. As far as the degree of greenness of vegetation was concerned, the TDVI appeared to be the most sensitive.

Change detection was performed in two ways: (i) VI differences and (ii) RGB- NDVI. The VI differences were computed from the two VI paired images, i.e., VI 2000 –VI 2003 and VI 2003 –VI 2006 and RGB-NDVI was performed using the three dates of NDVI imagery as RGB composite (Sader and Winne, 1992).

5.3.1 Vegetation Indices differences

Figure 5.7 shows vegetation index values across the study area in 2000, 2003 and 2006. As can be seen from the figure, very low index values relate to bare soil, mostly black colour that dominate in the north and in the north west of the study area,

especially in the agricultural land surrounded the forest. Relatively high vegetation index values in the center of the image represent high vegetation cover, mostly tree covers. Visual image inspection and also field checks showed that vegetation indices appear to overestimate the amount of vegetation cover in El Rawashda forest.

Changes in vegetation cover have been highlighted by subtracting 2000 vegetation index values from 2003 values and 2003 values from 2006 values (figure 5.7). Changes from 2000 to 2003 showed increased vegetation cover in the south and east south in the difference image, while changes from 2003 to 2006, showed increased vegetation cover in the center and in the west of the differencing image. These areas provide clear evidence for management related differences in vegetation cover.

To illustrate vegetation changes within El Rawashda forest, threshold have been applied to the change maps to calculate the increase, decrease and no change in vegetation cover (table 5.13).

5.3.2 5.3.2 RGB-NDVI

The RGB composite based on NDVI permits to display and understand the principal environmental dynamics, distinguishing different change classes on vegetation by different colour tones (Figure 5.8). Moreover it represents an important way to move across the dense forest areas allowing new clearing processes along their perimeter.

The visual comparisons of RGB-NDVI (2000-03-06) images are provided in Figure 5.8. Areas in red in the visual RGB-NDVI color composites indicate forest biomass decrease between 2000 and 2006. Areas in yellow are forest biomass loss between 2003 and 2006. The cyan colour indicates the regeneration between 2000 and 2006. The magenta colour displays the reduction between 2000 and 2003 and the regeneration between 2003 and 2006. The green colour displays the reduction before 2000 and after 2006. The blue colour indicates the regeneration between 2000 and 2006. Areas in black and white indicate no change.

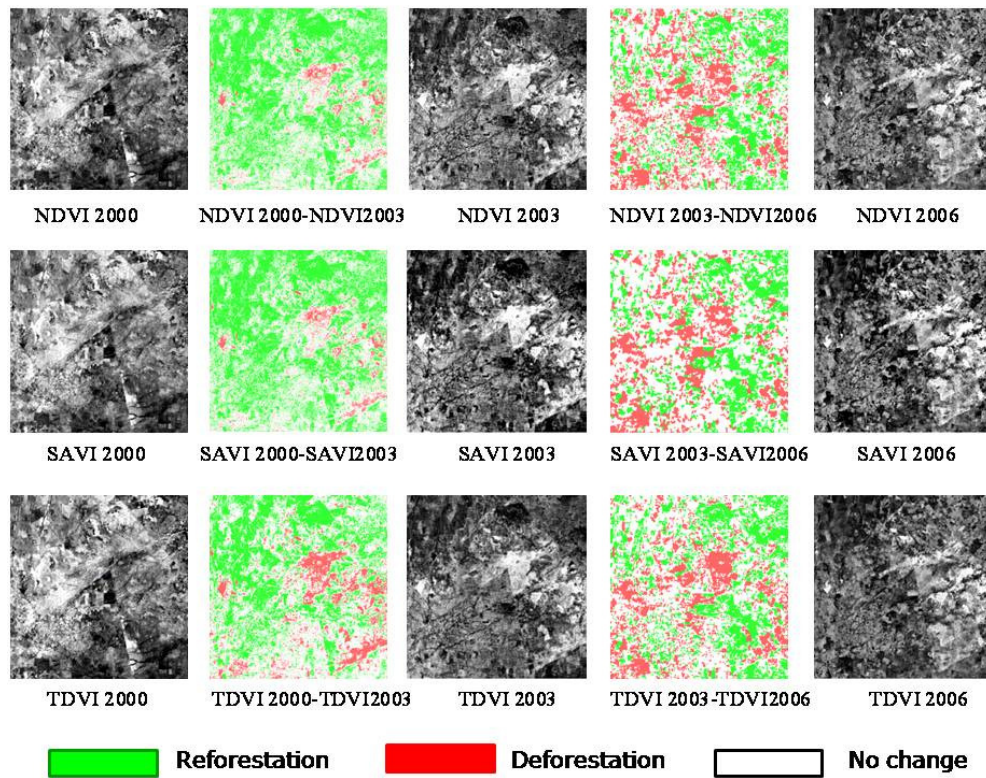
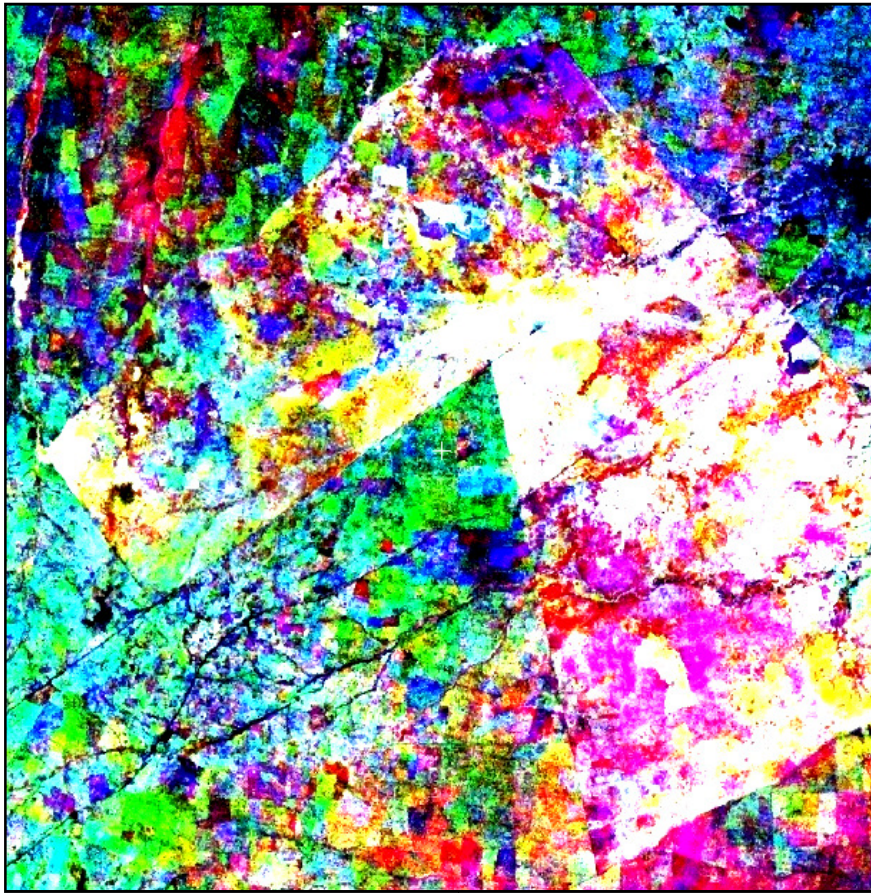


Figure 5.7: Resultant images of the NDVI, SAVI and TDVI transformation and image differencing.

Table 5.13: The percentage of increase, decrease and no change in vegetation cover

<i>VI</i>	<i>+ Change %</i>	<i>- Change %</i>	<i>No Change %</i>
NDVI2000-2003	48.7	5.0	46.3
NDVI2003-2006	26.6	26.8	46.5
SAVI2000-2003	48.8	5.0	46.2
SAVI2003-2006	25.2	28.0	46.6
TDVI2000-2003	40.0	12.9	50.1
TDVI2003-2006	32.5	26.7	51.6




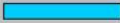


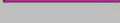



Computer Display: Image colour	RED 2000 NDVI	GREEN 2003 NDVI	BLUE 2006 NDVI	Interpretation relative to Forest canopy changes
	Low	Low	High	Cleared before 2000, regrow 2003-2006.
	Low	High	High	Cleared before 2000, regrow 2000-2006.
	Low	High	Low	Cleared before 2000, regrow 2000-2003, cleared 2003-2006.
	High	Low	Low	Cleared 2000-2003, No grow.
	High	Low	High	Cleared 2000-2003, Regrow 2003-2006
	High	High	Low	Cleared 2003-2006.
	High	High	High	No change, high NDVI Forest.
	Low	Low	Low	No change, low NDVI, Urban, pasture, other.

Figure 5.8: Simplified interpretation of three-date RGB-NDVI color composite imagery

5.4 Application of Tasseled Cap for change detection

The application of Tasseled Cap was performed in two ways: 1. RGB combination was derived from TC components of the three acquisitions separately. 2. RGB-TCG was performed using the green component of three dates of TCT imageries as RGB composite.

5.4.1 Derivation of Tasseled Cap Transformation

Figure 5.9 gives the resultant images for the derived tasseled cap transformation of the three acquisitions separately.

The RGB 123 combination resulted following the operation of a tasseled cap transformation using the first three bands proved to be particularly useful (figure 5.9). With this combination the grass land, shown in blue, can be best separated from closed forest, which shown in green in both ETM 2000 and Aster 2006 but in Cyan colour in ETM 2003. It is also possible to clearly identify the open forest and bare land which appears as red colour in all images.

The differentiation on average spatial resolution satellite images between forests and agricultural crops may be performed in the third tasseled cap dimension (wetness layer). In the greenness/ brightness projection there may appear some separation between close forest, open forest and grass land, with a specific localization of the data of the forest, whereas in the greenness/wetness projection the separation is clear, being well highlighted in the composite color images.

The differentiation based on the wetness index between forests and other crops consists in the fact that the shading phenomenon is significantly stronger in coppice as compared with agricultural crops or grassy land. Kimes et al. (1981) have shown that, relatively thick coppice tend to behave similarly to agricultural crops or grassy land with relation to the incidental radiation spread phenomenon, in the case of less thick coppice, characterized by the existence of several empty spaces, the low-frequency transmission occurrence is increased, this resulting in the amplification of the shadowing phenomenon and in the increase of the shadow percentage in the field of vision of the sensor. Moreover, any thinned out coppice containing a considerable percentage of visible trunks, as compared to agricultural crops leads to an increase in the occurrence of projected shadows both in the sublevels of the coppice and on the leaves or pins from the crown canopy of the trees.

The consideration of the shadowing phenomenon as the main cause of the different spectral behavior in the wetness component is supported both theoretically and practically. The inverse relation between radiation spread and wavelength suggests that surfaces lighted up only by the diffuse radiation may receive relatively more light in the visible and close infrared specter rather than in medium infrared (SWIR), which leads to value of the wetness component higher than could be noted in directly illuminated identical surfaces. As for the practical aspect, the simulation of the sensor signals using reflectance panels set within the range 0, 4-2, 5 μm , determines the tasseled cap values originating from shadow-like panels to be placed at the end of the raw of data simulated the same way as in the case of agricultural crops and soil reflectance.

5.4.2 Derivation of Greenness component for change detection

For change as far as the vegetation is concerned, the green layer was only used. The reflectance based greenness image, however, nearly similar to the NDVI image, and they both reveal the spatial pattern of green vegetation. For this reason the TCG composite was tried in same way as RGB-NDVI (Sader and Winne, 1992).

Figure 5.10 portrays a comparison of the Greenness component of TCT with the Normalized Difference Vegetation Index (NDVI), using ETM 2000 as an example.

The visual comparison of RGB-TCG (2000-03-06) images is provided in Figure 5.11. To some extent it resembles RGB-NDVI, but it detects changes more precisely. Note that it displays the re-growth from 2003 to 2006 in blue colour in the south east of the study area better than RGB-NDVI. Moreover it detects the re-growth from 2000 to 2003 in the north west side of the study area more clearly.

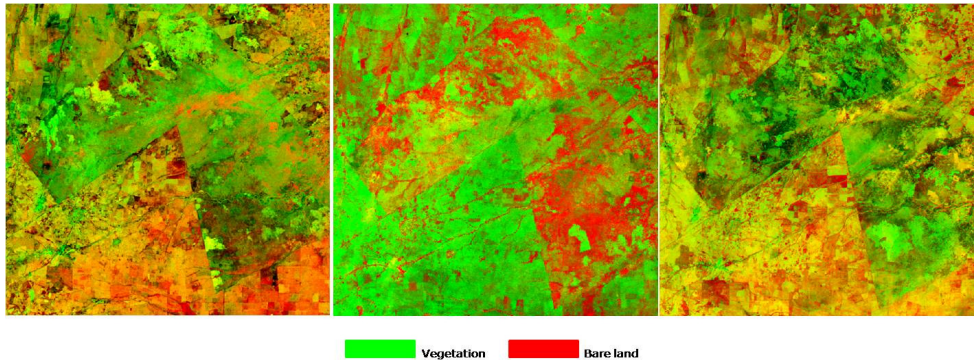


Figure 5.9: RGB composite of Tasseled Cap Transformation of ETM 2000 (left), ETM 2003 (middle) and Aster 2006 (right).

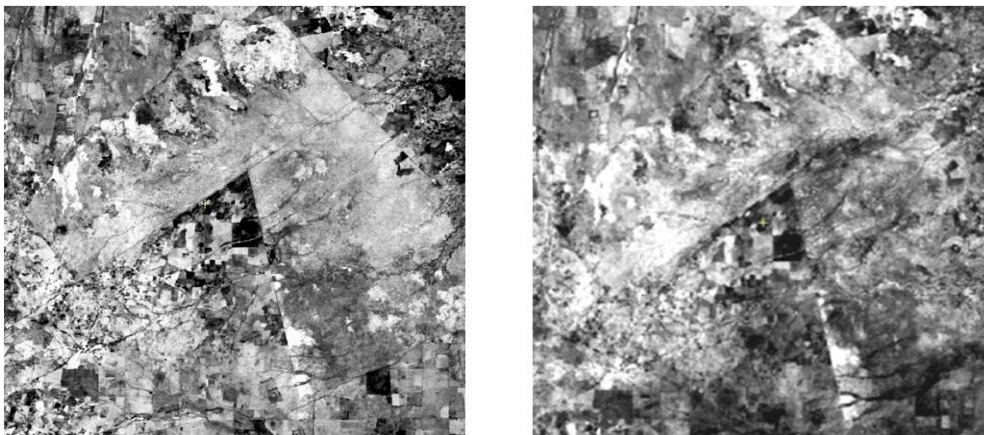
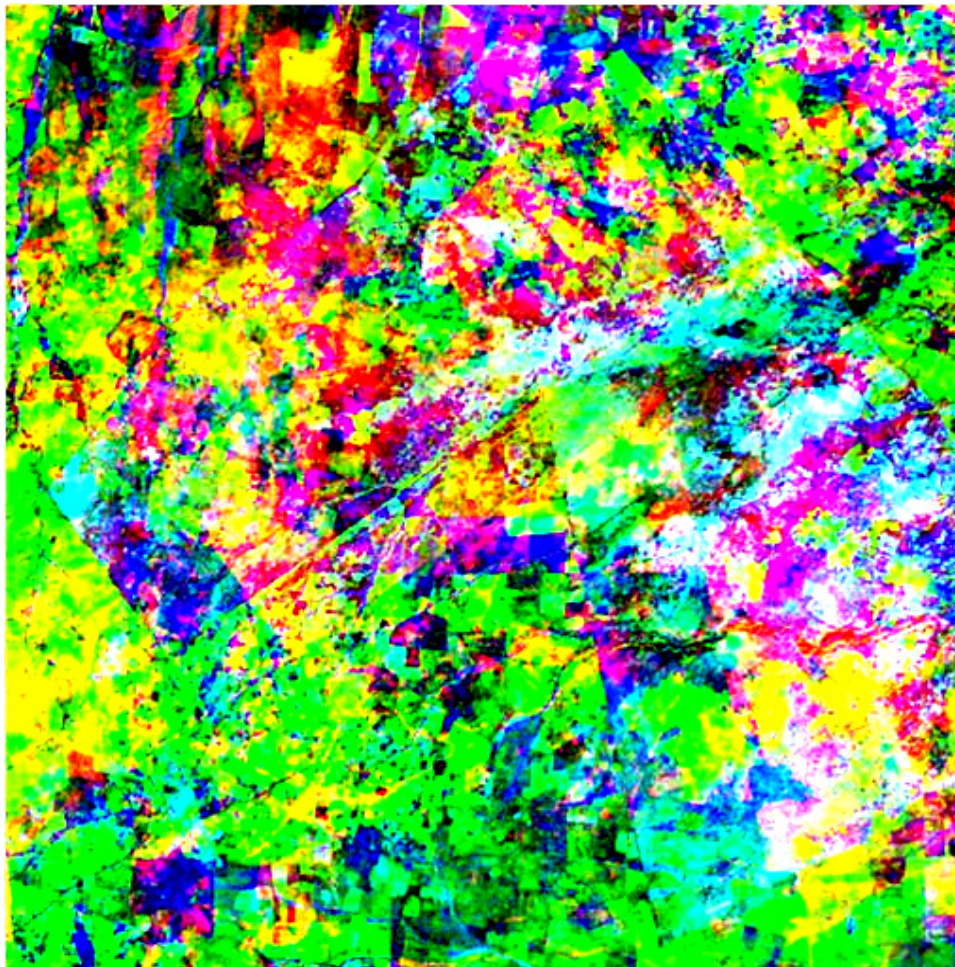


Figure 5.10: A comparison of the Greenness component of TCT (right) with the Normalized Difference Vegetation Index NDVI (left) for ETM 2000











Computer Display: Image colour	RED 2000 NDVI	GREEN 2003 NDVI	BLUE 2006 NDVI	Interpretation relative to Forest canopy changes
	Low	Low	High	Cleared before 2000, regrow 2003-2006.
	Low	High	High	Cleared before 2000, regrow 2000-2006.
	Low	High	Low	Cleared before 2000, regrow 2000-2003, cleared 2003-2006.
	High	Low	Low	Cleared 2000-2003, No grow.
	High	Low	High	Cleared 2000-2003, Regrow 2003-2006
	High	High	Low	Cleared 2003-2006.
	High	High	High	No change, high NDVI Forest.
	Low	Low	Low	No change, low NDVI, Urban, pasture, other.

Figure 5.11: Simplified interpretation of three-date RGB-TCG color composite imagery

5.5 Change Vector Analysis: An Approach for Detecting Forest Changes

For the whole study area, the CVA based on TCT is used to detect the deforestation for the two change pairs, and in this case a change image was prepared for each of the two intervals covered by the triplicate.

5.5.1 Analysis of the change image 2000/2003

The change image referring to the years 2000 and 2003 (Figure 5.12) shows an intensive dynamics related to the clear cut of primary vegetation, in a period characterized by the advancement of land occupation activities (agriculture and cattle raising) mainly in the south east, north east and west of the forest. In the other hand, the figure displays an increase of grass land or agricultural crops in the areas surrounding the forest. Two classes show this type of change specifically, with the decrease in brightness values indicating biomass loss (i.e. deforestation). A more detailed analysis of the associated colour code suggests that each of these classes represents information related to more specific changes: red colour indicates change from grass land to bare land or open forest, while green colour shows change from bare land to grass land or close forest. The magenta sector code represents change from grass land to close or open forest and the blue sector code is an indication of no change.

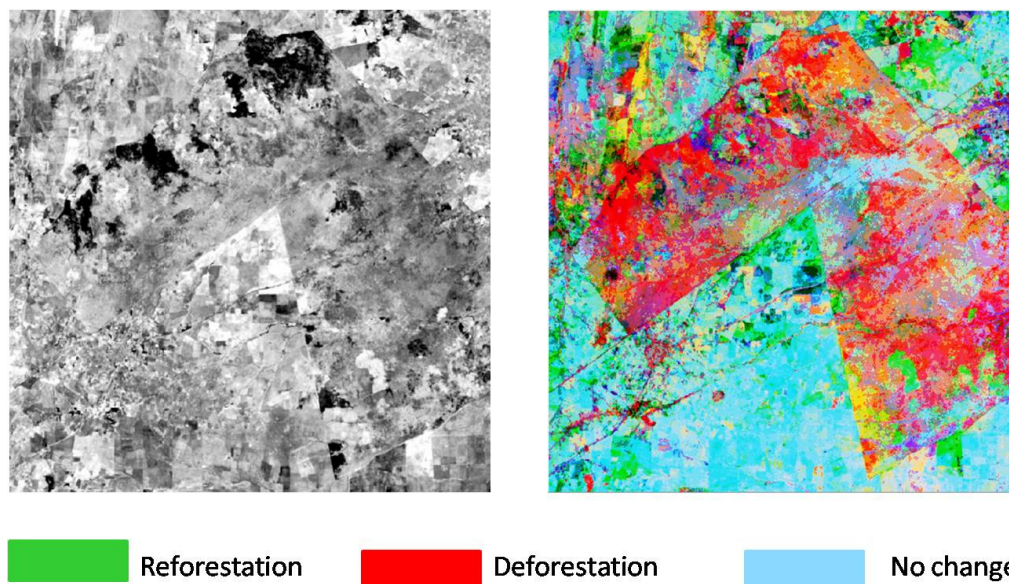


Figure 5.12: Change vector based on Tasseled Cap images from the year 2000 to 2003, magnitude (left) and direction (right)

5.5.2 Analysis of the change image 2003/2006

The Change Image referring to the period 2003/2006 (Figure 5.13), presents those elements which indicate an evolution on the land use/land cover processes. The Classes, referring to the loss of biomass, appear now with less intensity. They are more probably related to the opening of small clearances in already occupied lots for subsistence agriculture of colonists.

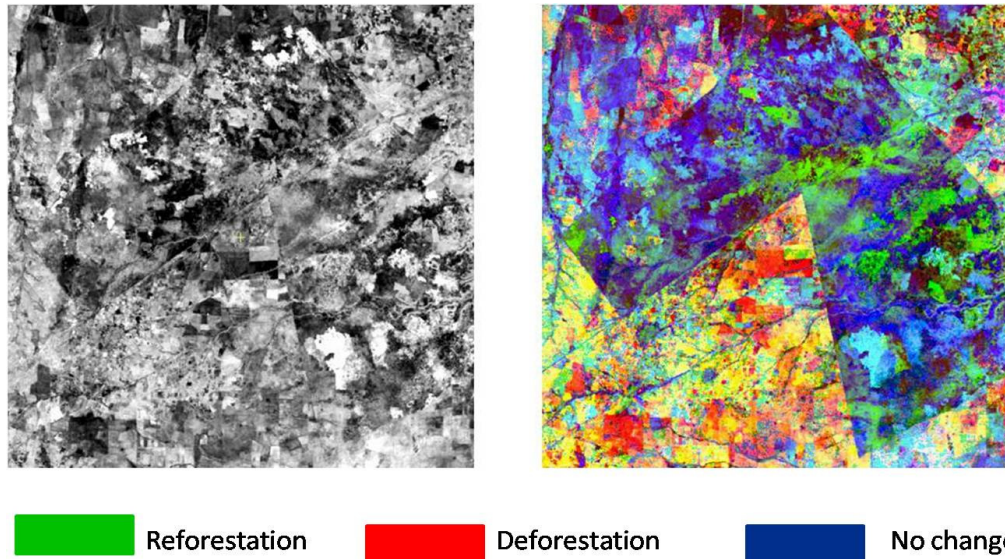


Figure 5.13: Change vector based on Tasseled Cap images from the year 2003 to 2006, magnitude (left) and direction (right)

During this second period, the area presents landscapes with higher complexity, because of the consolidation phase of rural properties and settlements, such as: different cultures in several stages of growth, diversified pastures, and re-growth sections at variable ages (shown by interference of different colours). Within this thematic diversification, the areas which were clear cut during the first period and re-growth in the second period can be better discriminated on the north east and south west inside the forest region. One can also perceive that, due to government incentives some lots get three to four cultivation cycles.

5.6 Mapping with Conventional and Selective Principal Component Analysis

5.6.1 Generation of PCA Components

The resultant images of the Principal Component Analysis generated from the three dates images are displayed in figure 5.14 while the statistics of the components are summarized in tables 5.14, 5.15 and 5.16.

Based on the eigenvalues, eigenvectors and correlation matrixes of the ETM_2000, ETM_2003 and Aster_2006 data, the first components (pc1s) contain 93.3%, 92.2% and 90.7% of the original information of the images data respectively. The lower components (i.e. pc3, pc4 etc.) are not useful and almost highlighted the redundant information. In the factor loading tables, the pc1 for the image ETM_2000 is best loaded by band 1, but negatively correlated with the other bands and pc 2 is also best loaded by band 1. In ETM_2003 pc1 is best loaded by band 3 while the pc2 is best loaded by band 5. In case of Aster_2006, the pc1 is best loaded by band 3 and pc2 is best loaded by band 2. This information was used to understand the relationship between bands and components.

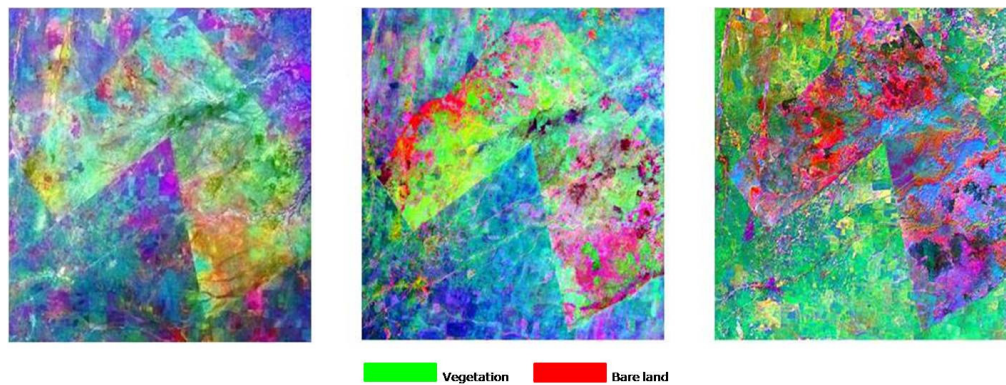


Figure 5.14: Images of the first three Principal components generated from ETM 2000 (left), ETM 2003 ETM 2003 (middle) and Aster 2006 (right)

Table 5.14: PCA Statistics of ETM_2000

Correlation Matrix	Band 1	Band 2	Band 3	Band 4	Band 5
Band1	1	-0.0069	0.0015	-0.0066	-0.0246
Band2	-0.0069	1	-0.0132	-0.0164	-0.0184
Band3	0.0015	-0.0132	1	0.0062	-0.0184
Band4	-0.0066	-0.0164	0.0062	1	0.0039
Band5	-0.0246	-0.0184	0.0024	0.0039	1

	Eigen-value	%Variance
pc1	757.2907	93.39%
pc2	36.4522	4.5%
pc3	11.2493	1.39%
pc4	2.7714	0.34%
pc5	1.5788	0.19%

Eigen-vectors	pc1	pc2	pc3	pc4	pc5
Band 1	0.9987	-0.0014	0.0001	-0.0003	-0.0008
Band 2	0.0016	0.9998	-0.0112	-0.0040	-0.0035
Band 3	-0.0010	-0.0110	-0.9994	-0.0029	-0.0005
Band 4	0.0005	0.0039	-0.0034	0.9998	0.0055
Band 5	-0.0019	0.0041	0.0018	-0.0045	0.9969

Factor Loadings	pc1	pc2	pc3	pc4	pc5
Band1	0.9599	0.9730	0.9733	0.9786	0.9127
Band2	-0.1884	-0.2143	-0.1211	0.1805	0.3509
Band3	-0.1677	-0.0587	0.1596	0.0903	-0.2000
Band4	-0.0016	0.0458	-0.0023	0.0247	-0.0371
Band5	-1221	0.0400	0.0017	-0.0156	0.0332

5.6.2 Change detection with Multitemporal PCA: the conventional approach

Table 5.17 summarizes the results of the PCA for the period 2000 to 2003. Table 5.11A shows the eigenvalues of each PC, and their associated percentages of explained variance. It can be seen that the first 3 PCs of the PCA performed on the 10 reflective bands of images explain 96.93% of the observed variance. These 3 PCs are shown in figure 5.15. The first variable or component (PC1) contains the higher variance present in the data while the subsequent variables contain decreasing proportions of scatter data. Experiments have shown that the first components contain the unchanged spectral information, while the changed information is contained in the latter components (Byrne et al, 1980). Table 5.17 B displays the loadings of the 10 Landsat bands. The loading factors for all bands of the two images exhibit a high magnitude in PC1, where all bands are positive (Table 17B), indicating that PC1 is related to general brightness. It is noteworthy that the PC1 loading factors are negative in all ETM_2000 bands except band 1 and positive in all ETM_2003 bands except band 5, which means that band 1 in ETM_2000 is positively correlated with PC1 whereas band 5 is negatively correlated with PC1.

Table 5.18 summarizes the results of the PCA for the period 2003 to 2006. Table 5.18A shows the eigenvalues of each PC, and their associated percentages of explained variance. It can be seen that the first 3 PCs of the PCA performed on the 10 reflective bands of images explain 97.46% of the observed variance. These 3 PCs are shown in figure 5.16. Similarly as in the first period, the first variable or component (PC1) contains the higher variance present in the data while the subsequent variables contain decreasing proportions of data scatter. Table 12B displays the loadings of the 10 Landsat and Aster bands. The loading factors for all bands of the two images exhibit a high magnitude in PC1, where all bands are positive (Table 5.18B), indicating that PC1 represented overall scene brightness. It is noteworthy that the PC2 loading factors are negative in all ETM_2000 bands and positive in all ETM_2003 bands except band 4 and band 5.

Visual analysis of the three PC layers for the two periods (figure 5.15 and figure 5.16) clearly shows that the change in vegetation is best detected using the second principle component (PC2). It is evident that high values (black) in PC2 represent increase in vegetated areas. These changes are more obvious in the RGB images of the three layers in green colour.

Table 5.15: PCA Statistics of ETM_2003

Correlation Matrix	Band 1	Band 2	Band 3	Band 4	Band 5
Band1	1	0.9722	0.9299	0.8986	-0.4671
Band2	0.9722	1	0.9613	0.9254	-0.5038
Band3	0.9299	0.9613	1	0.9477	-0.5218
Band4	0.8986	0.9254	0.9477	1	-0.4738
Band5	-0.4671	-0.5038	-0.5218	-0.4738	1

Eigen-vectors	pc1	pc2	pc3	pc4	pc5
Band 1	-0.9620	-0.1623	0.1863	-0.1130	0.0213
Band 2	0.1750	-0.9728	0.1146	0.0998	0.0093
Band 3	-0.1117	-0.1603	-0.9217	-0.3171	0.1075
Band 4	-0.1566	0.0363	-0.2633	0.9036	0.2978
Band 5	0.0822	0.0201	0.1818	-0.2461	0.9482

Factor Loadings	pc1	pc2	pc3	pc4	pc5
Band1	0.9559	0.0356	0.2196	0.1624	-0.1109
Band2	0.9800	0.0044	0.1672	0.0879	0.0772
Band3	0.9883	-0.0139	0.0264	-0.1205	-0.0092
Band4	0.9731	0.0715	-0.1974	0.0901	0.0021
Band5	-0.5304	0.8361	0.0778	-0.0495	0.0017

	Eigen-value	%Variance
pc1	291.7998	92.24%
pc2	12.1675	3.85%
pc3	7.4982	2.37%
pc4	3.8332	1.21%
pc5	1.0355	0.33%

Table 5.16: PCA Statistics of Aster_2006

Correlation Matrix	Band 1	Band 2	Band 3	Band 4	Band 5
Band1	1	0.9792	0.9505	0.8242	0.7598
Band2	0.9791	1	0.9700	0.8349	0.7563
Band3	0.9506	0.9700	1	0.8648	0.7804
Band4	0.8242	0.8349	0.8642	1	0.9371
Band5	0.7597	0.7565	0.7805	0.9371	1

Eigen-vector	pc1	pc2	pc3	pc4	pc5
Band 1	0.9826	0.0675	-0.1669	0.0223	0.0385
Band 2	0.0335	-0.9591	-0.1765	0.2097	-0.0611
Band 3	0.1506	-0.1021	0.9195	0.3217	0.1334
Band 4	-0.0941	0.2389	-0.2983	0.9044	0.1643
Band 5	-0.0414	-0.0891	-0.0801	-0.1842	0.9746

Factor Loadings	pc1	pc2	pc3	pc4	pc5
Band1	0.9591	0.2215	-0.1440	0.0431	-0.0977
Band2	0.9691	0.2266	-0.0517	0.0366	0.0779
Band3	0.9761	0.1583	0.1255	-0.0734	-0.0220
Band4	0.9383	-0.3295	0.0457	0.0876	-0.0071
Band5	0.8734	-0.4156	-0.1642	-0.1689	0.0168

	Eigen-value	%Variance
pc1	988.60	90.76%
pc2	77.87	7.15%
pc3	11.90	1.09%
pc4	7.47	0.69%
pc5	3.44	0.32%

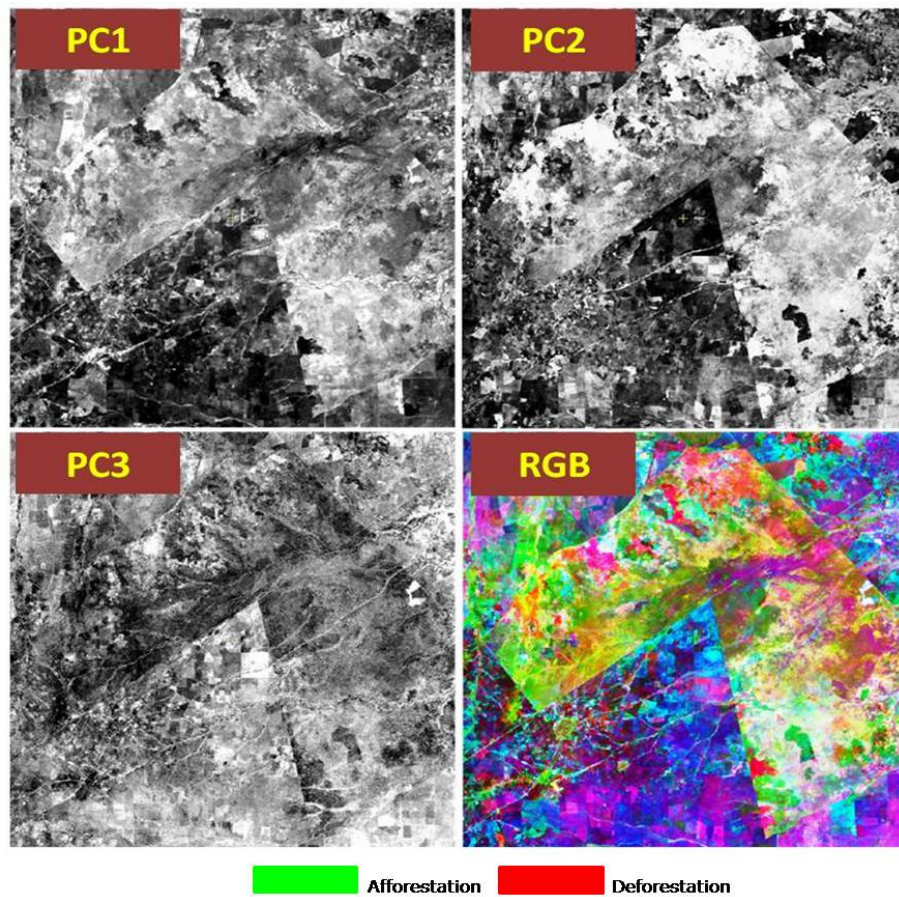


Figure 5.15: PCA generated from 10 bands combination of ETM_2000 and ETM-2003

Table 5.17: PCA Statistics of 10 bands combination of ETM_2000 and ETM_2003 data

17 A			17 B											
	Eigen-value	%Variance	Loading-factors	pc1	pc 2	pc 3	pc 4	pc 5	pc 6	pc 7	pc 8	pc9	pc 10	
pc1	805.32	69.69%		Band 1	0.8994	-0.3637	0.1613	0.1311	0.0541	-0.0010	0.0378	0.0350	-0.0348	0.0702
pc2	287.10	24.84%		Band 2	0.9067	-0.3754	0.1806	0.0282	0.0300	-0.0110	-0.0473	-0.0396	-0.0097	-0.0279
pc3	27.73	2.40%		Band 3	0.9262	-0.2920	0.1195	-0.1774	-0.0048	-0.0346	0.0234	-0.0059	0.0445	0.0220
pc4	13.10	1.13%		Band 4	0.9648	-0.1907	-0.1441	-0.0870	-0.0368	-0.0126	-0.0426	0.0231	-0.0345	-0.0052
pc5	7.32	0.63%		Band 5	0.9232	-0.1116	-0.2965	0.1850	-0.0200	0.0410	0.0014	-0.0579	0.0263	0.0019
pc6	4.28	0.37%		Band 6	0.6092	0.7508	0.1281	0.1016	-0.1178	-0.0300	-0.0776	0.0469	0.0312	0.0302
pc7	3.75	0.33%		Band 7	0.6156	0.7679	0.1149	0.0480	-0.0890	0.0112	-0.0506	-0.0321	-0.0541	0.0055
pc8	2.36	0.20%		Band 8	0.6150	0.7687	0.0378	-0.0899	-0.0179	0.0323	0.1072	-0.0276	-0.0013	-0.0151
pc9	1.67	0.14%		Band 9	0.6348	0.7425	-0.0795	-0.0114	0.1891	-0.0283	-0.0569	-0.0016	-0.0059	0.0038
pc10	1.05	0.09%		Band 10	0.2373	-0.4533	-0.2390	0.2651	-0.1210	-0.7295	0.1650	-0.0836	-0.0450	-0.0149

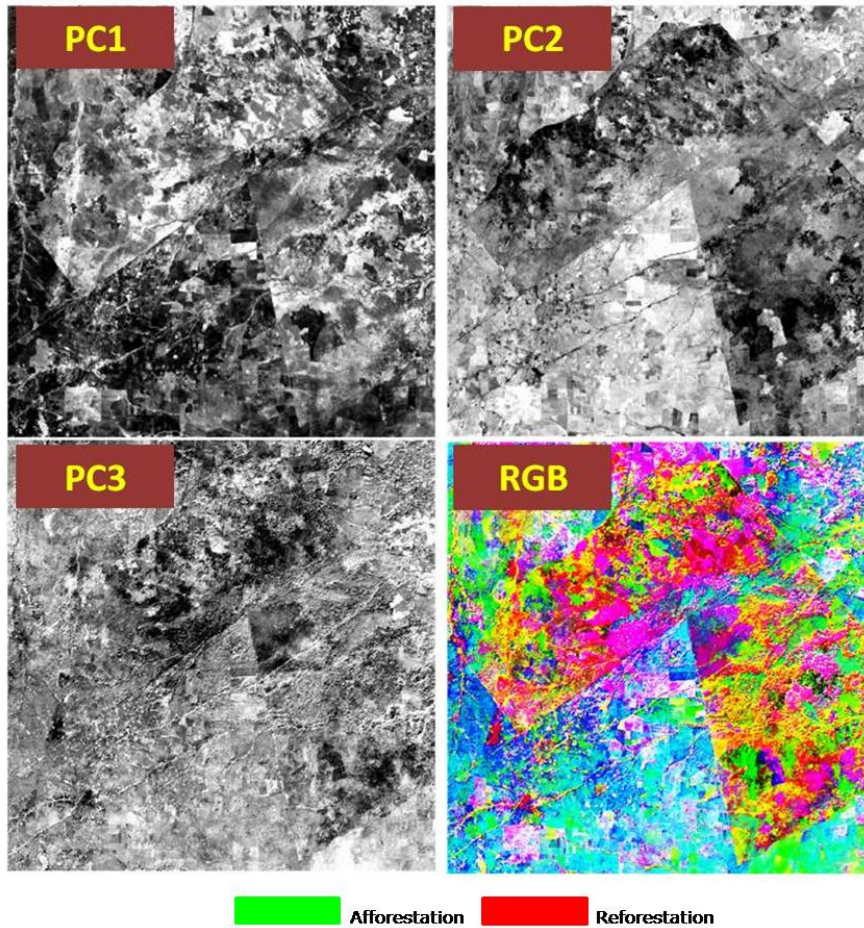


Figure 5.16: PCA generated from 10 bands combination of ETM 2003 and Aster 2006

Table 5.18: PCA Statistics of 10 bands combination of ETM_2003 and Aster_2006 data

18 A			18 B										
	Eigen-value	%Variance	Loading-factors	pc1	pc 2	pc 3	pc 4	pc 5	pc 6	pc 7	pc 8	pc9	pc 10
pc1	1012.3	74.91	Band 1	0.4475	-0.8280	0.1776	0.1000	-0.0509	-0.1740	-0.0633	0.0646	0.1189	0.1058
pc2	242.9	17.98	Band 2	0.4502	-0.8553	0.1681	0.0497	-0.0420	-0.1332	-0.0498	0.0457	0.0393	-0.0768
pc3	61.7	4.57	Band 3	0.4568	-0.8694	0.1076	-0.0618	0.0460	-0.0251	-0.0321	-0.0639	-0.0842	0.0139
pc4	11.6	0.86	Band 4	0.4865	-0.8444	0.0389	0.0481	0.0260	0.1504	0.1364	0.0332	0.0328	-0.0009
pc5	8.5	0.63	Band 5	0.0861	0.5346	-0.2152	0.5126	0.5660	-0.2184	0.1193	-0.0067	-0.0308	-0.0010
pc6	5.8	0.43	Band 6	0.9412	0.2239	0.1814	0.1160	-0.0827	0.0017	0.0298	-0.1027	0.0223	-0.0031
pc7	3.7	0.28	Band 7	0.9503	0.2323	0.1841	0.0401	-0.0449	-0.0042	0.0242	0.0651	-0.0389	0.0034
pc8	2.5	0.19	Band 8	0.9646	0.1688	0.1395	-0.0888	0.1067	0.0304	-0.0218	0.0002	0.0333	-0.0036
pc9	1.4	0.11	Band 9	0.9432	-0.0116	-0.3161	-0.0598	-0.0252	-0.0510	-0.0514	0.0019	0.0072	-0.0002
pc10	0.4	0.04	Band 10	0.8908	-0.1201	-0.3634	0.1615	-0.0114	0.1118	-0.1208	-0.0120	0.0029	0.0007

5.6.3 Change detection with Selective PCA

Table 5.19 and table 5.20 summarize the results of the selective PCA for the period 2000 to 2003 and for the period 2003 to 2006 respectively. The second component (PC2) of the NIR band exhibited the strongest vegetation gradient, having high positive factor loadings for the NIR band for both dates (0.96 and 0.85, respectively) for the first period. For the second period, PC2 have a negative factor loading (-0.88) for the NIR bands for time 1 but positive loading (0.46) for time 2. Based on these results, PC2 of the NIR was selected for use in analysis of vegetation change (figure 5.17).

Table 5.19: PCA Statistics from 10 bands of ETM_2000 and ETM_2003 data by band wise

19 A				19 B											
		Eigen-value	%Variance	Loading-factors	pc1	pc 2	pc 1	pc 2	pc 1	pc 2	pc 1	pc 2	pc1	pc 2	
T1b2- T2b2	pc1	1012.3	70.40	Band 1	-0.9108	0.3170	-0.9587	0.2889	-0.9515	0.2358	-0.6603	-0.6645	-0.8419	0.3597	
	pc2	242.9	29.60	Band 2	-0.8853	0.3145	-0.9390	0.2843	-0.9690	0.2485	-0.6732	-0.6925	-0.8536	0.3781	
T1b3- T2b3	pc1	61.7	69.54	Band 3	-0.8590	0.2419	-0.9140	0.2068	-0.9506	0.9685	-0.7600	-0.6483	-0.8966	0.3176	
	pc2	11.6	30.46	Band 4	-0.8817	0.1507	-0.9080	0.1053	-0.9301	0.0605	-0.7864	-0.5310	-0.9734	0.2308	
T1b4- T2b4	pc1	8.5	70.26	Band 5	-0.8763	0.0880	-0.8698	0.0376	-0.8608	-0.0146	-0.7338	-0.4037	-0.9309	0.1368	
	pc2	5.8	29.74	Band 6	-0.5947	-0.7905	-0.5397	-0.7792	-0.4957	-0.7955	-0.7940	0.4234	-0.5818	-0.6644	
T1b5- T2b5	pc1	3.7	68.76	Band 7	-0.5744	-0.7495	-0.5547	-0.8238	-0.5126	-0.8308	-0.8307	0.4426	-0.5978	-0.6882	
	pc2	2.5	31.24	Band 8	-0.5617	-0.7410	-0.5415	-0.8070	-0.5160	0.8540	-0.8510	0.4576	-0.6091	-0.7062	
T1b7- T2b7	pc1	1.4	79.06	Band 9	-0.5382	-0.7093	-0.5130	-0.7809	-0.4893	-0.8301	-0.8832	0.4670	-0.6260	-0.7106	
	pc2	0.4	20.94	Band 10	-0.5583	-0.6775	-0.5239	-0.7416	-0.4973	-0.7891	-0.8452	0.4324	-0.6654	-0.7433	
T1 (ETM2000), T2 (ETM2003)				Band 1 – Band 5 (ETM2000), Band 6 – Band 10 (ETM2003)											

Table 5.20: PCA Statistics from 10 bands of ETM_2003 and Aster_2006 data by band wise

20 A				20 B											
		Eigen-value	%Variance	Loading-factors	pc1	pc 2	pc 1	pc 2	pc 1	pc 2	pc 1	pc 2	pc1	pc 2	
T1b2-T2b2	pc1	160.1	84.40	Band 1	-0.3414	-0.9349	-0.3470	-0.9056	-0.4419	-0.8164	-0.4966	-0.7464	-0.4388	0.4627	
	pc2	29.6	15.60		-0.3293	-0.9098	-0.3431	-0.9367	-0.4484	-0.8482	-0.5076	-0.7714	-0.4430	0.5002	
T1b3-T2b3	pc1	260.7	81.57	Band 3	-0.3078	-0.8724	-0.3222	-0.9028	-0.4679	-0.8806	-0.5347	-0.7788	-0.4635	0.5192	
	pc2	58.9	18.43		-0.3360	-0.8286	-0.3471	-0.8554	-0.4718	-0.8199	-0.5808	-0.8105	-0.5283	0.4697	
T1b4-T2b4	pc1	294	76.22	Band 5	0.0195	0.4896	0.0428	0.5218	0.1092	0.5336	0.1233	0.4950	0.0222	-0.9959	
	pc2	91.7	23.78		-0.9972	0.0720	-0.9762	0.0749	-0.9285	0.2135	-0.7990	0.2298	-0.7600	-0.0231	
T1b5-T2b5	pc1	322.1	82.20	Band 7	-0.9762	0.0714	-0.9963	0.0850	-0.9463	0.2252	-0.8081	0.2416	-0.7564	-0.0094	
	pc2	69.7	17.80		-0.9505	0.0283	-0.9705	0.0336	-0.9865	0.4664	-0.8449	0.1990	-0.7803	0.0125	
T1b7-T2b7	pc1	102	86.25	Band 9	-0.8318	-0.0934	-0.8455	-0.0969	-0.8758	0.0038	-0.9882	0.1551	-0.9371	0.0349	
	pc2	16.2	13.75		-0.7730	-0.1813	-0.7738	-0.1866	-0.8062	-0.0952	-0.9438	0.0268	-0.9996	0.0112	
T1 (ETM2003), T2 (Aster2006)				Band 1– Band 5 (ETM2003), Band 6– Band 10 (Aster2006)											

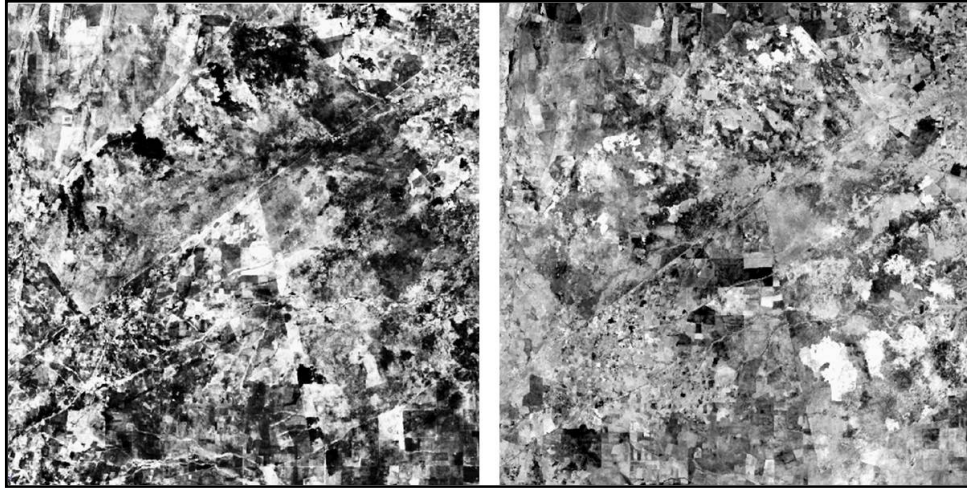


Figure 5.17: PC2 generated from NIR of ETM_2000 and NIR of ETM_2003 (left), and PC2 generated from NIR of ETM_2003 and NIR of Aster-2006

5.7 Change Detection based on Multivariate Alteration Detection (MAD)

MAD process was applied to every pair of images of the two periods. As a result we obtain as many MAD bands as input channels. The MAD components have maximum variance subject to the condition that the pixel intensities are statistically uncorrelated with each other. Figure 5.18 shows a scatter plot of MAD1 vs. MAD2 for ETM_2000 and ETM_2003. It is clear that the components are uncorrelated. Assuming that different kinds of changes will generally be uncorrelated with one another, these changes will be distributed among different MAD components. Noise will be concentrated in lower order components (Canty et al., 2001).

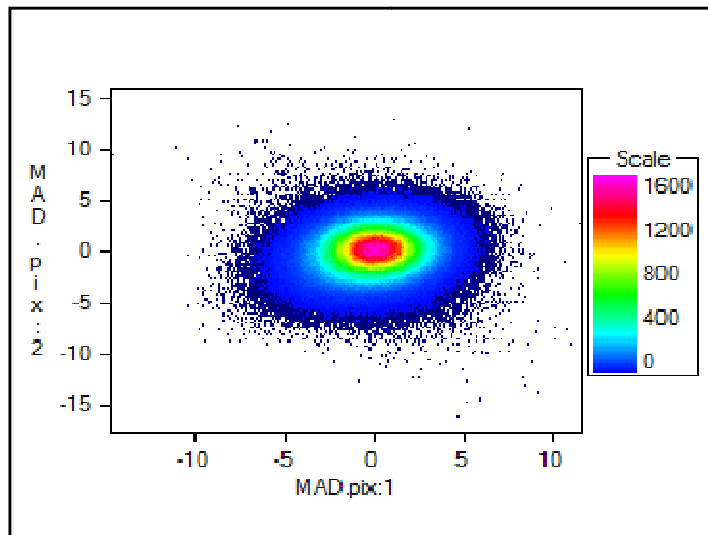


Figure 5.18: Scatter plot MAD1 vs. MAD2

5.7.1 MAD Interpretation

The interpretation of the resulting change images was based on correlations between the transformed variates and the original data. Table 5.21 and Table 5.22 show the correlations between the MAD and the original bands of the first period (2000 to 2003) and the second period (2003 to 2006) respectively.

For the first period, MAD 3 correlation shows a weighted mean of NIR with positive correlation in ETM_2000 image (0.42) and negative correlation in ETM_2003 image (-0.49). Therefore MAD 3 is probably an indicator of vegetation changes. Actually, if we consider MAD 3 (Figure 5.19) we can identify slight positive and negative changes in different parts of the forest, which are effected by intense shadowing of Acacias trees. The correlation of MAD 4 shows a weighted mean of all channels with positive correlation in ETM_2000 image and negative correlation in all ETM_2003 band except band 1. Therefore MAD 4 is probably an indicator of shadow-induced changes. Actually, if we consider MAD 4 in figure 5.19 we can identify clearly positive change in white colour located in the south region inside the forest in different pars outside the forest and negative changes located in the north region of the forest. In MAD2 and MAD 5 there are smaller changes that are uncorrelated to each other. MAD 6 is weakly correlated to all bands in both years and shows scanner noise.

For the second period, the correlation of MAD 3 and MAD 5 have highest correlation in all channels, with negative correlation in ETM image and positive correlation in Aster image. Therefore MAD 3 and MAD 5 are probably indicators of vegetation changes. Actually, if we consider MAD 3 and MAD 5 (Figure 5.20) we can identify positive and negative changes more clearly than in other MAD components. MAD 2 shows small areas of changes in vegetation and has slightly low correlation with the original bands. MAD 1 and MAD 4 are uncorrelated with all bands in both years, MAD 1 shows image noise.

Table 5.21: Correlation matrix of the MAD components with the original ETM_2000 and ETM_2003 bands

<i>Original bands</i>	<i>MAD 1</i>	<i>MAD 2</i>	<i>MAD 3</i>	<i>MAD 4</i>	<i>MAD 5</i>
ETM_2000b2	0.10	0.22	0.29	0.25	0.04
ETM_2000b3	0.03	-0.15	0.37	0.27	0.05
ETM_2000b4	0.04	0.07	0.42	0.30	-0.06
ETM_2000b5	0.01	0.04	0.40	0.37	-0.04
ETM_2000b7	0.02	0.02	0.29	0.35	0.07
ETM_2003b2	-0.01	-0.02	0.10	0.25	0.20
ETM_2003b3	-0.16	-0.18	-0.48	-0.34	0.01
ETM_2003b4	-0.17	-0.18	-0.49	-0.36	-0.02
ETM_2003b5	-0.16	-0.16	-0.48	-0.38	-0.03
ETM_2003b7	-0.14	-0.13	-0.44	-0.38	0.01

Table 5.22: Correlation matrix of the MAD components with the original ETM 2003 and Aster 2006 bands

<i>Original bands</i>	<i>MAD 1</i>	<i>MAD 2</i>	<i>MAD 3</i>	<i>MAD 4</i>	<i>MAD 5</i>
ETM_2003b2	0.01	-0.18	-0.35	-0.19	-0.33
ETM_2003b3	-0.13	-0.19	-0.33	-0.15	-0.36
ETM_2003b4	-0.09	-0.20	-0.28	-0.05	-0.4
ETM_2003b5	-0.07	-0.22	-0.14	-0.17	-0.39
ETM_2003b7	0.06	0.56	0.23	-1.31	0.23
Aster_2006b1	-0.05	0.04	0.61	0.14	0.23
Aster_2006b2	0.09	0.06	0.63	0.10	0.24
Aster_2006b3	0.06	0.04	0.61	0.02	0.30
Aster_2006b4	0.01	0.31	0.36	0.13	0.39
Aster_2006b5	0.02	0.16	0.24	0.22	0.38

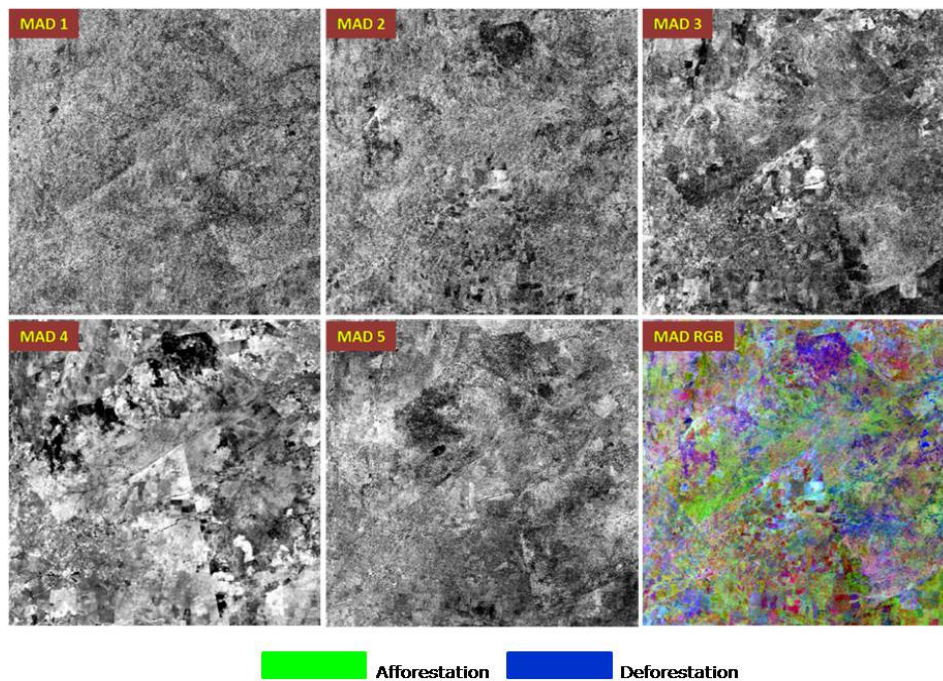


Figure 5.19: MAD components of ETM2000 and ETM2003 and the first three components as RGB

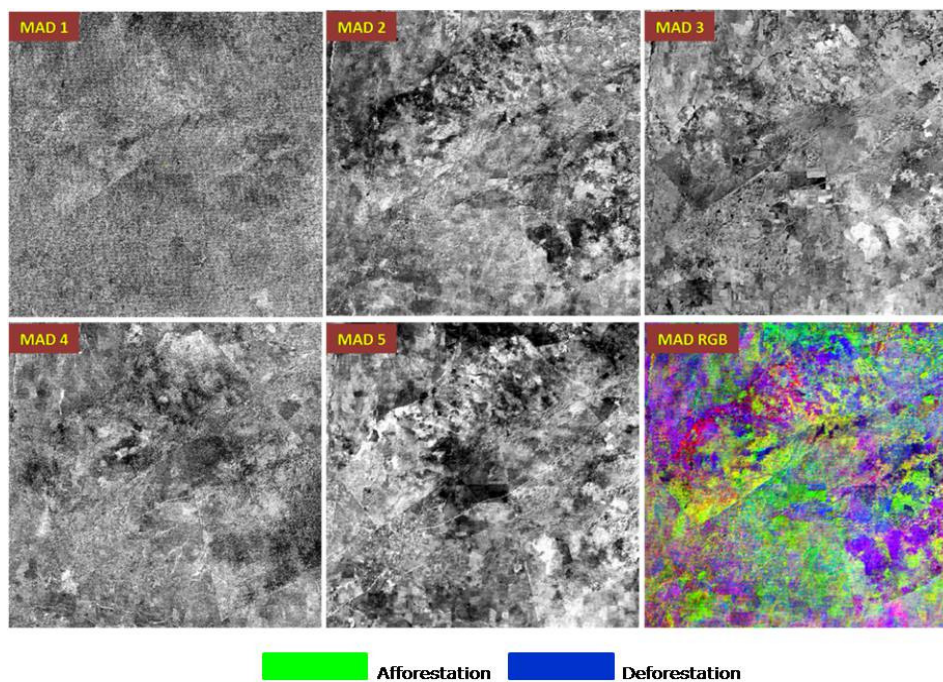


Figure 5.20: MAD components of ETM2003 and Ater2006 and the first three components as RGB

5.7.2 Maximum autocorrelation factor (MAF) analysis

To find maximum change areas with high spatial autocorrelation a MAF post-processing of the MAD variates was applied. Figure 5.21 and Figure 5.22 show the MAF/MADs of the first period images (2000 to 2003) and of the second period images (2003 to 2006) respectively. In both cases areas that are very bright or very dark are maximum change areas and with high spatial autocorrelation. It is noted that in contrast to MAD components, the change information from all bands is concentrated in the first two or three MAF/MADs whereas the low order MADs are quite noisy. If we consider MAD/MAF 1 of the first period we realized that positive change areas are shown as white colour in the south region inside the forest boundary and in different places outside the forest boundary. If we consider MAD/MAF 1 of the second period, the positive change areas again shown as white colour in the south, east and small patches in north parts inside the forest. MAD/MAF RGB of the first three components in both periods detects changes more clearly than MAD RGB components.

For discriminating change and no-change pixels a procedure suggested by Bruzzone and Prieto (2000), was applied to MAD/MAF components to determine automatically the decision thresholds for change and no change. These change areas are shown in Figures 5.23 for the first and second periods.

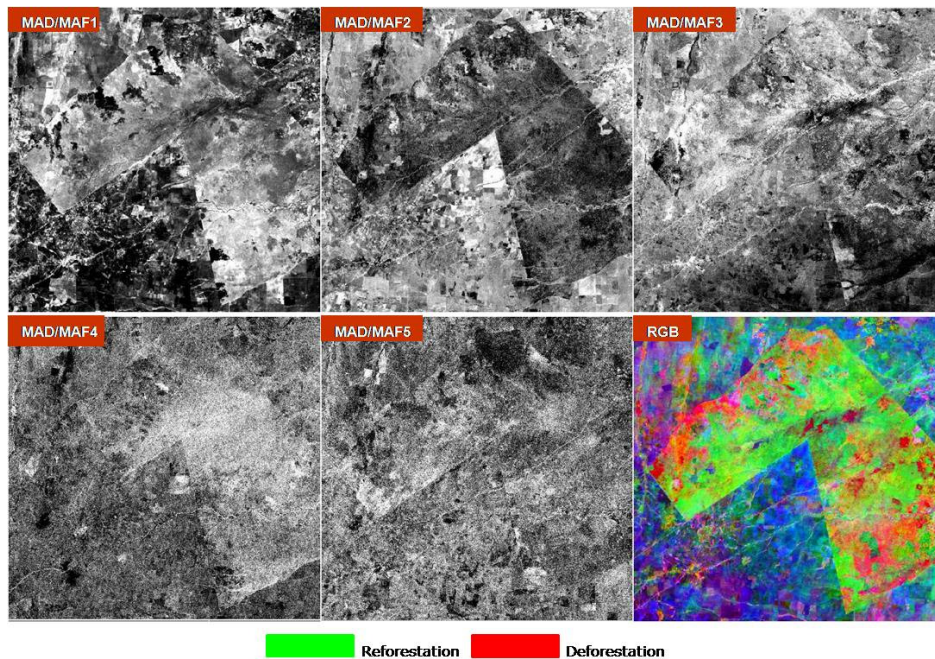


Figure 5.21: MAD/MAF components of ETM2000 and ETM2003 and the first three components as RGB

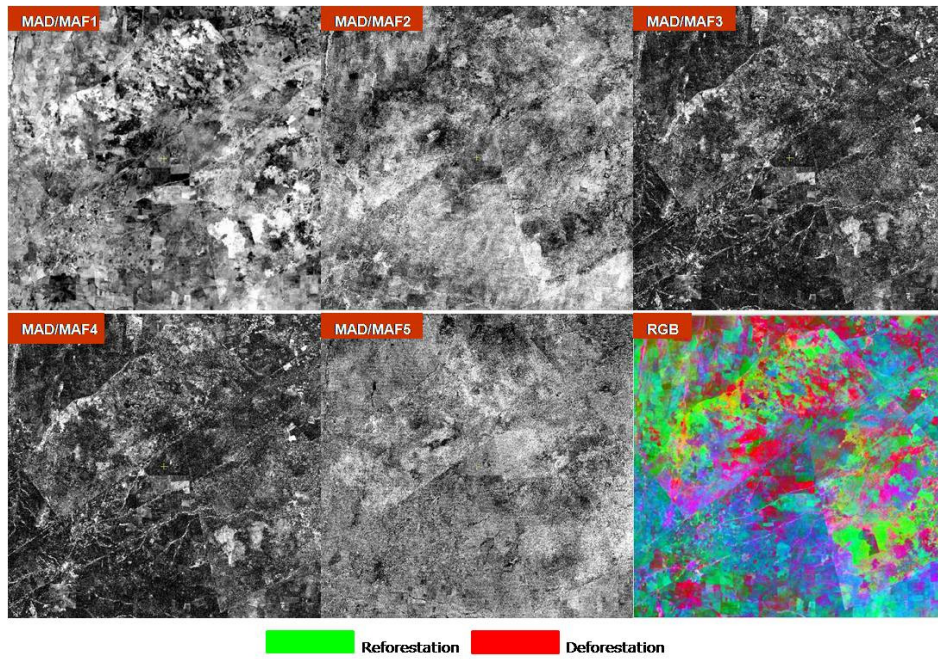


Figure 5.22: MAD/MAF components of ETM_2003 and Aster_2006 and the first three components as RGB

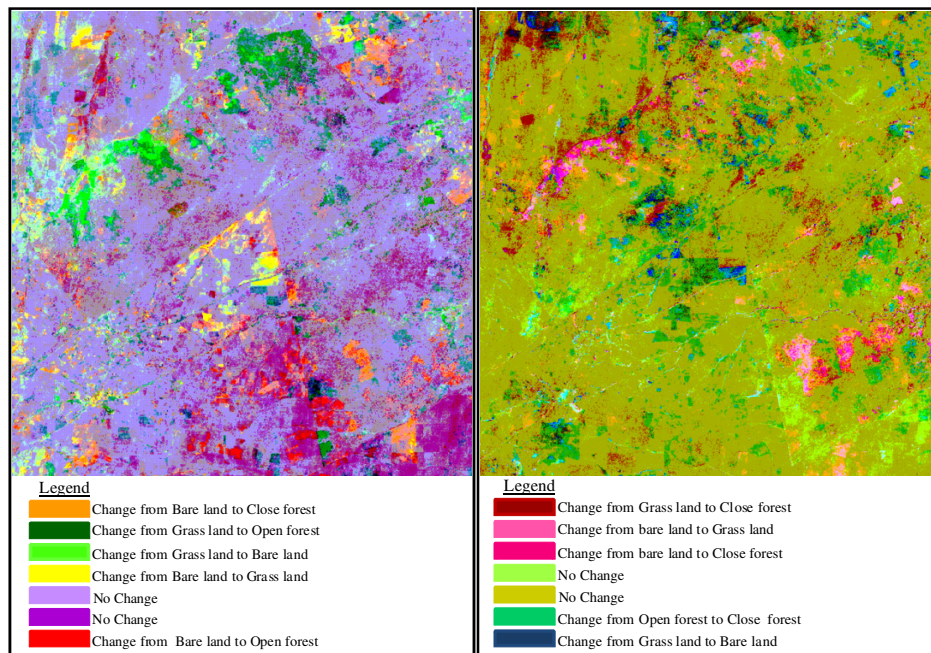


Figure 5.23: Changes given by the MAD/MAF of the first three components from ETM_2000 and ETM_2003 (left) and from ETM_2003 and Aster_2006 (right) with automatic threshold

5.8 Accuracy assessments for change detection techniques

Figure 5.24 and table 5.23 show the assessment of overall vegetation change using different change detection methods for the first period (2000 - 2003). The software eCognition was used for manual generated classification to develop a reference map (Figure 5.26).

Land cover changed map with a higher accuracy produced by Post classification comparison (PCC), this method correctly detect vegetation loss and gain. All the tested methods detected the presence of change in a given local area equally well, but TDVI shows omission in detecting vegetation gain in many areas. PCC and CVA mapped vegetation loss in most areas in a more spatially complete and accurate manner.

Figure 5.25 and table 5.24 show the assessment of overall vegetation change using different change detection methods for the first period (2003 - 2006). The software eCognition was used for manual generated classification to develop a reference map. For this period also land cover changed map with a higher accuracy produced by Post classification comparison (PCC), the method detected the presence of reforestation and deforestation in most areas in a very accurate manner. Land cover changed maps with lowest accuracy were all produced with VI differencing technique.

Table 5.25 and figure 5.27 illustrate the accuracy assessment for change detection techniques from the 2000 and 2003 dates. Accuracy of the change image was estimated at change/no change detection level. The highest accuracy was obtained by PCC (90.6%) The accuracy assessments for the others change detection methods were 60.8% (NDVI), 62.5% (SAVI), 59.5% (TDVI), 53.1% (TCA), 84.4% (PCA), 75% (MAD) and 65.3% (CVA) respectively.

Table 5.26 and figure 5.28 illustrate the accuracy assessment for change detection techniques from the 2003 and 2006 dates. The highest accuracy was also obtained by PCC (87%) Accuracy of the change image was estimated at change/no change detection level (Fig. 1) the accuracy assessments were 59.2% (NDVI), 59.9% (SAVI), 60.1% (TDVI), 62.2% (TCA), 68.6% (PCA), 60.09% (MAD) and 71.6% (CVA) respectively.

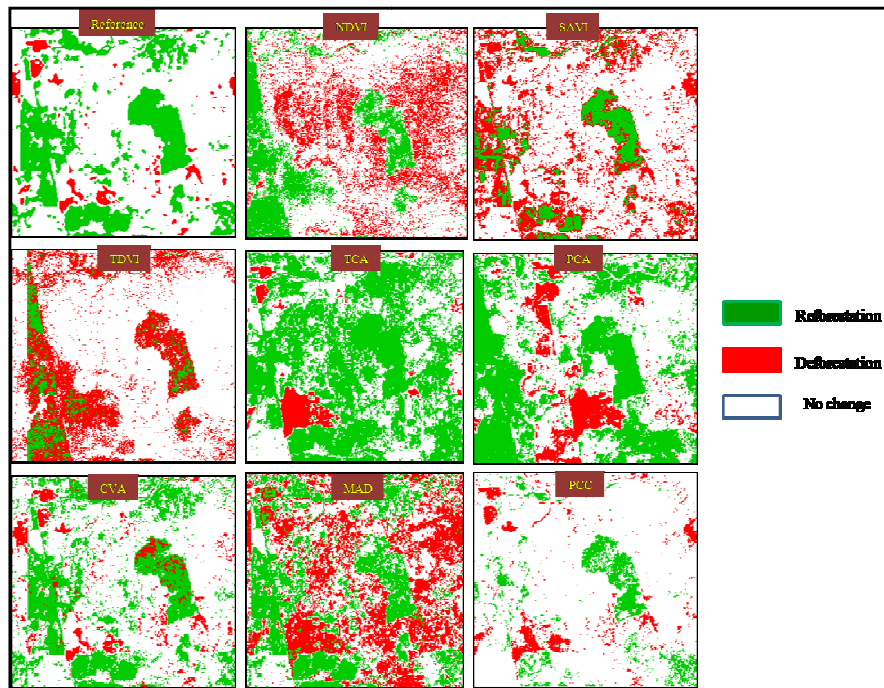


Figure 5.24: Change / no change map given by different change detection techniques (2000-2003)

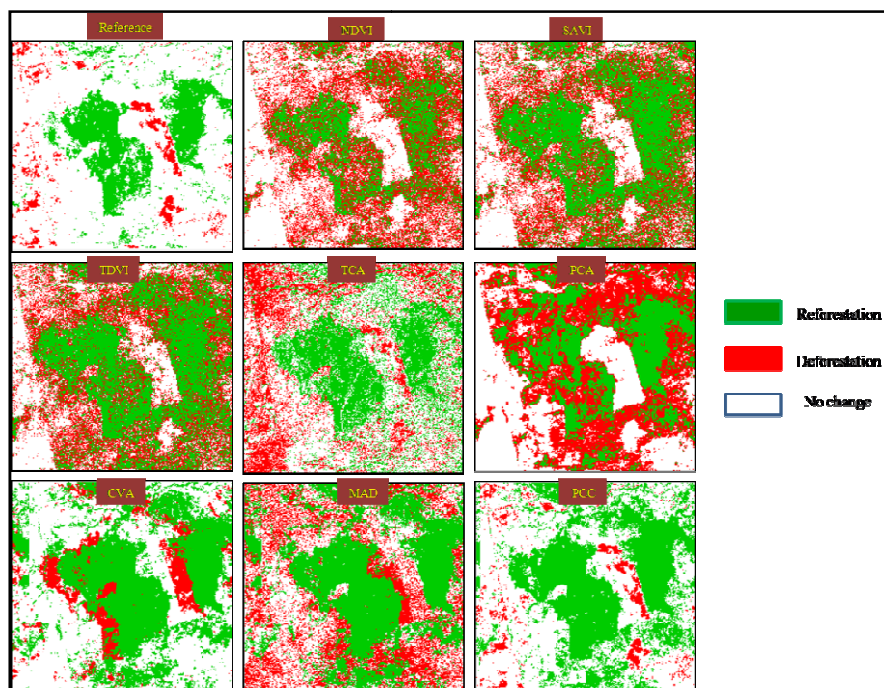


Figure 5.25: Change / no change map given by different change detection techniques (2003-2006)

Table 5.23: Percentages of Reforestation, Deforestation and No change (2000-2003)

<i>Method</i>	<i>Reforestation</i>	<i>Deforestation</i>	<i>No change</i>
Reference	28.0	7.7	64.3
NDVI	48.4	12.6	39.0
SAVI	50.0	9.9	40.1
TDVI	36.2	25.6	38.2
TC	51.7	14.2	34.1
CVA	51.6	6.4	42.0
PCA	32.4	13.3	54.3
MAD	27.1	24.7	48.2
PCC	36.4	5.6	58.2

Table 5.24: Percentages of Reforestation, Deforestation and No change (2003-2006)

<i>Method</i>	<i>Reforestation</i>	<i>Deforestation</i>	<i>No change</i>
Reference	20.0	20.0	20.0
NDVI	32.4	32.4	32.4
SAVI	32.4	32.4	32.4
TDVI	26.6	26.6	26.6
TC	22.3	22.3	22.3
CVA	29.3	29.3	29.3
PCA	26.0	26.0	26.0
MAD	32.1	32.1	32.1
PCC	26.9	26.9	26.9

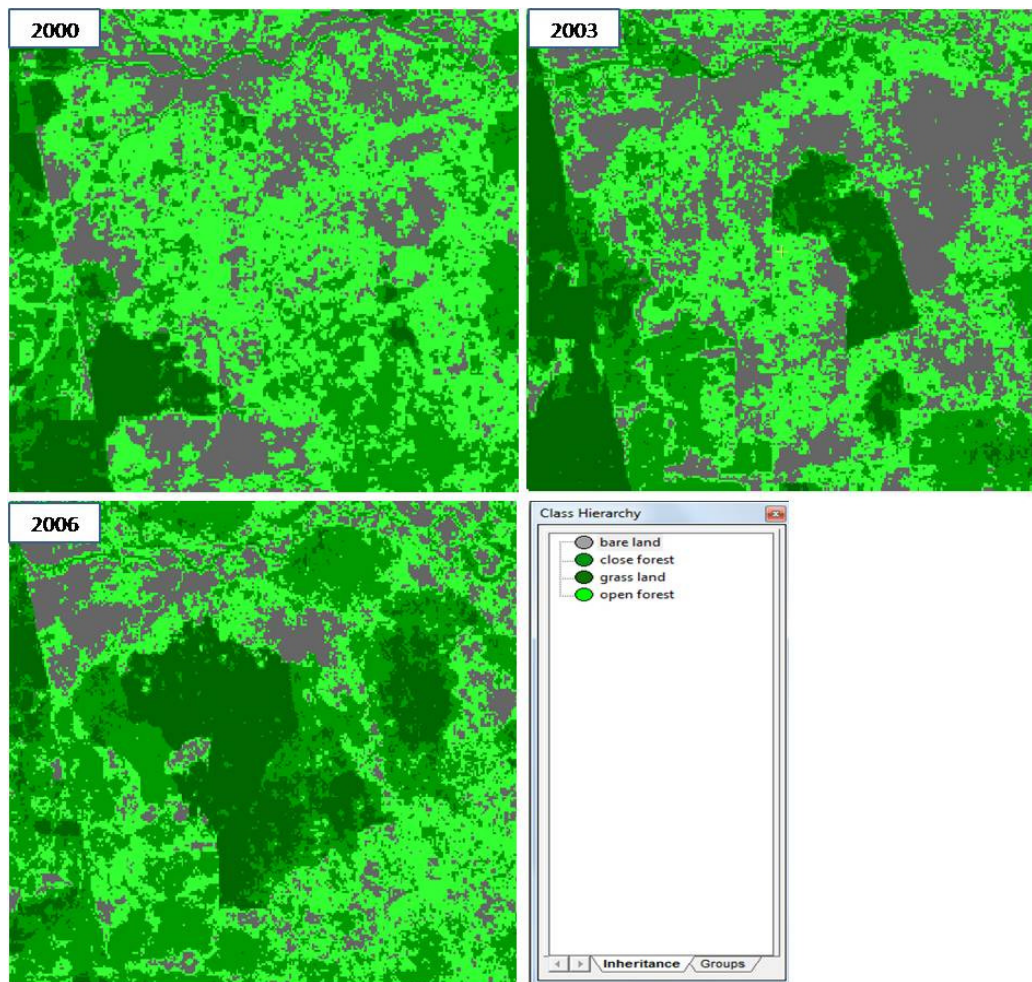


Figure 5.26: Classification of the references images

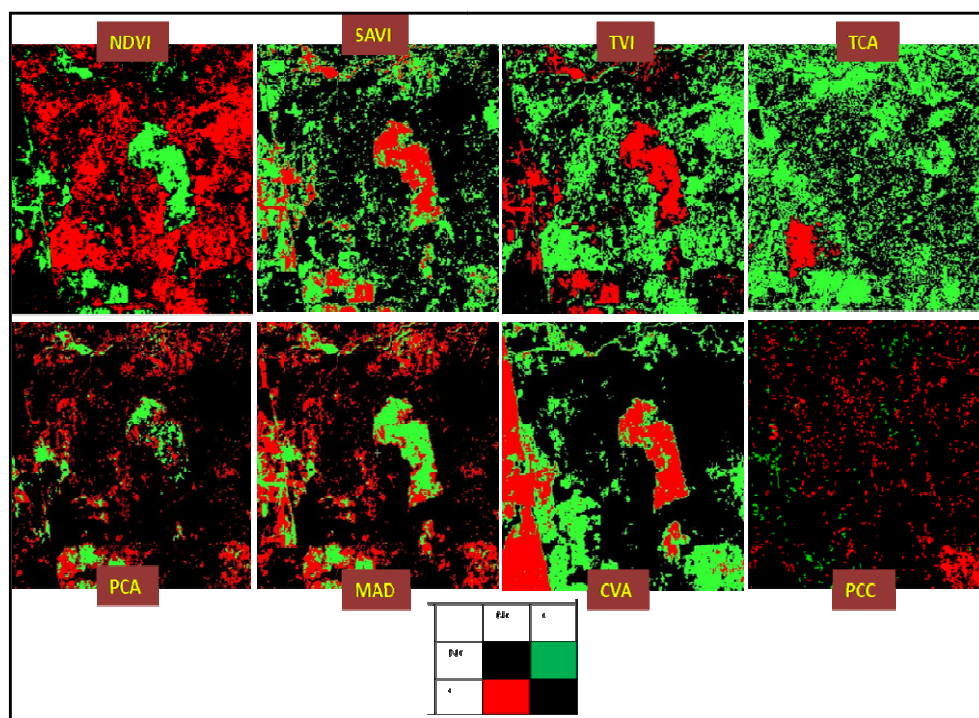


Figure 5.27: Accuracy map given by different change detection techniques (2000-2003)

Table 5.25: Comparison between different change detection techniques and its overall accuracy [%] (2000-2003)

	Reference					Reference			
		NC	C	Σ			NC	C	Σ
	NDVI	38335	5859	44194		CVA	19774	12502	32276
	60.8	19261	673	19934		63.3	9759	22093	31852
	Σ	57596	6532	64128		Σ	29533	34595	64128
	Reference					Reference			
		NC	C	Σ			NC	C	Σ
	SAVI	37559	17023	54582		PCA	52956	2865	55821
	62.5	7015	2531	9546		84.4	7153	1154	8307
	Σ	44574	19554	64128		Σ	60109	4019	64128
	Reference					Reference			
		NC	C	Σ			NC	C	Σ
	TDVI	37611	19885	57496		MAD	41990	3655	45645
	59.5	6115	517	6632		75	12368	6115	18483
	Σ	43726	20402	64128		Σ	54358	9770	64128
	Reference					Reference			
		NC	C	Σ			NC	C	Σ
	TC	30205	28868	59073		PCC	34730	919	35631
	53.1	1226	3829	5055		90.6	5126	23371	28479
	Σ	31431	32697	64128		Σ	39838	24290	64128

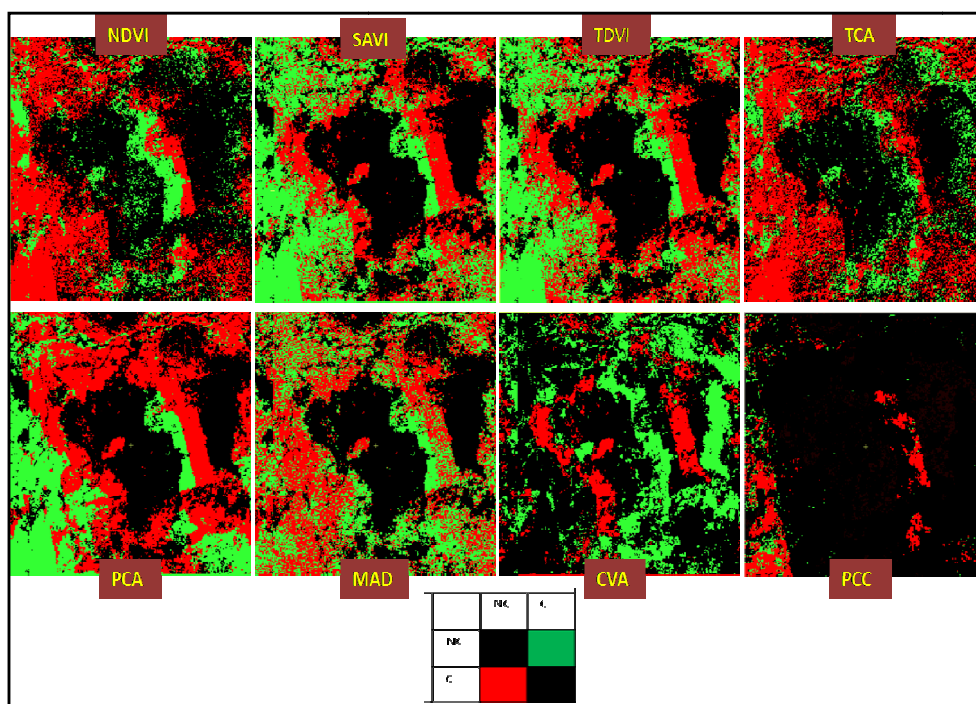


Figure 5.28: Accuracy map given by different change detection techniques (2003-2006)

Table 5.26: Comparison between different change detection techniques and its overall accuracy [%] (2003-2006)

NDVI 54.1	Reference			
		NC	C	Σ
	NC	20752	17186	38536
	C	8875	17215	26190
	Σ	29727	34401	64128

SAVI 58.1	Reference			
		NC	C	Σ
	NC	21334	17381	38535
	C	8997	17896	26193
	Σ	30331	34397	64128

TDVI 59.1	Reference			
		NC	C	Σ
	NC	20034	17989	38003
	C	8204	18521	26725
	Σ	28238	36510	64128

TCA 61.2	Reference			
		NC	C	Σ
	NC	21421	8169	29605
	C	17134	20397	37531
	Σ	30331	34397	64128

CVA 71.6	Reference			
		NC	C	Σ
	NC	30926	11208	45910
	C	7608	14984	22593
	Σ	38535	26193	64128

PCA 59.5	Reference			
		NC	C	Σ
	NC	22821	15614	38535
	C	5113	21080	26193
	Σ	28034	36694	64128

MAD 60.1	Reference			
		NC	C	Σ
	NC	21239	12421	33660
	C	13772	17276	31048
	Σ	28034	36694	64128

PCC 57.0	Reference			
		NC	C	Σ
	NC	36488	539	37029
	C	7774	19325	27099
	Σ	44264	19863	64128

6 Discussion

One of the difficulties in this research is the unavailability of ground truth and reference data for the classification of imagery of 2000 and 2003. There is no source of data available for the land cover maps of the corresponding years. These maps were manually made based on unsupervised classification using the software eCognition, these maps were used as references to evaluate the accuracy of change detection methods.

Also, it was not possible to separate annual crop fields from grass land in the classification. The difficulty to separate these two classes can be possibly attributed to spectral overlapping resulted from the similarity in regeneration of both land cover classes, for that reason they are merged onto one land cover class (grass land).

The accuracy assessment is a fundamental part of the process of image classification because it gives an idea of the validity of the results. In the present research, the overall classification accuracy obtained were 88.4%, 91.9% and 92.1% for the years 2000, 2003 and 2006 respectively, which are reasonable compared to the accuracy that proposed by Anderson et al. (1976): 85% to 90% for land use and land cover assessment for planning and management purposes. The generalization of classes certainly contributed to improvements in the accuracy. Moreover, results of the user accuracy for all classes which ranged from 80% to 100% with the three classified images can be seen optimistic and susceptible of errors.

Detection of land-cover changes is one of the most interesting aspects of the analysis of multitemporal remote sensing images (Coppin et al., 2004). In this study, we performed many approaches to detect land-cover changes in El Rawashda forest. Methods, Post-Classification Comparison and vegetation indices are straightforward techniques and easy to apply. Some area of changes detected by vegetation indices differencing, are not detected by post classification. Also, vegetation indices differencing managed to detect some sharp changes in the forest while post-classification failed. A more detailed classification system may help to detect these changes. Positive and negative changes can be well revealed by post classification method because of its ability to classify forest class with more accuracy while, for instance the method provided detail information about increase and decrease in vegetation areas of the all four classes for the periods from 2000 to 2003 and from 2003 to 2006, whereas vegetation indices differencing demonstrated the weak performance in the detection of this category. This is may be attributed to spectral overlapping between close forest plantation classes, grass and open forest. This confusion was solved by cooperating the expertise knowledge of the study area and visual interpretation with the post classification method during the process of image classification thus enabling the detection of this change, while with vegetation indices differencing this knowledge cannot be incorporated.

Vegetation indices differencing yielded low accuracies, while Post classification yielded high accuracy. These results agree with Virk et al. (2006) who found that Post classification provided more accurate representation of significant forest change, whether deforestation or reforestation. Mas (1999) also found that Post classification to be more accurate than raw image and vegetative index differencing for monitoring land cover changes in a coastal region of Mexico.

The Post classification results confirmed the finding of Abd El-Kawy et al. (2011) that they applied supervised classification to four Landsat images collected over time (1984, 1999, 2005, and 2009). The authors provided recent and historical LULC conditions for the western Nile delta and they concluded that visual interpretation was not only useful in increasing the classification accuracy of the Landsat images, but it was also helpful in identifying areas with the effective use of water for irrigation and areas of private land reclamation. The result is also agreed with the recent finding of Bharti et al. (2011), who reported an upward shift of timberline vegetation by 300 m. Their analysis based on multi-temporal remote sensing data to detect timberline changes in the subalpine vegetation, using post classification comparison method. The authors managed to compare fir patches to see the changes in timberline vegetation. However, Foody (2001) applied Post classification to detect land cover change around the southern limits of the Sahara desert and found that it underestimated the areas of land cover change, and where change was detected; the magnitude of change was overestimated.

Within vegetation indices, NDVI and SAVI behaved similarly at detecting vegetation, whereas, TDVI showed better linearity at the function of the rate of vegetation cover, this may be attributed to the fact that TDVI does not saturate like NDVI or SAVI. Similar results have been reported in Ozbakir and Bannari (2008).

An RGB-NDVI change detection strategy to detect major decreases or increases in forest vegetation was developed as well. This method avoids the need of setting a predefined histogram threshold, but it obviates the need for a high degree of a priori knowledge and requires substantial a posteriori interpretation. In this study the accuracy assessment of this method was not counted, it was only visually assessed and found to be more effective than NDVI image differencing as it distinguish different change classes on vegetation by different colour tones. The result achieved by this study corresponds to those from the literature, (Hayes and Sader, 2001).found the RGB-NDVI method to be more accurate than NDVI image differencing and principal component analysis

Another effective method was tested for the study area, the Tasseled Cap Transformation. This method performed better than the vegetation indices. This may be attributed to the fact that the Tasseled Cap transformation successfully preserve and highlight information relevant to forest disturbance while simultaneously reducing the amount of information that must be processed. The green layer derived structure of the Tasseled Cap Transformation revealed spatial pattern of green vegetation nearly similar to the NDVI image, however it provided slightly better advantage over the NDVI in highlighting pixels that move from grass land to bare land in very dark color.

The Tasseled Cap green layer (GTC) composite of the three images was proposed to detect the change in vegetation of the study area. We found that the RBG-TCG worked better than RGB-NDVI. For instance, the RBG-TCG detected some areas of changes that RGB-NDVI failed to detect them, moreover RBG-TCG displayed different changed areas with more strong colours.

Change vector analysis (CVA) based on Tasseled Cap transformation (TCT) was applied for detecting and characterizing land cover change. Transformation of the multispectral data to some indices which represent vegetation and bare soil components is widely used in the CVA. The typical one is analyzing change vector within the plane of vegetation, defined by the greenness and brightness of the tasseled cap transformation (Kauth and Thomas, 1976).

The results support the CVA approach to change detection. The calculated date to date change vectors contained useful information, both in their magnitude and their direction. The finding obtained demonstrated the capacity to detect and stratify different types of changes in terms of vegetation gain and loss. The Change Vector images of the period 2000-2003, allowed detecting the deforested area of primary vegetation in different areas inside the forest. In the other hand, the technique illustrated an increase of grass land or more probably agricultural crops in the buffer areas surrounding the forest. In the second period (2003-2006), the Change Image presented the loss of vegetation with less intensity and regeneration in other areas that appeared with open vegetation or bare land in the first period. In the two change maps of the CVA and especially in developmental analyses, it was clear that the performance of the CVA procedure is sensitive to its parameter settings and that additional studies to optimize their selection and to normalize differences in scene conditions are desirable. For the short term, additional testing and development; work are needed to gain more understanding of the forest spectral signatures. It is believed that working level interaction with field personnel in such efforts would be desirable and of substantial benefit to both researcher and field manager. These results obtained from satellite data analysis could facilitate the understanding of the changes that took place in the forest.

This result obtained by applying CVA based on TCT agreed with the findings of Siwe and Koch (2008), the authors implemented Change Vector Analysis (CVA) technique on multitemporal multispectral Landsat data from the Thematic Mapper (TM) and Enhanced Thematic Mapper (ETM) sensors to monitor the dynamics of forest change in the mount Cameroon region. CVA was applied to compare the differences in the time-trajectory of the tasseled cap greenness and brightness for two successive time periods 1987 and 2002. The authors concluded that the technique demonstrated immense potentials in monitoring forest cover change dynamics especially when complemented with field studies.

An attempt to increase the performance of Change Vector Analysis technique was reported recently by Chen et al. (2011). The authors proposed a new method named CVA in posterior probability space (CVAPS), which analyzes the posterior probability by using CVA. The authors proved that the main drawbacks in CVA were alleviated effectively by using CVAPS and concluded the new method is potentially useful in land use and land cover change detection.

A powerful tool for time series analysis is the principal components analysis (PCA). This method was tested for change detection in the study area by two ways: Multitemporal PCA and Selective PCA. The interpretation of both methods mainly depended on the statistics from the transformation, including the variance/covariance matrix, the correlation matrix, and the component eigenvectors and loadings. Both methods found to offer the potential for monitoring forest change detection. The first three components are able to explain virtually all of the original variability in reflectance values. Later components thus tend to be dominated by noise effects. By rejecting these later components, the volume of data is reduced with no appreciable loss of information.

The PCA technique also showed major and minor spectral changes, reduces the dimensionality of the data, and provided a much more change information than other change detection techniques. However, the results are difficult to interpret. The PCA technique had a better performance over vegetation differencing and tasseled Cap in viewing areas that are changing, but does not indicate the direction of change like

change vector analysis. Despite these deficiencies, PCA is recommended for change detection because the technique provides insight into patterns of ecological dynamics and can identify areas that are undergoing change so that we can focus on those areas with further investigations.

Based on the statistical results of the loading factors and on visual interpretation, our result pointed that the change in vegetation is best detected using the second principle component (PC2). This result confirmed the finding of Virk et al. (2006) and Toomey et al. (2005) that the second component exhibited the strongest vegetation gradient and having high positive factor loadings for the NIR band. However, Cakir et al. (2006) reported that the first Principal Component (PC1) corresponds to sharp contrast between vegetation and non-vegetation features.

Combining with supervised classification, PCA was found to improve the classification accuracy of all classes. This finding is in accordance with other previous studies, for instance, Akhter (2006), who attempts to use the statistical Principal Component Analysis method for checking the performance in defining the various land cover classes and concluded that PCA imagery improved the classification accuracy for specific classes. More recently, Sulieman and Buchroithner (2007) evaluate combinations of original bands and groups of indices and feature components subjected to Standardized Principal Component Analysis and pointed that Standardized Principal Component generated from indices and feature components can be recommended to obtain more accurate classifications for areas covered by sparse heterogeneous vegetation for other regions in the Sahelian Zone of Africa.

A recently proposed approach, the multivariate alteration detection (MAD), in combination with a posterior maximum autocorrelation factor transformation (MAF) was used to demonstrate visualization of vegetation changes in the study area. The MAD transformation provides a way of combining different data types that found to be useful in change detection.

Instead of selecting Pseudo Invariant Feature visually, an automatic normalization method has been developed by Canty et al. (2004) based on Multivariate Alteration Detection. This transformation generates a set of mutually orthogonal difference images of decreasing variance having the same dimension as the original multispectral images. According to Nielsen et al. (1998), this transformation is invariant to linear scaling of the input data and can use different data types. However, this approach has not been assessed for vegetation change detection applications.

The interpretation of the resulting change images was based on correlations between the transformed variates and the original data. The study revealed that, Mad3 is probably an indicator of vegetation changes as it showed a weighted mean of NIR and MAD4 is probably an indicator of shadow-induced changes as it showed a weighted mean of all channels. This finding disagreed with the result pointed by Frank and Canty (2003) that Mad2 is sensitive to vegetation changes and MAD1 is probably an indicator of shadow-induced changes.

The result also showed that the use of the maximum autocorrelation factor transformation improved the result of the MAD components as it removes noise and excludes minor change information and on the other hand explained the major changed areas with more strong colours which made the results easier to interpret.

Change in forest classes for the two periods shown in Figure 6.1. For the two periods the greatest change appeared in close forest class. Change in open forest class within the first period 2000 to 2003 comprised higher percentage than grass land, whereas in the second period 2003 to 2006 the percentage of change greater in grass land. Bare land revealed the least percentage of change in both periods.

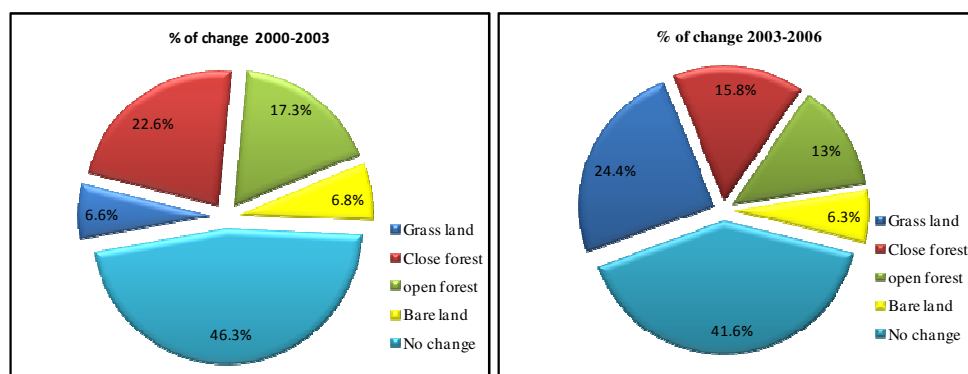


Figure 6.1: Change of forest classes

Accuracy assessment is an important final step addressed in the study to evaluate the different change detection techniques. A quantitative accuracy assessment at level of change/no change pixels was performed to determine the threshold value with the highest accuracy. Figure 6.2 summarizes the result of the accuracy assessment of eight methods tested. Among the various accuracy assessment methods presented the highest accuracy was obtained using the post-classification comparison based on supervised classification of each pair images. The good performance of this approach can be attributed to the high classification accuracy of 2000, 2003 and 2006 classified images and to the fact that accuracy has been improved by grouping classes which presented the most common spectral confusion.

Results of accuracy assessments of the two time periods confirmed this output, for instance, the accuracy assessment of post classification comparison for the two periods were 90.6% and 87% consequently.

Some authors carried out comparative studies of change detection techniques and generally found that post classification comparison was less effective than enhancement procedures such as image regression (Singh 1986) or image differencing and PCA (Muchoney and Haak 1994). However, the result confirmed the finding of Mas (2007) who compared six techniques and pointed that post-classification comparison proved to be the best method of 86.8% accuracy.

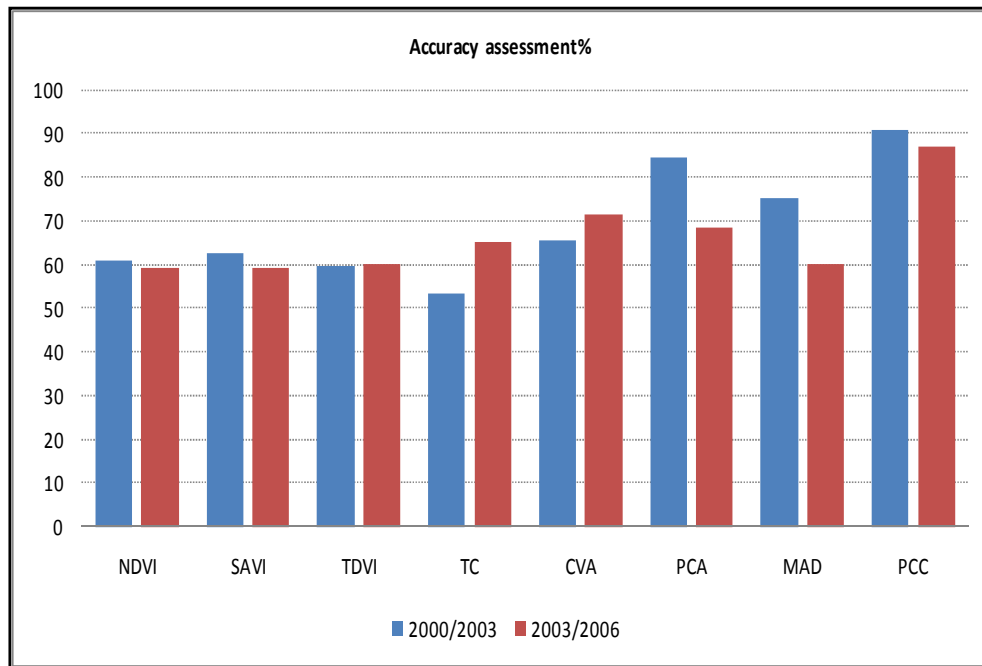


Figure 6.2: Accuracy assessments of change detection techniques

The performance of the PCA was confused as it counted a high accuracy of 84.4% for the first period and significant less accuracy of 68.6% for the second period. Hayes and Sader (2001) reported 74% accuracy assessment for PCA. Another confusing results obtained by multivariate alteration detection which counted accuracy of 75% for the first period and 60.1% for the second period.

Change vector analysis achieved quite good performances of 65.3% and 71.6% for the two periods respectively. However a high result of 86% was obtained by Lunetta et al. (2004) using change vector analysis.

In this study vegetation indices and tasseled cap showed the least accuracy assessments for the two time periods whereas Hayes and Sader (2001) reported accuracy of 82% for NDVI.

Different change detections methods used in this research are viewed to be complementary to each other. The combined use of different change detection algorithms (hybrid schemes) such as change vector analysis based on Tasseled Cap analysis and supervise classification based on Principal component analysis were found to minimize commission errors . Multivariate change detection technique that process the full dimensionality (spectral and temporal) of the image data such as Multivariate alteration detection and Change vector analysis, have demonstrated potential as a means to detect, identify, map and monitor changes, moreover, they are excelling at providing rich qualitative detail about the nature of the change and effective techniques to capture all kind of changes.

For all tested methods, precise registration of multi-date imagery is a critical prerequisite of accurate change detection. However, residual misregistration at the

below-pixel level somewhat degrades area assessment of change events at the change/no-change boundaries. It is clear that temporal trajectory analysis offers the greatest opportunities to study the dynamic processes and their effect on vegetation and meet all challenges in land use land cover change, but its major drawback is the limitations on the available time series length.

During the past six decades, the Gedarif State in eastern Sudan lost its status as one of the main sources of food production in the country, due to large-scale degradation of its rich soil as well as other natural resources, particularly through unsuccessful land use policies and practices (Elsiddig, 2003). In the absence of obvious management practices and the absence of participation of local in the management process, natural forest reserves and forests outside the reserves are constantly exposed to strong pressure from people that depend on local forests. Benefiting from unsuccessful control and the easy access to the forest that is provided by the Authorized forest harvesting, they provided in random felling , agriculture (by permanent or shifting cultivation), gathering wood, charcoal burning and collection of other forest products and herding of cattle.

El Rawashda forest is surrounded by seven villages from the south and east borders, and by the two large towns of Gedarif and El-Showak. Rain fed agricultural schemes have taken up all the land surrounding these forests. El Rawashda forest is engulfed by the vast rain-fed agricultural schemes where extensive land clearances have been practiced. To avert conflict between the peasants and the pastoralists, transhumant routes have been laid on. Being at the cross roads of animal migration passages, transgression over the forest by the nomads and their herds is inevitable. Proximity to the transhumant routes and the villages confer a disadvantage and pressure on the limited vegetation of the El Rawashda forest. The huge numbers of animals roaming are exceeding the carrying capacity of the forest. Such situation, however, has lead to the disappearance of superior species and the dominance of inferior species. In addition, the transgression of the dwellers within the vicinity of the forest remains the prime threat through illegal tree cutting and charcoal production. The excessive cutting of the trees and overgrazing have systemically depleted the natural vegetation of El Rawashda forest. Nevertheless it has been considered as the main morph dynamic aspect of vegetation thinning in El Rawashda forest. Vegetation thinning, loss of arboreal cover together with the excessive runoff have rendered the soil prone to erosion in the forest. Thus, the need for effective management measures is inevitable (Gadalla, 1995).

Forest degradation is detected more in south and east parts of the forest; this may be attributed to the fact that, El Rawashda forest is bordered by seven villages on the southern and eastern boundaries. People living in these villages derive their income from various combinations of the three main forms of land use: agriculture, grazing, and forest exploitation. Farmers did not adopt any measure to combat land degradation. Their farms were located on forest land, they benefited from agriculture that aimed at maintaining the soil productivity with trees, in addition to other economic activities such as gum tapping, collecting and trading on forest products and charcoal burning which lead to forest degradation.

In many areas in Sudan firewood for domestic purposes is still collected rather than produced or purchased. Few rural households consider tree planting as a solution to the fuel crisis, many social forestry programs have been created in close consultation with residents who are designed to serve. Such programs will improve the knowledge of the local people and they will be aware of the economic and environmental

consequences of deforestation and therefore they will be prepared and willing to participate in forestry activities and contribute to the management of the forest reserves.

Forest planting projects should be relevant to the needs and priorities of the people living in the area. Success of tree planting projects should not be measured through the achievement of numerical targets. Increasing the number of trees in an area may have little beneficial effect unless it is closely related to the needs and priorities of the people living there. The management and utilization of existing tree resources should be a key element in any program of forest social development. Proper scientific management of woodlands with local participation not only could supply valuable yields of fuel wood and poles to neighboring communities, but could also provide many other useful woodland products while fulfilling an equally important conservation function.

Problems of environmental degradation, fodder production and fuel wood supply cannot be solved by reforestation alone. What is required is an integrated land-use approach which involves agriculture, livestock, land settlement, forestry and the socio-economic set-up. The remedy to this problem lies in either the establishment of range lands north of El Rawashda forest, the allocation of these lands to the nomads whereby they could grow crops and later graze their animals on their residues, or the reopening of grazing routes.

7 Conclusions and outlook

7.1 Conclusions

The objective of this research was to examine the effectiveness of eight algorithms in detecting land-cover changes for two periods (2000 - 2003 and 2003 - 2006) including 1) the ability to differentiate change from no-change and 2) the ability to detect different kinds of change. The study also aimed to determine the change detection technique that had the highest accuracy in detecting vegetation cover changes and use this method to produce land cover change map for the study area.

Consideration of the study leads to the following conclusions.

- Post-classification comparison revealed the highest accuracy and furthermore presents the advantage of giving information about the nature of the changes.
- There are other promising techniques for assessing vegetation cover changes and produced reasonable accuracy such as multivariate alteration detection and change vector analysis. Both methods can use any number of spectral bands from multi-date satellite data to produce change images that yield information about the direction of differences in pixel values. MAD is seen as an important method in future automated change detection applications.
- The application of the automatic threshold determination procedures of MAF/MAD revealed good results. We recommend using the MAF/MAD transformed variables because their ability to enhance signal-to-noise is very strong and moreover they are straightforward methods for visualization of changes.
- This study presents a new simple and logical technique to display and quantify forest change using three dates of satellite imagery. Instead of using RGB-NDVI (Sader and Winne, 1992), the tasseled cap transformation's greenness layer (GTC) was used. By simultaneously projecting each date of GTC layer through the red, green, and blue (RGB) computer display write functions, major changes in GTC (and hence vegetation cover) between dates will appear in combinations of the primary (RGB) colours. We recommend using this technique because it allows interpretation of forest changes for three dates at a time. Analysis of three or more dates allows trends to be examined at more than one interval of time. Moreover, the method requires no thresholding for change/no change area and additional information can be interpreted from a three-date RGB-GTC that cannot be interpreted from the thresholding of two-date change images.
- Quantitative analysis of the accuracy assessment of change detection techniques is a difficult task because of the different nature of change detection. For example, how does one obtain reference data for images that were taken in the past? Which change detection technique will work best for a given change in the environment?
- It is also difficult to determine which change detection methods are most effective because most studies on change detection have not included

quantitative accuracy assessments. So far no standard accuracy assessment techniques or procedures for change detection have been developed.

- Results indicated that the principal land cover changes in the study area (e.g., deforestation and forest regeneration) can be monitored accurately by remote sensing.
- Analysis of the literature provides ample evidence to support the conclusion that multi-date satellite imagery can be effectively used to detect and monitor changes in forests. At the same time we support the observation of Collins & Woodcock, (1996) that one of the challenges facing the community of remote sensing research is to develop a better knowledge of the change detection process so as to realize how to fit applications and change detection techniques.
- El Rawashda forest is the largest forest in east Sudan of 52080 square hectares. It is well understood that El Rawashda forest had degraded and the degradation had induced a decline in agricultural productivity. However, to date, no studies have evaluated this degradation. To our knowledge, ours is the first study to classify and assess vegetation change in these classes in the forest.
- It is important to mention that although the total vegetation of the forest seemed to be increased within the two periods, but 8.1% and 1.3% of the total closed forest area has been decreased in the first period (2000 – 2003) and the second period (2003 – 2006) respectively. So this may lead to misunderstanding because the vegetation cover includes grasses, weeds and other inferior regeneration, for example degradation of *Acacia seyal* (superior species) replaced by *Acacia nubica* (inferior species).

7.2 Outlook

The present study supports future application for a detailed study of forest cover changes assessment. Clearly, this work needs to be pursued further, to improve the quality and the accuracy of our results. In future work a comprehensive change detection for Sudan forests should be carried out to assess the rate of deforestation, Studies are also needed to make better prediction of forest attributes from remote sensing data using different local studies to extract forest biomass.

The capability of using remote sensing imagery for change detection will be enhanced by improvements in satellite data and by the integration of remote sensing, GIS techniques, beside field studies, practical expert and ecosystem simulation models. Although this study provides evidence that supports certain forest change detection methods, there is a need for further work to establish long-term validation programs for such monitoring and compare these methods against more recent change detection methods such as object classification and fuzzy classification.

Clearly, as change-detection studies become more popular, the urgency for developing procedures to determine the accuracy of the different techniques becomes increasingly important. Upcoming work should involve the development of a comprehensive change detection and interpretation system.

For the future, we plan to combine pixel- based and object- based approach to improve the accuracy of classification. Pixel classification approaches are based on statistical analysis of individual pixels, while object based classification incorporate as much information on spatial neighbourhood properties as possible into the classification process, so we can integrate spectral analysis with spatial information. This can provide a valuable tool for mapping forests, a capability that should be a great value to resource managers.

The study also suggests several other possible studies as an extension to this one to complement the understanding of land cover change processes in El Rawashda forest. Research should include multitemporal socioeconomic data, which is going to be possible after the release of the 2008 Census data. The comparison of socioeconomic data will give valuable insights and a clearer picture of the socioeconomic drivers of deforestation in El Rawashda forest. Also study to test the hypothesis whether the changing socio-economic development in the region leads to changes in the relationship between population density and deforestation.

The study pointed out that RGB-GTC technique detects more changes than RGB-NDVI. However more research is needed regarding this issue. Also in this research no attempt was made to classify forest changes using RGB-GTC output, our research from RGB-GTC only provided useful information as a draft of changing. The study proposed automated classification on three or more dates of GTC by unsupervised cluster analysis (Sader et al., 2003), thus the Change and no change categories can be labeled and dated. The utility of the RGB-GTC technique for supporting forest inventories and updating forest resource information systems is needed to presented and discussed.

Future directions of this research could include more field data and statistical analysis will definitively verify the results of the study. Ground data indicating the spatially known deforestation and reforestation locations would allow for a definitive assertion that different methods are or are not able to detect accurate changes. Better ground data that could more explicitly identify where forest regeneration occurred would allow

better accuracy assessment. Further statistical analysis could be used to explain why some methods detected less biomass loss while others detected more biomass gain. The reasons of differences in accuracy of each method derive from preliminary findings of previous studies. By using spectral statistics and more precise ground-truth data one could provide a more definitive explanation of the strengths and weaknesses of each method.

Monitoring of trends and impact of interventions on drought and desertification is a central issue to the success of efforts in combating drought and desertification; the establishment of well-functioning monitoring institutionally is strongly needed in Sub-Saharan Africa. This could be work through strengthening the information base on drought and desertification and sharing of best practices through programs at regional, sub-regional and national level. These programs should entail activities to: strengthen collection of information through targeted research; establish comprehensive information systems; develop and apply methodologies for monitoring land degradation; and promote networking and centers of excellence. These programs could be supported by The Global Environment Facility (GEF) through its implementing agencies namely UNEP, UNDP and World Bank. Information systems should be composed of low-cost raster based image analysis and GIS tools with standard overlay and query procedures. Standardized data of specific networks of regions should be integrated with national and international environmental plans. A methodology for monitoring Sahelian regions must be able to detect, quantify and map the spatiotemporal patterns of land cover and land use change.

More monitoring and accurate data are needed concerning deforestation at different regions in our country. Sudan would not be able to fulfill its obligations to implement the international agreements to combat desertification and to promote sustainable dry land development without accurate identification of deforested regions and the causes for desertification and environmental degradation. Proper management of forest is an essential task of this research.

8 References

- A Systematic Survey. Department of Electrical, Computer, and Systems Engineering Rensselaer Polytechnic Institute, USA.
- Abbadi, K. A. B., & Ahmed, A. E. 2006. Brief overview of Sudan economy and future prospects for agricultural development. Food aid forum, WFP, Khartoum.
- Abd El-Kawy, O., Rod, J., Ismail, H., & Suliman. 2011. Land use and land cover change detection in the western Nile delta of Egypt using remote sensing data. *Applied Geography*, 31(2): 483-494.
- Abdalla, A. A., & Abdel Nour, H. O. 2001 .The Agricultural Potential of Sudan. Retrieved from: [Uhttp://www.aboutsudan.com/conferences/U](http://www.aboutsudan.com/conferences/U).
- Abdelnour, H. O. 1999. Implementation of national forest programmes in Sudan. A case study. Paper presented at FAO-Turkey workshop, Istanbul. 46 p.
- Akhter, M. 2006. Remote sensing for developing an operational monitoring scheme for the Sundarban Reserved Forest, Bangladesh. PHD thesis. Faculty of Forest, Geo and Hydro Sciences Institute of Photogrammetry and Remote Sensing. Technische Universität Dresden, Germany.
- Allen, T., & Kupfer, J. 2000. Application of Spherical Statistics to Change Vector Analysis of Landsat Data-Southern Appalachian Spruce-Fir Forests. *Remote Sensing of Environment*, 74(3):482–493.
- Almeida-Filho, R., & Shimabukuro, Y. 2002. Digital processing of a Landsat-TM time series for mapping and monitoring degraded areas caused by independent gold miners, Roraima State, Brazilian Amazon. *Remote Sensing of Environment*, 79(1):42–50.
- Anderson, R., Hardy, E., Roach, T., & Witmer, R. 1976. A land use and land cover classification system for use with remote sensor data. U.S. Geological Survey Professional 964. 28 pp.
- Anttila, P. 2002. Updating stand level inventory data applying growth models and visual interpretation of aerial photographs. *Silva Fennica*, 36(2):549–560.
- Asner, G., Bustamante, M., & Townsend, A. 2003. Scale dependence of biophysical structure in deforested areas bordering the Tapajo's National Forest, Central Amazon. *Remote Sensing of Environment*, 87(4):507–520.
- Asner, G., Keller, M., Pereira, R., and Zweede, J. 2002. Remote sensing of selective logging in Amazonia - Assessing limitations based on detailed field observations, Landsat ETM+, and textural analysis. *Remote Sensing of Environment*, 80(3):483–496.
- Ayoub A.T. 1998. Extent, severity and causative factors of land degradation in the Sudan. *Journal of Arid Environments*, 38: 397 – 409.
- Büttner, G., Feranec, J., & Jaffrain, G. 2002. Corine land cover update 2000. Technical report, European Environmental Agency, Copenhagen, Denmark.

- Baatz, M., & Schäpe, M., 2000. Multiresolution segmentation: An optimization approach for high quality multi-scale image segmentation. In: Strobl, J., Blaschke, T., Griesebner, G. (Eds.), *Angewandte Geographische Informations- Verarbeitung XII*. WichmannVerlag, Karlsruhe, pp. 12-23.
- Baatz, M., Hoffmann, C., & Willhauck, G., 2008. Progressing from object-based to object-oriented image analysis. In: Blaschke, T., Lang, S., Hay, G.J. (Eds.), *Object based image analysis*. Springer, Heidelberg, Berlin, New York, pp. 29-42.
- Bannari A., Asalhi H. & Teillet P.M. 2002. Transformed difference vegetation index (TDVI) for vegetation cover mapping. *International Geoscience and Remote Sensing Symposium*, Toronto, Ontario, Canada, *Proceedings on CD-Rom*, paper I2A35-1508.
- Bastin, G.N. & Ludwig, J.A. 2006. Problems and prospects for mapping vegetation condition in Australia's arid rangelands. *Ecological management and Restoration*, 7(s1): 71-74.
- Benz, U.C., Hofmann, P., Willhauck, G., Lingenfelder, I., & Heynen, M. 2004. Multiresolution, object-oriented fuzzy analysis of remote sensing data for GIS-ready information. *ISPRS Journal of Photogrammetry and Remote Sensing*, 58: 239-258.
- Biging, G. S., Colby, D. R., & Congalton, R. G. 1998. Remote sensing change detection: environmental monitoring methods and applications, chapter Sampling systems for change detection accuracy assessment, pp. 281–308.
- Blaschke, T. 2010. Object based image analysis for remote sensing. *ISPRS Journal of Photogrammetry and Remote Sensing*, 65: 2-16.
- Blaschke, T., Burnett, C., & Pekkarinen, A. 2004. Remote Sensing Image Analysis: Including the Spatial Domain, chapter Image Segmentation Methods for Object-based Analysis and Classification, pp. 211–236.
- Booth, D. T. & Tueller, P.T. 2003. Rangeland monitoring using remote sensing. *Arid Land research and management*, 17(4): 455-467.
- Bruzzone, L., & Pireto, D. 2000. Automatic analysis of the difference image for unsupervised change detection .*IEEE Trans. Geosci. Remote Sen*, 38 (3):1171-1182.
- Bruzzone, L., & Prieto, D. 2000. An adaptive parcel-based technique for unsupervised change detection. *International Journal of Remote Sensing*, 21(4):817–822.
- Byrne, G., Crapper, P. & Mayo, K. 1980. Monitoring Land-Cover Change by Principle Components Analysis of Multitemporal Landsat Data. *Remote Sensing of Environment* 10: 175-184.
- Cakir, H., Khorram, S., & Nelson, S. 2006. Correspondence analyses for detecting land cover change. *Remote Sensing of Environment*, 102(3-4):306–317.
- Canty, M. 2005. *Image Analysis and Pattern Recognition for Remote Sensing book*. Juelich Research Center, Germany, 69-78.
- Canty, M., & Niemeyer, I. 2002. Analysis of digital satellite imagery. In Jasani, B. and Stein, G., editors, *Commercial Satellite Imagery. A tactic in nuclear weapon deterrence*, p 67–78. Springer, Berlin Heidelberg

- Canty, M., Nielsen, A., & Schmidt, M. 2003. Automatic radiometric normalization of multitemporal satellite imagery. *Remote Sensing of Environment*, 91: 441–451.
- Canty, M., Nielsen, A., & Schmidt, M. 2004. Automatic radiometric normalization of multitemporal satellite imagery. *Remote Sensing of Environment*, 91(3-4):441–451.
- Central Intelligence Agency, CIA world factbook, 2011. Retrieved from: www.cia.gov/library/publications/the-world-factbook.
- Chavez, P. S.; & Kwarteng, A. Y. 1989. Extracting spectral contrast in Landsat Thematic Mapper Image data using selective principal component analysis. *Photogrammetric Engineering and Remote Sensing*, 55: 339-348.
- Chavez, P., & MacKinnon, D. 1994. Automatic detection of vegetation changes in the southwestern United States using remotely sensed images. *Photogrammetric Engineering and Remote Sensing*, 60(5):571–583.
- Chen, J., Chen, X., Cui, X., & Chen, J. 2011. Change Vector Analysis in Posterior Probability Space: A New Method for Land Cover Change Detection. *Geoscience and Remote Sensing Letters, IEEE*, 2(8): 317 – 321.
- Cicone, E. P. & Cicone, R. C. 1984. A physically-based transformation of thematic mapper data-the tm tasseled cap. *IEEE Transactions of Geoscience and Remote Sensing GE*, 22(3): 256-263.
- Cohen, W. B. & Fiorella, M. 1998. Remote sensing change detection: environmental monitoring methods and applications, chapter Comparison of methods for detecting conifer forest change with thematic mapper imagery, pp. 89–102.
- Collins, J., & Woodcock, C. 1996. An assessment of several linear change detection techniques for mapping forest mortality using multitemporal landsat TM data. *Remote Sensing of Environment*, 56(1):66–77.
- Collins, J., & Woodcock, C. 1999. Geostatistical estimation of resolution-dependent variance in remotely sensed images. *Photogrammetric Engineering and Remote Sensing*, 61:41–50.
- Coppin, P. P., and M. E. Bauer 1994. Processing of multitemporal landsat TM imagery to optimize extraction of forest cover change features. *IEEE Transactions of Geoscience and Remote Sensing*, 32(4): 918-927.
- Coppin, P., & Bauer, M. 1996. Digital change detection in forest ecosystems with remote sensing imagery. *Remote Sensing Reviews*, 13:207–234.
- Coppin, P., Jonckheere, I., Nackaerts, K., Muys, B., & Lambin, E. 2004. Digital change detection methods in ecosystem monitoring: a review. *International Journal of Remote Sensing*, 25(9):1565–1596.
- Coppin, P., Nackaerts, K., Queen, L. & Brewer, H. 2001. Operational monitoring of green biomass change for forest management. *Photogrammetric Engineering and Remote Sensing*, 67(5):603–611.
- Crist, E. P. 1985. A thematic mapper tasseled cap equivalent for reflectance factor data. *Remote Sensing of Environment*, 17: 301-306.
- Crocetto, N., & Tarantino, E., 2009. A Class-Oriented Strategy for Features Extraction from Multidate ASTER Imagery. *Remote Sensing*, 1: 1171-1189.

- Currit, N. 2005. Development of a remotely sensed, historical land-cover change data base for rural Chihuahua, Mexico. *International Journal of Applied Earth Observation and Geoinformation*, 7(3):232–247.
- De Sherbinin, A. 2005. Remote Sensing in Support of Ecosystem Management Treaties and Transboundary Conservation. Palisades, NY: CIESIN at Columbia University. Retrieved from: http://sedac.ciesin.columbia.edu/rs-treaties/RS&EMTreaties_Nov05_screen.pdf
- Desclée, B. 2007. Automated object-based change detection for forest monitoring by satellite remote sensing: Applications in temperate and tropical regions. PHD thesis. Faculté d'ingénierie biologique, agronomique et environnementale Département des Sciences du Milieu et de l'Aménagement du Territoire, Université catholique de Louvain .
- Desclée, B., Bogaert, P., & Defourny, P. 2006. Forest change detection by statistical object-based method. *Remote Sensing of Environment*, 102: 1–11.
- Duggin, M., Rowntree, R., Emmons, M., Hubbard, N., Odell, A., Sakhavat, H. 1986. The Use of Multidate Multichannel Radiance Data in Urban Feature Analysis. *Remote Sensing of Environment*, 20: 95-105.
- Gadalla, S. 1995. The Importance of Forest Resource Management in Eastern Sudan: The Case of El Rawashda and Wad Kabo Forest Reserves, in: OSSREA (ed) managing Scarcity : Human adaptation in East African Drylands, OSSREA, Addis Ababa, pp 139 - 146.
- Elmoula, M. E. A. 1985. On the problem of resource management in the Sudan. Monograph Series, Institute of Environmental Studies, University of Khartoum, (4) 131 p.
- Elmubarak, S. O. 2002. Impacts of decentralization on sustainable management of forest resources in the Sudan. A case study: Kassala and Gedarf States. M.Sc. Thesis. Institute of Environmental Studies, University of Khartoum, Sudan. 80 p.
- Elmuola, M. E. A. 1985. On the problem of resource management in the Sudan. Environmental monograph series no. 4. Institute of Environmental Studies, University of Khartoum, Sudan. 131 p.
- Elsiddig, E. A. 1996. Investigation on management systems in natural forest reserves: A case study: Elrawashda and Wad Kabo. A consultancy report for FAO/FNC, Khartoum. 80 p.
- Elsiddig, E. A. 2003. Management of dryland forest reserves in Sudan based on participatory approach. In: Alsharan, A.A., Wood, W.W., Goudie, A.S., Fowler, A. & Abdellatif, E.A. Desertification in the third millennium. Belkan Publishers, Lisse, The Netherlands, pp. 361-364.
- Eltayeb, G. E. 1985. Environmental management in the Sudan: Gadaref district study area. Institute of Environmental Studies, University of Khartoum, Sudan. 201 p.
- Environs Using Multi-Temporal Landsat Thematic Mapper Data. *International Journal of Remote Sensing*, 19(9): 1651–1662.
- FAO. 2001. Global forest resources assessment 2000- main report. FAO, forestry paper No. 140, Food and Agriculture Organization of the United Nations, Rome.

- FAO. 2002b. Law and sustainable development since Rio: Legal trends in agriculture and natural resource management. Legislative Study No.73, FAO, Rome.
- FNC. 2000. The annual afforestation and programme – present and future, FNC Khartoum.50 p.
- Foody, M. 2001. Monitoring the magnitude of land-cover change around the southern limits of the Sahara. *Photogrammetric Engineering & Remote Sensing*, 67(8):841–847.
- Frank, M., & Canty, M. 2003. Unsupervised Change Detection for Hyperspectral Images. AVIRIS workshop, popo.jpl.nasa.gov.
- Franklin, J., Phinn, S. R., Woodcock, C. E., & Rogan, J. 2003. Rationale and conceptual framework for classification approaches to assess forest resources and properties. In: Wulder, M. A. and Franklin, S. E (Eds) *Remote Sensing of Forest Environments concepts and case studies*, Kluwer Academic Publishers, USA.
- Franklin, S. E., L.M. Moskal, M.B., & La ugh. 2000. Interpretation and classification of partially harvested forest stands in the Fundy model forest using multitemporal landsat TM digital data. *Canadian Journal of Remote Sensing*, 26(4): 318-333.
- Franklin, S. E., Lavigne, M. B., Wulder, M. A., & Stenhouse, G. B. 2002. Change detection and landscape structure mapping using remote sensing. *The Forestry Chronicle*, 78(5): 618-625.
- Franklin, S. E., Lavigne, M. B., Wulder, M. A., & McCaffrey T. M. 2002. Large-area forest structure change detection: An example. *Canadian Journal of Remote Sensing*, 28(4): 588-592.
- Franklin, S., Lavigne, M., Wulder, M., & McCaffrey, T. 2002. Large-area forest structure change detection: An example. *Canadian Journal of Remote Sensing*, 28(4):588–592.
- Fuller, D. O. 2001. Forest fragmentation in Loudoun County, Virginia, USA evaluated with multitemporal Landsat imagery. *Landscape Ecology*, 16: 627-642.
- Fung, T. 1990. An Assessment of TM Imagery for Land-Cover Change Detection. *IEEE Transactions on Geoscience and Remote Sensing*, 28: 681-684.
- Fung, T., & LaDrew, E. 1987. Application of principal component analysis to change detection, *Photogrammetric Engineering & Remote Sensing*, 53(12):1649-1658.
- Fung, T., & LeDrew, E. 1988. The determination of optimal threshold levels for change detection using various accuracy indices. *Photogrammetric Engineering and Remote Sensing*, 54(10):1449–1454.
- Gamanya, R., de Maeyer, P., & De Dapper, M. 2009. Object-oriented change detection for the city of Harare, Zimbabwe. *Expert Systems with Applications*, 36 (1), 571_588.
- Gao, B. C. 1996. NDWI - A normalized difference water index for remote sensing of vegetation liquid water from space. *Remote Sensing of Environment*, 58(3):257–266.
- García-Haro, F. J., Gilabert, M. A., & Meliá, J. 1996. Linear spectral mixture modeling to estimate vegetation amount from optical spectral data. *International Journal of Remote Sensing*, 17 (17), 3373– 3400.

- Geist, H. 2006. Our earth's changing land: an encyclopedia of land-use and land-cover change. Greenwood Press.
- Glover, E. K. 2005. Tropical dryland rehabilitation: A case study on participatory forest management in Gedarif, Sudan. PhD Dissertation. Faculty of Agriculture and Forestry of the University of Helsinki, Finland.
- Gopal, S., & Woodcock, C. 1996. Remote sensing of forest change using artificial neural networks. *IEEE Transactions on Geoscience and Remote Sensing*, 34(2):398–404.
- Greenberg, J., Kefauver, S., Stimson, H., Yeaton., C. & Ustin, S. 2005. Survival analysis of a neotropical rainforest using multitemporal satellite imagery. *Remote Sensing of Environment*, 96(2):202–211.
- Guild, L., Cohen, W., & Kauffman, J. 2004. Detection of deforestation and land conversion in Rondonia, Brazil using change detection techniques. *International Journal of Remote Sensing*, 25(4):731–750.
- Häme, T., Heiler, I., & Miguel-Ayanz, J. 1998. An unsupervised change detection and recognition system for forestry. *International Journal of Remote Sensing*, 19(6):1079–1099.
- Hansen, M. J., S. E. Franklin, Woudsma, C., & Peterson, M. 2001. Forest structure classification in the North Columbia Mountains using the landsat tm tasseled cap wetness component. *Canadian Journal of Remote Sensing*, 27(1): 20-32.
- Hardisky, M., Klemas, V., & Smart, R. 1983. The influence of soil salinity, growth form, and leaf moisture on the spectral radiance of *Spartina alterniflora* canopies. *Photogrammetric Engineering and Remote Sensing*, 49:77–83.
- Harrison, M. N., & Jackson, J. K. 1958. Ecological classification of the vegetation of the Sudan. *Forest Bulletin No. 2*. Ministry of Agriculture, Khartoum.45 p.
- Hay, G.J., & Castilla, G. 2008. Geographic Object-Based Image Analysis (GEOBIA): A new name for a new discipline. In: Blaschke, T., Lang, S., Hay, G. (Eds.), *Object Based Image Analysis*. Springer, Heidelberg, Berlin, New York, pp. 93_112.
- Hayes, D., and Sader, S. 2001. Comparison of change-detection techniques for monitoring tropical forest clearing and vegetation regrowth in a time series. *Photogrammetric Engineering and Remote Sensing*, 67(9):1067–1075.
- Healey, S., Cohen, W., Yang, Z., & Krankina, O. 2005. Comparison of Tasseled Cap-based Landsat data structures for use in forest disturbance detection. *Remote Sensing of Environment*, 97(3):301–310.
- Heikkonen, J., & Varjo, J. 2004. Forest change detection applying Landsat Thematic Mapper difference features: a comparison of different classifiers in Boreal forest conditions. *Forest Science*, 50 (5): 579-588.
- Heute, A.R. 1988. A soil-adjusted vegetation index (SAVI). *Remote Sens. Environ*, 29:295-309.
- Hotelling, H. 1936. Relations between two sets of variates. *Biometrika*, 28:321–377.
- Hussein, S.G. 1991. Environmental degrdation in a semi-arid range land in Northern Sudan. *Desertification Bulletin*. 19p.

- Ibrahim, A. M. 2002. An overview of forest policy and legislation in the Sudan: With special reference to environmental concerns and impact on forestry. Workshop on Tropical Dryland Rehabilitation, Hytiälä Forestry Research Station, University of Helsinki. 9p.
- Jensen, J. R. 1996. Introductory Digital Image Processing(3rd ed.). Upper Saddle River, NJ: Prentice Hall.
- Jensen, J. R. 2000. Remote Sensing of the Environment: An Earth Resource Perspective. Upper Saddle River, New Jersey, Prentice Hall.
- Jin, S., & Sader, S. 2005. Comparison of time series tasseled cap wetness and the normalized difference moisture index in detecting forest disturbances. Remote Sensing of Environment, 94(3):364–372.
- Johnson, R.D., & E.S. Kasischke. 1998. Change Vector Analysis: A Technique for Multispectral Monitoring of Land Cover and Condition. International Journal of Remote Sensing, 19(3): 411-426.
- Jolly, A., Guyon, D., & Riom, J. 1996. Use of middle-infrared Landsat Thematic Mapper data for representation of clearcuts in the Landes region. International Journal of Remote Sensing, 17(18):3615–3645.
- Jörn, L. 2007. Is prosopis a curse or a blessing? – An ecological-economic analysis of an invasive alien tree species in Sudan. PhD Dissertation.Faculty of Agriculture and Forestry of the University of Helsinki, Finland.
- Kass, M., Witkin, A., & Terzopoulos, D. 1988. Snakes: Active contour models. International Journal of Computer Vision, 1(4):321–331.
- Kauth, R. J., & Tomas, G. S. 1976.The Tasseled Cap - A Graphic Description of the Spectral-Temporal Development of Agricultural Crops as Seen by Landsat. Symposium on Machine Processing of Remotely Sensed Data, Purdue University, West Lafayette, Indiana, IEEE.
- Kayitakir'e, F., Giot, P., & Defourny, P. 2002. Automated delineation of the forest stands using digital color orthophotos: Case study in Belgium. Canadian Journal of Remote Sensing, 28(5):629–640.
- Kumar, P., Rani, M., Pandey, P., Majumdar, A., & Nathawat, M., 2010. Monitoring of Deforestation and Forest Degradation Using Remote Sensing and GIS: A Case Study of Ranchi in Jharkhand , India, 2(4).
- Kwarteng, A.Y., & P. S. Chavez Jr. 1998. Change Detection Study of Kuwait City and Environs Using Multi-Temporal Landsat Thematic Mapper Data. International Journal of Remote Sensing, 19:1651–1662.
- Laing. R. G. 1953. Mechanization in agriculture in the rainlands of the Sudan, Ministry of Agriculture, Khartoum-Sudan.
- Lambin, E., and A. Strahler. 1994. Change Vector Analysis in Multitemporal Space: A Tool to Detect and Categorize Land-Cover Change Processes Using High Temporal- Resolution Satellite Data. Remote Sensing of Environment, 48: 231-244.
- Lang, S., & Tiede, D. 2007. Definiens Developer. GIS Business, 34-37.

- Larsson, H., & Pilesjo, P. 1990. Remote sensing for forest management in semi-arid environments. Twenty-third International Symposium on Remote Sensing of Environment.
- LEE, S., KIM, C., and Rho, D. 2007. Ecological Change Detection of Burnt Forest Area using Multi-temporal Landsat TM Data. Retrieved from: <http://proceedings.esri.com/library/userconf/proc02/pap1255/p1255.htm>
- Li, X., & A. Yeh. 1998. Principle Component Analysis of Stacked Multi-Temporal Images for the Monitoring of Rapid Urban Expansion in the Pearl River Delta. *International Journal of Remote Sensing*, 19(8): 1501-1518.
- Lillesand, T. M. & Kiefer, R. W. 1987. *Remote Sensing and Image Interpretation*, 2nd ed., John Wiley & Sons, New York, NY.
- Lillesand, T., M., & Kiefer, R. W. 2000. *Remote Sensing and Image Interpretation*. 5th ed. John Wiley & Sons, Inc.
- Lorena, R.B., Santos J.R., Shimabukouro Y.E., Brown I.F & Kulx H.J.H. 2002. A change vector analysis techniques to monitor land use/land cover in SW Brazilain Amazon: Acre state in: *PECORA- 15 integrated remote sensing at global regional and local scale*, Denver, Colorado/USA, pp.8-15.
- Lowell, K. 2001. An area-based accuracy assessment methodology for digital change maps. *International Journal of Remote Sensing*, 22: 3571–3596.
- Lu, D., Batistella, M., & Moran, E. 2004. Multitemporal spectral mixture analysis for Amazonian land-cover change detection. *Canadian Journal of Remote Sensing*, 30(1):87–100.
- Lu, D., Mausel, P., Batistella, M., & Moran, E. 2005. Land-cover binary change detection methods for use in the moist tropical region of the Amazon: A comparative study. *International Journal of Remote Sensing*, 26(1):101–114.
- Lu, D., Mausel, P., Brondizio, E., & Moran, E. 2004. Change detection techniques. *International Journal of Remote Sensing*, 25(12):2365–2407.
- Lu, D., Mausel, P., Brondizio, E., & Moran, E. 2004. Change detection techniques. *International Journal of Remote Sensing*, 25(12):2365–2407.
- Lunetta, R. 1999. Applications, project formulation and analytical approach. In: Lunetta, R. and C. Elvidge (eds): *Remote sensing Change Detection : Environmental Monitoring and Applications*. Taylor & Francis. London.
- Lunetta, R. S., & Elvidge, C. D. E. 1999. Applications, Project formulation, and analytical approach, *Remote Sensing Change Detection: Environmental Monitoring Methods and Applications*. Taylor & Francis .London, pp.1–20.
- Lunetta, R., Johnson, D., Lyon, J., & Crotwell, J. 2004. Impacts of imagery temporal frequency on land-cover change detection monitoring. *Remote Sensing of Environment*, 89(4):444–454.
- Lyon, J., Yuan, D., Lunetta, R., & Elvidge, C. 1998. A change detection experiment using vegetation indices. *Photogrammetric Engineering and Remote Sensing*, 64(2):143–150.
- Malila, W. 1980. Change vector analysis: An approach for detecting forest changes with Landsat. In *Proceedings of the 6th annual Symposium on Machine*

- Processing of Remotely Sensed Data, Purdue University, West Lafayette, Ann Arbor, ERIM. Indiana, pp. 326–335
- Mas, J. F. 1999. Monitoring land-cover changes: A comparison of change detection techniques. *International Journal of Remote Sensing*, 20(1): 139-152.
- Maselli, F. 2004. Monitoring M forest conditions in a protected Mediterranean coastal area by the analysis of multiyear NDVI data. *Remote Sensing of Environment*, 89: 423-433.
- Mather, P. 1987. Computer processing of remotely sensed images - An introduction. Biddles Ltd, Guildford and Kings's Lynn.
- McDonald, A. J., Gemmell, F. M. & Lewis, P. E. 1998. Investigation of the utility of spectral vegetation indices for determining information on coniferous forests. *Remote Sensing of Environment*, 66(3):250–272.
- Meinel, G., & Neubert, M. 2004. A comparison of segmentation programs for high resolution remote sensing data. In *Proceedings of the XXth ISPRS Congress*. Istanbul, Turkey.
- Michalek, J., & Wagner, T. 1993. Multispectral Change Vector Analysis for Monitoring Coastal Marine Environment. *Photogrammetric Engineering & Remote Sensing*, 59: 381- 384.
- Michener, W., & Houhoulis, P. 1997. Detection of vegetation changes associated with extensive flooding in a forested ecosystem. *Photogrammetric Engineering and Remote Sensing*, 63(12):1363–1374.
- Miller, A., Bryant, E., & Birnie, R. 1998. Analysis of land cover changes in the Northern Forest of New England using multitemporal Landsat MSS data. *International Journal of Remote Sensing*, 19(2):245–265.
- Ministry of Environment & Physical Development (MEPD). 2003. Sudan's First National Communications under the United Nations Framework Convention on Climate Change. Volume 1.
- Morisette, J. T., & Khorram, S. 2000. Accuracy assessment curves for satellite-based change detection. *Photogrammetric Engineering and Remote Sensing*, 66: 875–880.
- Muchoney, M., & Haack, N. 1994. Change detection for monitoring forest defoliation. *Photogrammetric Engineering and Remote Sensing*, 10:1243–1251.
- Munoz, X., Freixenet, J., Cufi, X., & Marti, J. 2003. Strategies for image segmentation combining region and boundary information. *Pattern Recognition Letters*, 24(1-3):375–392.
- Mustafa, R. 2006. Risk Management in the Rain-fed Sector of Sudan: A case Study, Gedarif Area Eastern Sudan. Ph.D. Thesis, Faculty of Agricultural and Natural Sciences, University of Justus- Liebig Giessen.
- Nackaerts, K., Vaesen, K., Muys, B., & Coppin, P. 2005. Comparative performance of a modified change vector analysis in forest change detection. *International Journal of Remote Sensing*, 26(5):839–852.
- Nelson, R. 1983. Detecting forest canopy change due to insect activity using Landsat MSS. *Photogrammetric Engineering and Remote Sensing*, 49(9):1303–1314.

- Nielsen, A. A. 1996. Change detection in multi-spectral, bi-temporal spatial data using orthogonal transformations. 8th Australasian Remote Sensing Conference, Canberra, Australia.
- Nielsen, A. A., Conradsen, K., & Simpson, J. J. 1998. Multivariate alteration detection (MAD) and MAF post processing in multispectral, bitemporal image data: New approaches to change detection studies. *Remote Sensing of Environment*, 64(1): 1–19.
- Niemeyer, I. & Canty. 2003. Pixel based and object oriented change detection analysis using high resolution imagery. *Definiense Imaging*.
- Niemeyer, I. & Canty, M. 2001. Object-Oriented Post-Classification of Change Images. *Proc. SPIE's International Symposium on Remote Sensing, Toulouse*.
- Niemeyer, I., Canty, M., & Klaus, D. 1999. Unsupervised change detection techniques using multispectral satellite images. *IEEE International Geoscience and Remote Sensing Symposium, Hamburg. IGARSS*.
- Omer, S. A. 1989. Some Aspects of Socio-economic and Environmental Change in Simsim Area, The case of Sudanese-Canadian project.
- Pacifici, F. 2007. Change Detection Algorithms: State of the Art. *Tor Vergata University, Rome, Italy*.
- Pal, N., & Pal, S. 1993. A review on image segmentation techniques. *Pattern Recognition*, 26(9):1277–1294.
- Petit, C., Scudder, T., & Lambin, E. 2001. Quantifying processes of land-cover change by remote sensing: Resettlement and rapid land-cover change in southeastern Zambia. *International Journal of Remote Sensing*, 22:3435–3456.
- Pilon, P. G., P. Howath, J., & Bullock, R. A. 1988. An Enhanced Classification Approach to Change Detection in Semi-Arid Environments. *Photogrammetric Engineering & Remote Sensing*, 54: 1709-1716.
- Prenzel, B., & Treitz, P. 2005. Comparison of structure- and function-based schemes for classification of remotely sensed data. *International Journal of Remote Sensing*, 26(3):543-561.
- Radke, R., Andra, S., Al Kofahi, O., & Roysam, B. 2005. Image change detection algorithms: A systematic survey. *Ieee Transactions on Image Processing*, 14(3):294–307.
- Radke, R., Andra, S., Kofahi, O., & Roysam, B. 2004. Image Change Detection Algorithms: A systematic Survey
- Richards, J. A. 1986. *Remote sensing Digital Image Analysis: An Introduction*. Springer-Verlag, Berlin.
- Richards, A. 1993. *Remote sensing digital image analysis. An introduction (2nd.)*. Berlin: Springer-Verlag. 340 p.
- Ridd, M., & Liu, J. 1998. A comparison of four algorithms for change detection in an urban environment. *Remote Sensing of Environment*, 63(2):95–100.
- Rogan, J., Franklin, J., & Roberts, D. 2002. A comparison of methods for monitoring multitemporal vegetation change using Thematic Mapper imagery. *Remote Sensing of Environment*, 80(1):143–156.

- Rogan, J., Miller, J., Stow, D., Franklin, J., Levien, L., & Fischer, C. 2003. Land-cover change monitoring with classification trees using Landsat TM and ancillary data. *Photogrammetric Engineering and Remote Sensing*, 69(7):793–804.
- Rogerson, P. 2002. Change detection thresholds for remotely sensed images. *Journal of Geographical Systems*, 4(1):85–97.
- Rosin, P. 2002. Thresholding for change detection. *Computer Vision and Image Understanding*, 86(2):79–95.
- Sader, A., Bertrand, M., & Wilson, E. 2003. Satellite change detection of forest harvest patterns on an Industrial forest landscape. *Forest Science*, 49(3): 341-353.
- Sader, S. A., Hayes, D. J., Hepinstall J. A., Coan, M. C., & Soza, C. 2001. Forest change monitoring of a remote biosphere reserve. *International Journal of Remote Sensing*, 22(10): 1937-1950.
- Sader, S., & Winne, J. 1992. RGB-NDVI color composites for visualizing forest change dynamics. *International Journal of Remote Sensing*, 13(16):3055–3067.
- Saksa, T., Uutera, J., Kolstrom, T., Lehtikainen, M., Pekkarinen, A., & Sarvi, V. 2003. Clear-cut detection in boreal forest aided by remote sensing. *Scandinavian Journal of Forest Research*, 18(6):537–546.
- Saura, S. 2002. Effects of minimum mapping unit on land cover data spatial configuration and composition. *International Journal of Remote Sensing*, 23(22):4853–4880.
- Schmidt, H. & Karnieli, A. 2001. Sensitivity of vegetation indices to substrate brightness in hyper-arid environment: The Makhtesh Ramon Crater (Israel) case study. *International Journal of Remote Sensing*, 22:3503-3520.
- Schott, J., Salvaggio, C., & Volchok, W. 1988. Radiometric scene normalization using pseudoinvariant features. *Remote Sensing of Environment*, 26:1–7.
- Schroeder, T., Cohen, W., Song, C., Canty, M., & Yang, Z. 2006. Radiometric correction of multi-temporal Landsat data for characterization of early successional forest patterns in western Oregon. *Remote Sensing of Environment*, 103: 16–26.
- Schroeder, T., Cohen, W., Song, C., Canty, M., & Yang, Z. 2006. Radiometric correction of multi-temporal Landsat data for characterization of early successional forest patterns in western Oregon. *Remote Sensing of Environment*, 103(1):16–26.
- SeifEldin A., & Obeid M., 1970. Grazing and seedling growth in *Acacia senegal*. *Journal of Applied Ecology*, 1. (8).
- Singh, A. 1986. Change Detection in a Tropical Forest Environment of Northeastern India Using Landsat. *Remote Sensing and Tropical Land Management*, edited by M. J. Eden and J. T. Parry, John Wiley & Sons, London, England, pp. 237-254.
- Singh, A. 1989. Review Article: Digital Change Detection Techniques Using Remotely-Sensed Data. *International Journal of Remote Sensing*, 10(6): 989-1003.
- Siwe, R., & Koch, B. 2008 Change vector analysis to categorize land cover change processes using the Tasseled cap as biophysical indicator. *Environmental Monitoring and Assessment*, 145 (1-3): 227-235.

- Skakun, R., Wulder, M., & Franklin, S. 2003. Sensitivity of the Thematic Mapper Enhanced Wetness Difference Index (EWDI) to detect mountain pine beetle red-attack damage. *Remote Sensing of Environment*, 86(4):433–443.
- Small, C. 2002. High resolution spectral mixture analysis of urban reflectance. High spatial resolution commercial imagery workshop CD. Lamont-Doherty Earth Observatory, Columbia University.
- Sohl, T.L. 1999. Change Analysis in the United Arab Emirates: An Investigation of Techniques. *Photogrammetric Engineering and Remote Sensing*, 65(4): 475- 484.
- Soille, P., & Pesaresi, M. 2002. Advances in mathematical morphology applied to geoscience and remote sensing. *IEEE Transactions on Geoscience and Remote Sensing*, 40(9):2042–2055.
- Song, C., Woodcock, C., Seto, K., Lenney, M., & Macomber, S. 2001. Classification and change detection using Landsat TM data: When and how to correct atmospheric effects? *Remote Sensing of Environment*, 75(2):230–244.
- Sudan Meteorological Department, 1970. Climatological Normals 1941-70, Gadaref, Sudan.
- Suliman, H., & Buchroithner, M. 2007. Multi-Temporal Classification of Abandoned Agricultural Land in Gadarif Region, Sudan, Using Original Bands, Indices and Feature Components of Spaceborne Imagery. *IEEE Proceedings for Fourth International Workshop on the Analysis of Multitemporal Remote Sensing Images*, Leuven, Belgium.
- Sunar, F.1998. An Analysis of Change in a Multi-date Data Set: A Case study in The Ikitelli Area, Istanbul, Turkey. *International Journal of Remote Sensing*, 19: 225-235.
- Tarongi, J., & Camps, A. 2010. Normality Analysis for RFI Detection in Microwave Radiometry. *Remote Sensing*, 2: 191-210.
- The higher council for environment and natural resources (hcnr). 2009. Sudan's fourth national report to the convention on biological diversity.
- Toll, D. L., Royal, J. A., & Davis, J. B. 1980. Urban Area Up-date Procedures Using Landsat Data. *Proceedings, American Society of Photogrammetry*, Falls Church, Virginia. 12 p.
- Toomey, M., & Vierling, L. 2005. Multispectral remote sensing of landscape level foliar moisture: techniques and applications for forest ecosystem monitoring. *Canadian Journal of Forest Research*, 35 :(5) 1087-1097, 10.1139/x05-043
- Tothill. J. D. 1948. *Agriculture in the Sudan*, Oxford.
- United Nation Environment Programme. 2007. Sudan Post-Conflict Environmental Assessment. Urban Fringes. *IEEE Transactions on Geoscience & Remote Sensing*, 31: 136-145.
- Vincent, L. & Soille, P. 1991. Watersheds in digital spaces: An efficient algorithm based on immersion simulations. *IEEE Transactions on Pattern Analysis and Machine Intelligence*, 13:583–589.

- Vink, A. T. 1987. Integrated Landuse Plan for Rawashda Forest Reserve (1987-1991). Fuelwood Development for Energy in Sudan GCP/SUD/033/NET. Field Document No. 27. Forests National Corporation. 100 p.
- Virk, R., & King, D. 2006. Comparison of Techniques for Forest Change Mapping Using Landsat Data in Karnataka, India. *Geocarto International*, 21. (4).
- Volcani, A., Karnieli, A., & Svoray, T. 2005. The use of remote sensing and GIS for spatio-temporal analysis of the physiological state of a semi-arid forest with respect to drought years. *Forest Ecology and Management*, 215(1-3):239–250.
- Wallace, J., Behn, G., & Furby, S. 2006. Vegetation condition assessment and monitoring from sequences of satellite imagery. *Ecological Management and Restoration*, 7(s1), 31-36.
- Walter, V. 2004. Object-based classification of remote sensing data for change detection. *Isprs Journal of Photogrammetry and Remote Sensing*, 58(3-4):225–238.
- Wang, F. 1993. A Knowledge-Based Vision System for Detecting land Changes at Urban Fringes. *IEEE Transactions on Geoscience & Remote Sensing*, 31: 136-145.
- White, R., Murray, S., & Rohweder, M. 2000. *Grassland Ecosystems*. World Resources Institute, Washington, D.C.
- Wilson, E., & Sader, S. 2002. Detection of forest harvest type using multiple dates of Landsat TM imagery. *Remote Sensing of Environment*, 80(3):385–396.
- Wily, L. 2003. Governance and land relations: A review of decentralization of land administration and management in Africa. International Institute for Environment and Development (IIED), UK. 90p.
- Woodcock, C., Macomber, S., Pax-Lenney, M., & Cohen, W. 2001. Monitoring large areas for forest change using Landsat: Generalization across space, time and Landsat sensors. *Remote Sensing of Environment*, 78(1-2):194–203.
- World Bank. 2003. Sudan: Country Economic Memorandum, Stabilization and Reconstruction report. Report No. 26420-SU, Washington, D.C.
- Yacouba, M. 1999. Niger's experiences in decentralised management of natural resources. Paper presented at the DFID workshop on land rights and sustainable development in Sub-Saharan Africa: Lessons and ways forward in land tenure policy, Sunningdale, UK, 16-19pp.
- Yang, L., & Huang, C. 2002. Mapping large-area impervious surface and forest canopy density using Landsat 7 ETM+ and high resolution imagery. 2002 High spatial resolution commercial imagery workshop CD, Raytheon ITSS, USGS EROS Data Center.
- Zhang Lu, 2004. Change Detection in Remotely Sensed Imagery Using Multivariate Statistical Analysis, Ph.D Dissertation, Wuhan University, China.
- Zhang, Q., and Ban, Y. 2010. Monitoring impervious surface Aprox using tasseled Cap transformation of Landsat data. *ISPRS TC VII Symposium*. Vol. XXXVIII, Part 7A.

Zhu, J., Guo, Q., & Harmon, T. 2010. Land use/ land cover change detection using object based change vector analysis in posterior probability space. Annual Meeting, Washington, DC Online Program.